Western&Graduate&PostdoctoralStudies

Electronic Thesis and Dissertation Repository

11-9-2017 5:00 PM

# Development of an Active Finger Motion Simulator: With In-Vitro Assessments of Tendon Loads and Joint Kinematics

Mohammad Haddara
*The University of Western Ontario*

Supervisor
Ferreira, Louis
*The University of Western Ontario*

Graduate Program in Biomedical Engineering
A thesis submitted in partial fulfillment of the requirements for the degree in Master of Engineering Science
© Mohammad Haddara 2017

Follow this and additional works at: https://ir.lib.uwo.ca/etd

Part of the Biomechanics and Biotransport Commons, and the Biomedical Devices and Instrumentation Commons

# Abstract

Musculoskeletal injuries of the finger far outnumber those of other joints. While in-vitro motion simulators are useful for studying joint biomechanics and evaluating surgical repairs, considerably less simulator development has been reported for the finger compared to other joints. Replication of active musculoskeletal movement during in-vitro testing has been shown to be more representative of in-vivo motion patterns; closed-loop motion controllers are the current state-of-the-art for in-vitro kinematics studies. However, an in-vitro motion simulator with closed-loop tendon load control and simultaneous tendon excursion control has not yet been reported for the finger. This thesis outlines the design and development of an active motion simulator for the study of finger joint kinematics, as well as forces and excursions of the flexor/extensor tendons. Performance of the system was verified in terms of tendon load control accuracy and motion repeatability, before conducting two cadaveric studies. An in-vitro study on the effects of wrist position and distal extensor tendon rupture verified that the new simulator produced expected finger kinematics and tendon loads. With the new simulator validated, its high sensitivity in measuring tendon loads was leveraged to observe the effects of A2 and A4 pulley excision and subsequent surgical repair. The thesis culminates with a summary of sample size analysis and statistical effect sizes that will aid future in-vitro finger studies with this simulator.

Keywords: Active Motion Simulator, Excursion, Flexors, Cadavers, Kinematics, Force, Pulley, Reconstruction.

# Co-Authorship Statement

**Chapter 1: Introduction and Literature Review**

Mohammad Haddara - Sole author

**Chapter 2: Development of a Finger Active Motion Simulator**

Mohammad Haddara - Developed platform & control system, study design, data collection, wrote code

Louis Ferreira – Study design, simulator design

Laura Kember – Study design, specimen preparation

Ruby Grewal – Pilot study protocol design

**Chapter 3: Effects of Wrist Position and Distal Extensor Rupture on Finger Kinematics and Tendon Loads: An In-Vitro Study**

Mohammad Haddara - Study design, data collection, statistical analysis

Louis Ferreira – Study design & protocol,

Troy Ng - Specimen preparation

**Chapter 4: Sequential A2 and A4 Pulley Sectioning and Reconstruction: Cadaveric Kinematics Study**

Mohammad Haddara - Study design, data collection, statistical analysis

Louis Ferreira - Study design

Brett Byers - Study design, specimen preparation, surgical excisions and reconstructions

**Chapter 5: Discussion & Future Work**

Mohammad Haddara - Sole author

# Acknowledgments

I would first like to start by thanking my supervisor, Dr. L. Ferreira, for giving me the incredible opportunity to work with him closely at the Hand & Upper Limb Centre (HULC) as a Masters Grad student. Thank you also for the unwavering support that I received from you not only throughout my thesis, but also since my second year of undergrad as a work study student. You've given me the opportunity to initiate my very own project, explore many different pathways, and you never failed to push me towards excellence and for that, I can't thank you enough. The skills that I have gained from my time working with you are extremely valuable and I will continue to use them throughout my professional career.

Jordan O'Brien, I cannot begin to explain how thankful I am for all the time and effort that you put in assisting me with my hardware and software troubleshooting. Thank you for all the early mornings you donated your help with experimental setup and data collection. It was definitely a pleasure working with you and I wish you nothing but success in your life.

To Dustin Dobranksy, a very close friend. Thank you for always being there for me when I needed help the most in term of any software difficulties or barriers I may have encountered. You truly are a great friend.

To Dr. Kember, Dr. Ng, and Dr. Byers, thank you for all the time that you put in with long and exhausting testing protocols. It if weren't for you, my thesis would not be where it is as of now so thank you to all three of you. It was definitely a pleasure working with such skilled surgeons.

To my sister, Raneem, you have been nothing but understanding throughout this entire process. You offered me comfort, kindness, and support and I love you with every part of my heart. Being my only sister, you and I have grown so close to one another over the years and I can't imagine my life without you so thank you for being you and for everything you do for me. I truly don't deserve the love that I get from you.

Finally, to my parents, Moustafa Haddara and Sahar El-Arousy. Where can I even begin explaining how much you both mean to me. Dad, you are, and will always be my role model.

# Table of Contents

# List of Tables

# List of Figures

# List of Appendices

# Chapter 1

## 1 Introduction and Literature Review

*OVERVIEW:* *This chapter begins with a review of the basic anatomy and biomechanics of the finger and then continues with an overview of flexor tendon injuries, and the complications following flexor tendon repair. Literature review regarding past and ongoing passive and active-motor assist studies is discussed. This chapter then concludes with an explanation behind the purpose of this study and the objective towards this research of developing an active motion flexor tendon simulator that allows for the study of the kinematics of finger joints and the forces within the tendons.*

## 1.1    Significance of the hand

As one of the most crucial and fascinating components of the body, the hand is an essential tool in one's everyday life. Its reliability and integrity is strongly reliant on the flexibility of its finger joints and the tendon mechanism driving the finger. The hand, amongst all other body parts, is very susceptible to many disorders and injuries to the fingers, most commonly within the tendons and the pulleys. Therefore, fine understanding of the anatomy of the hand is vital when trying to provide the highest quality of care to a patient suffering from a trauma. The following section will discuss the three main structures that formulate the essence of the finger; the joints, pulleys, and tendon mechanism.

## 1.2    Anatomical Background of the Finger

Each finger is comprised of three bones or 'phalanges'; the proximal phalanx phalange, middle phalanx phalange, and distal phalanx phalange. Together, they all make up the bone structure of the finger and are similar in their organization and function. They do however differ in their shapes and their joint's ranges of motion (ROM) [1]. The proximal phalanx is the third and largest phalange within the finger. The middle phalanx is the second, or middle, phalange, and the distal phalanx is the first phalange [2]. A joint is a connection made between bones in the body by a specialized set of tissues called cartilage. These tissues are commonly self-lubricating and can maintain smooth and flexible motion under large compressive and tensile loading conditions of the joints. They also allow for the movement within one degree of freedom; ensuring proper stability when undergoing full flexion and extension of the finger. There are three joints that are formed between the finger phalanges, the distal interphalangeal joint (DIP), proximal interphalangeal (PIP) joint, and the metacarpophalangeal (MCP) joint (*Figure 1.1*) [3].

### 1.2.1    Distal Interphalangeal Joint (DIP)

The DIP joint is located at the tip of the finger, between the distal and the middle phalanx. The range of motion of the joint varies between 0° and 65° [4].

### 1.2.2    Proximal Interphalangeal Joint (PIP Joint)

The PIP joint is located around the middle of the finger, between the middle and the proximal phalanx. The range of motion of the joint varies between 0° and 110° [4].

## 1.2.3     Metacarpophalangeal Joint (MCP joint)

The MCP joint is where the bones within the palm of the hand, called the metacarpals, meet the first finger phalange, the proximal phalanx. The metacarpals are long bones that provide the structure of the palm of the hand but provide little, to no movement, during the flexion of the joints. MCP joints are crucial for both power grip and sturdy activities. The MCP joints allow for the tip of the fingers to reach the palm of the hand through full flexion of the joint. The range of motion of the joint varies between 0° and 85° [4].
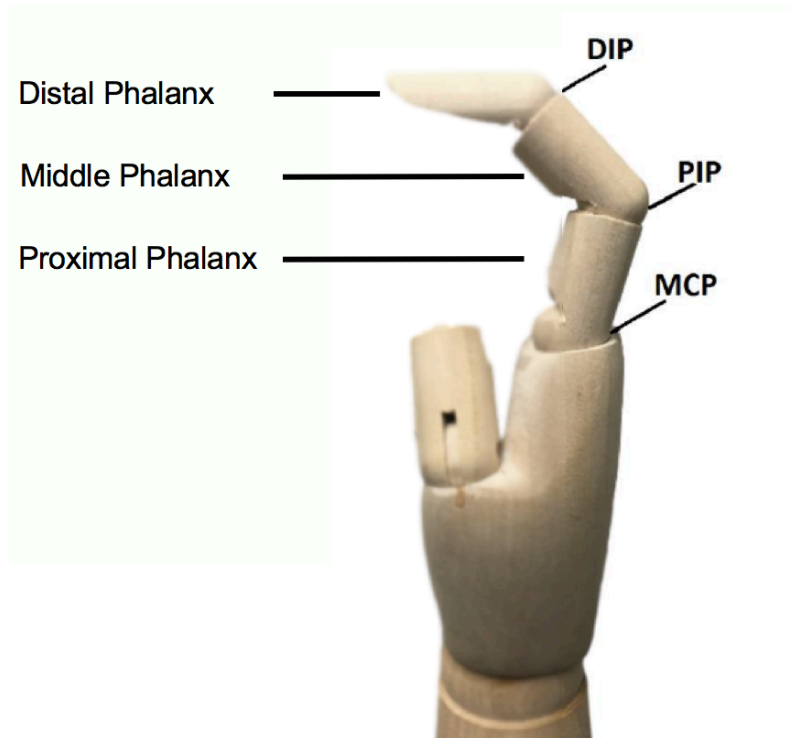


**Figure 1.1: Finger Segments and Joints**

Illustration of the finger bones along with the joints on a hand model

## 1.3   Tendons

### 1.3.1      Anatomy

Tendons are fibrous connective tissues that connect muscles to bone, functioning simply to transmit forces [5]. Within the hand, these tissues are categorized into flexor and extensor tendons, each with a distinct function, insertion point, and pathway along the finger. Every finger, excluding the fifth digit, consists of two long flexor tendons that run along the palmar side of the hand and one long extensor tendon that runs along the dorsal side of the hand; working collectively to achieve full flexion and extension of the finger [3]. In other words, consider a pulley-box mechanism where a rope is fed through a pulley and is tied to a hanging mass at one end and a linear motor at the other end. In this scenario, the weight resembles a single phalange, the rope represents the tendon, and the motor resembles the muscle in the forearm that applies tension within the tendon. As the rope is pulled from one end by the motor, the mass travels towards the point in which force is applied, and vice versa. Similar to the human finger, once the flexor tendons are pulled, the finger joints begin to rotate towards the direction in which force is applied, and vice versa when the extensor tendons are pulled instead. Although they differ in their insertion points, there are two types of long flexor tendons that work collectively to achieve full flexion of the finger; flexor digitorum profundus (FDP) and flexor digitorum superficialis (FDS). Both flexor tendons run along one another through pulleys and fibrous tissues called sheaths on the palmar side of the finger in a very fascinating, yet complicating organization. These tendon sheaths function as tunnels, lubricating the gliding movement of the two tendons against one another. They also allow the tendons to elastically deform when pulled, assisting in the smooth movement of the finger along its path of flexion or extension [6]. Both tendons are held tight enough within these sheaths to the extent that any possible increase in the size of the tendon can limit the motion of the tendons through the sheaths; jeopardizing mobility. Aside from the sheaths, pulleys at the joints also provide for smooth motion of the finger and function to maintain the flexor tendons close to bone [6] [7].

### 1.3.2      Flexor Digitorum Profundus

The profundus tendon is one of two long flexor tendons within the finger. It originates within a muscle in the forearm and inserts at the tip of the distal phalanx [4]. Its chief function is to achieve full flexion of the finger, including all of the finger joints.

### 1.3.3      Flexor Digitorum Superficialis

The second flexor tendon, superficialis, also functions to achieve full flexion of the finger joints. However, unlike FDP, FDS insert at the midline of the middle phalanx and therefore, is responsible for the flexion of only the MCP and the PIP joint, but not the DIP joint. In order to obtain a full flexion of the finger, a functional FDP tendon is crucial for the flexion of the most distal joint.

### 1.3.4      Extensor Tendon

Located along the dorsal side of the hand, extensor tendons work antagonistically to the flexor tendons, extending the finger and its joints back to their straightened position. Similar to the flexor tendons, the long extensor tendons originate from muscles at the forearm and insert at the most distal finger segment, the distal phalanx [8].

### 1.3.5      Pulleys

There are five different pulleys located along the finger; each with a significant role of maintaining and stabilizing the flexor tendons at the palmar sides of the phalanges close to bone [9]. The arrangement and function of the pulleys allow for any tensile force or excursion experienced by the flexor tendons to be translated into rotation and torque at the finger joints [10]. Pulleys A1, A3, and A5 overlie the MCP, PIP, and DIP joints, whereas the A2 and A4 pulleys are located along the phalanges, in-between the joints. The A1 pulley is approximately 8 mm in width and is the first annular pulley which arises from the proximal portion of the proximal phalanx [11]. The second annular pulley, A2, is approximately 20 mm in width and is clinically known to be the most important pulley, biomechanically, followed by the A4 pulley (7mm in width) as they both play a vital role in maintaining independent interphalangeal joint function and preventing tendon bowstringing [12][13]. Tendon bowstringing is a rare condition where the tendon translated away from the center of rotation of the MCP joint; altering the flexion moment arm of the joint [14]. A3 and A5 pulleys are 3mm and 4mm in width respectively [7].

## 1.3.6    Tendon Mechanism

All the fine and gross movements of the finger are achieved by a very complex tendon mechanism. The complexity and uniqueness of the tendon structure and arrangement of the long flexor tendons can be observed (*Figure 1.2*). The organization of the tendons is unique enough that the tendons not only glide against one another, but also through one another. The profundus tendon, FDP, physically runs though the superficialis tendon, FDS, to reach its insertion point at the distal phalanx. Such mechanism is the main reason behind the smooth motion of the finger during flexion.
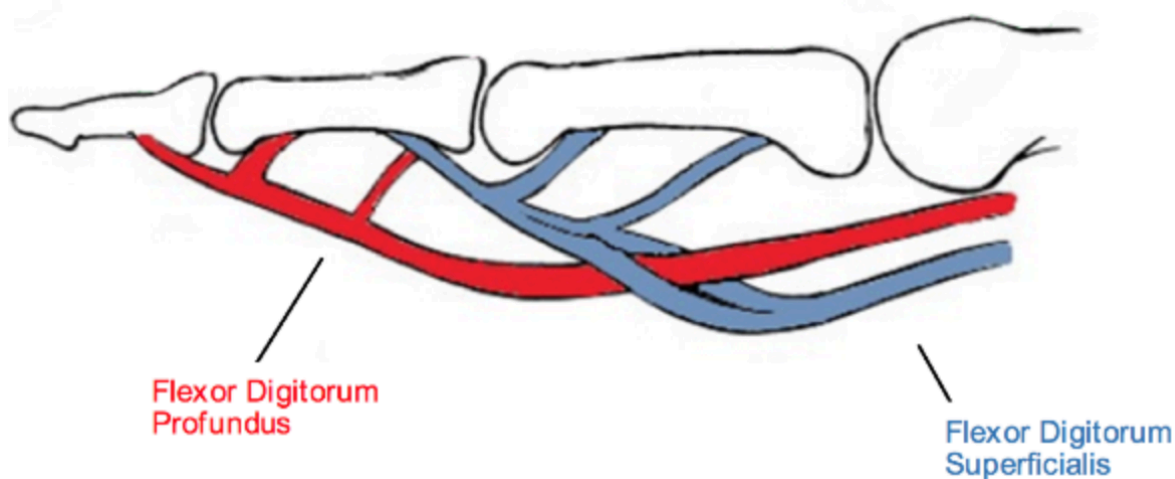


**Figure 1.2: Flexor and Extensor Tendons**

*The anatomy of the flexor tendons (flexor digitorum profundus and flexor digitorum superficialis) along the finger without the tendon sheaths securing them.*

## 1.4    Flexor Tendon Injuries

### 1.4.1    Challenges

Tendon injuries are fairly common and can become quite challenging and problematic. Such trauma can arise from severe physical activity such as sports or the accidental slicing of the tendon by a sharp object [5]. Depending on the degree of laceration, the cut or injury could affect one or both tendons. Once a flexor tendon is torn, it becomes impaired and can no longer function to mobilize the finger. Flexor tendon injuries are a puzzling problem for surgeons due to three main reasons. Firstly, flexor tendons cannot heal without surgical treatment as the two ends need to be surgically brought together for the healing to occur. Secondly, postoperative management needs to be carefully planned as mobilization has shown to be essential in improve gliding but can risk rupture. Lastly, due to the unique anatomy of the tendons running through flexor tendon sheaths to function, surgeons need to prevent any risk of increasing the bulkiness of the tendon through its sheath, which is not always possible from scarring as this affects the functional outcome of the tendon. Based on literature review, injuries to the hand and wrist account for approximately 20% of patient visits to emergency departments in the United States and they seem to impose a large economic burden as they annually account for $740 million U.S dollars and rank first in the order of most expensive injury types [15]. During a 10-year study, there was an incidence rate of 33.2 finger tendon injuries per 100,000 person-years [16]. Work-related injuries accounted for 24.9% of acute traumatic tendon injuries, food preparation and serving related occupations (14.4%), and transportation and material moving occupations (12.5%) [16].

### 1.4.2    Surgical Tendon Repair

There are various techniques that are used to repair tendons. These techniques normally involve approximating and suturing both cut ends of the tendon together. Many different considerations need to be taken into account once deciding to repair a flexor tendon. Early surgical repair, subsequently following injury offer a much better outcome in terms of functionality of the hands as opposed to a late surgical repair [5]. Generally, as time permits, the possibility of repairing a tendon decreases due to end swelling and increased risk of infections. Strickland et al. stated that the ideal tendon repair should have minimal gapping at the repair site, minimal interference with tendon vascularity, secure suture knots, smooth junction of tendon end and have sufficient strength for healing [17]. Handling of the tendons should be done with as little trauma as possible to prevent scaring and adhesion [18].

Depending on where the site of injury is along the hand, different surgical procedures are used (*Figure 1.3*). For example, Zone I injuries commonly involve the rupture of only the FDP whereas, Zone II, also known as the 'no man's land' is far more complex as there is a much closer interaction between both long flexor tendons, FDS and FDP, risking the chance of future complications [18]. Not only should tendons be handled carefully, the tendon sheaths and pulley systems should remain protected and salvaged. Most commonly in repair cases, the surgeon avoids repairing a lacerated tendon sheath as a repair decrease the overall width of the passage site, limiting the tendons from gliding smoothly to achieve its function [5]. Zone III and V injuries of the hand do not impose as big of a threat as zone II due to its large surface area and better vascularity and therefore, are not difficult to repair.
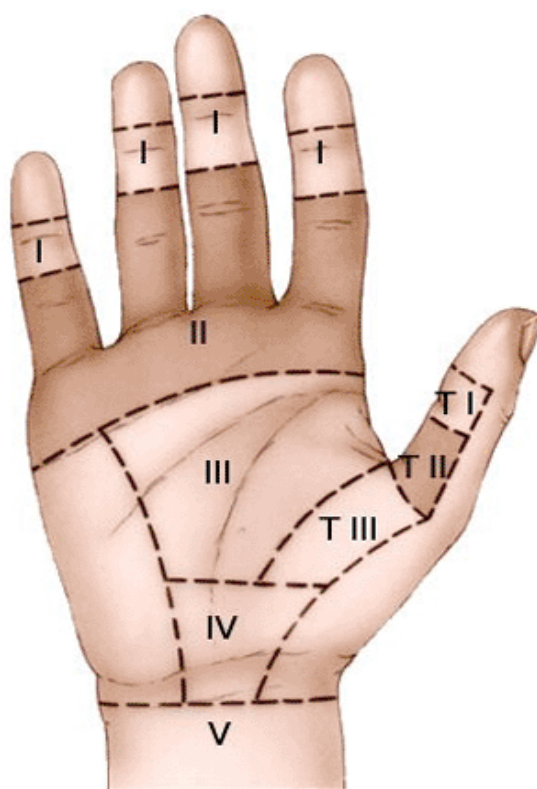
**Figure 1.3: Zones of the Hand**

*An illustration of the different zones of the hand. Zone I is the most commonly injured zone. Zone II (the shaded area), is commonly referred to as "no man's land" as injures in this area are very complex and have a high risk of future complications. Injuries to Zones III and IV are easy to repair and do not pose any added risks like Zone II.  [19], [20]*

### 1.4.3     Post-Op Healing

Unfortunately, not every post tendon repair recovery session is smooth. Approximately 59% to 90% of patients undergoing flexor tendon repair do experience improvement in their joint ROM. However, 5% to 33% of patients find no improvement in finger mobility and 8% experience worsening of symptoms, such as pain and discomfort [21][22]. Despite the improvement in technology and the advancement in surgical techniques and methods, flexor tendon complications following tendon repair manages to continue being a formidable challenge worldwide. Such complications can include infection, tendon rupture, pulley rupture, or adhesion formation [23]. The possibility of a tendon rupture or pulley is considered one the most critical complications as it requires immediate revision surgery where the surgeon is required to relocate the injury site and repair it once again. Urgent secondary surgical intervention usually occurs in 3-9% of patient cases [21]. Causes of tendon rupture can include overloading the tendons, misuse of the hand, or bulky tendons after repair. Another critical complication that can occur within patients is the adhesion simulation within the finger [24].

### 1.4.4     Adhesions

During recovery, the body undergoes a type of healing known as extrinsic healing [25]. The process involves the accumulation or layering of scar tissue around the site of injury for cells and tissue to reform and grow underneath, similar to a scab that forms over the skin once the skin breaks due to a cut. The main issue arises when excess scar tissue is laid down along one, or both tendons; increasing the thickness of the tendons and/or adhering the tendon to the surrounding tissues, the other tendon, or bone [26]. Thus, limiting the smooth gliding of the tendons through the anatomical tunnels and immobilizing the finger.

## 1.5    Pulley Injuries

Similar to tendons, pulleys within the finger are also at risk of injuries, most commonly within rock climbers. With the increasing number of people participating in indoor and outdoor rock climbing activities, injuries sustained by pulleys are on the rise [27]. Around 40% of all climbing injuries clinically documented are to the fingers, where 20-26% are solely to the pulleys [28][29]. Such injuries include partial or complete rupture of one or more annular pulleys, resulting in visible bowstringing. The A2 pulley is the most commonly injured of the five annular pulleys due to the configuration of the hand when attempting to grasp small holds, also known as the 'crimp' grip (*Figure 1.4*). The crimp grip was first described by Bollen in 1988 [27] as having the DIP joint undergo great hyperextension, whereas the PIP joint maintains a 90 degree flexion angle, producing tremendous force load on the A2 pulley. The forces at the A2 pulley are approximately $3 - 4$ times greater than at the fingertip which has been clinically estimated to be forces of around 380N [30]. Such large loading on the pulley can evidently lead to rupture.
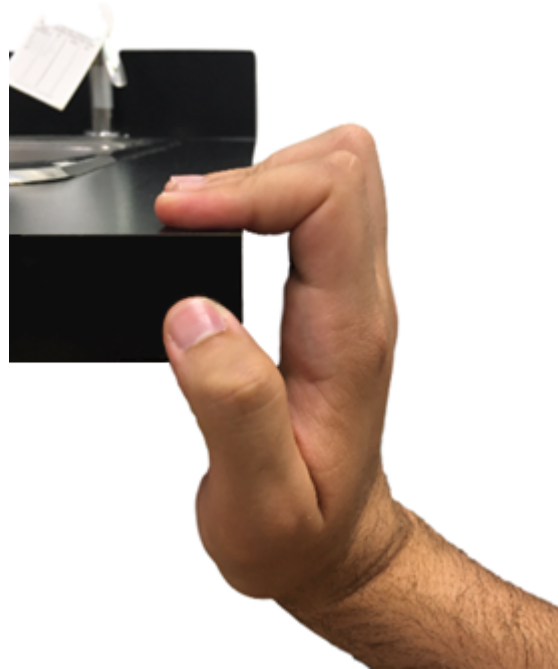


**Figure 1.4: The 'crimp' grip position**

*An illustration of the crimp grip position where the DIP joint experiences severe hyperextension with the PIP joint in a 90 degree flexed position.*

## 1.6  Wrist Biomechanics

### 1.6.1    Neutral Position

When describing the motions of the wrist joint, it is important to understand the anatomical neutral position in which all range of motion such as flexion-extension, radioulnar deviation, and a combination of these positions are defined. Neutral wrist position is defined as the palm of the hand parallel to the forearm (*Figure 1.5*).



**Figure 1.5: Wrist neutral position**

### 1.6.2    Flexed-Extended Position

The flexion-extension position of the wrist has a center of rotation around the centroid of the wrist. A healthy wrist can have a flexion-extension range of $60 - 80$ degrees and $60 - 75$ degrees respectively (*Figure 1.6*) [31]. In terms of our research, a 30-degree flexion-extension angle of the wrist was analyzed.
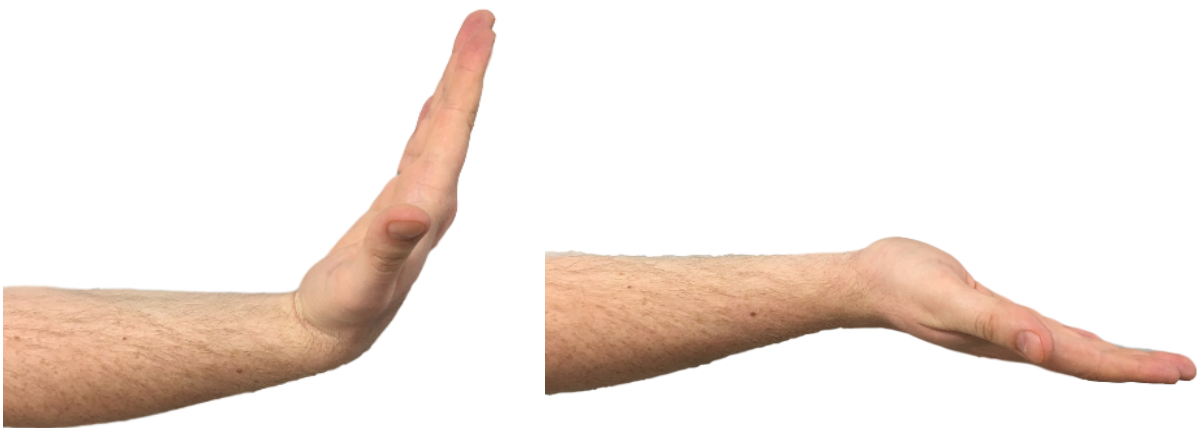


**Figure 1.6: Wrist Flexed and Extended**

*The wrists in 80° flexion and 20° extension*

## 1.6.3    Ulnar-Radial Deviation

Similar to flexion-extension, ulnar-radial deviation of the wrist occurs around the centroid of the wrist with a range of 30 – 39 degrees and 20 – 25 degrees respectively (*Figure 1.7)* [31]. For our research, a 30-degree ulnar deviation was only analyzed.



**Figure 1.7: Wrist Ulnar and Radial Deviated**

*Wrists in 30° ulnar deviation (left) and 20° radial deviation (right)*

## 1.7 Kinematics Measurement Systems

With current advancement in technology, there are numerous methods that are used in vivo, and in vitro, to measure the kinematics and range of motion of the finger joints. Such techniques range from the use of a simple goniometer, to an electro-magnetic tracking system.

### 1.7.1 Goniometer

Goniometer are one of the most common tools used for the measurement of angles up to 360 degrees [32]. In terms of finger kinematics, joint ranges can be measured by simply centering the fulcrum of the goniometer over the dorsal aspect of the joint of choice. Subsequently, aligning the proximal arm over the dorsal midline of the joint and the distal arm over the dorsal midline of the corresponding phalange (*Figure 1.8)* [31]. The angle in which the goniometer then forms is the angle of rotation of the joint. Although simple, calculating angles using such approach involves a large amount of human error by the operator.
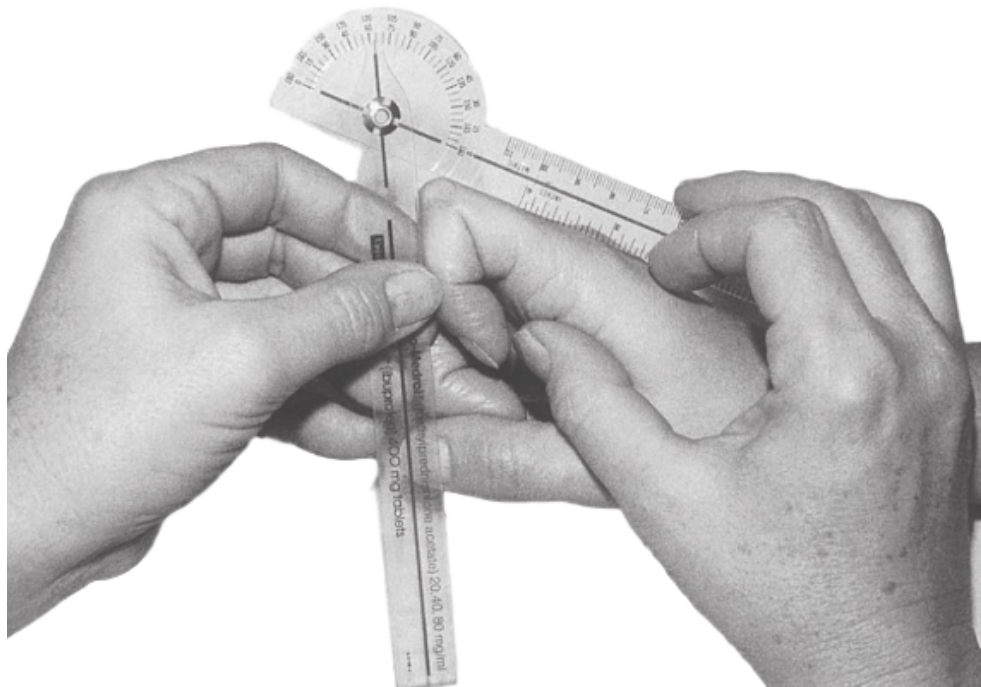


**Figure 1.8: Goniometer**

 *Image depicts the PIP joint being measured. by aligning the proximal goniometer arm over the dorsal midline of the proximal phalange with one hand whilst maintaining the PIP joint in flexion and aligns the distal arm with the dorsal goniometer arm with the other hand [33]*

## 1.7.2 Optical Tracking Systems

Optical tracking involves the use of infrared rays to locate an object in space. Objects that need to be tracked are equipped with retro-reflective markers, which then reflect the incoming rays back to the camera, notifying the system where the object is within space. Optical tracking is efficient when tracking finger joints and their angles [34] since it is capable of gathering its position in 2D, or 3D depending on the number of camera used, and relaying such information in the form of image coordinates with extreme precision. Similar to position, the rotation of the object in space can also be derived by placing multiple markers on the same object. With such configuration, the system is able to correctly develop the object's position and orientation and display it to the user. Active markers contain light emitting diodes (LEDs) that emit their own infrared light requiring a power source from either a battery or the terminal. The infrared rays emitted within the system are invisible to the naked eye, but its intensity is safe within the working environment. Advantages of optical tracking include tracking more than one object simultaneously and its low susceptibly to noise from its surroundings.

## 1.7.3 Electromagnetic Tracking Systems

Commonly used *in-vitro*, electromagnetic trackers function by emitting a magnetic field to its surrounding. Such field is picked up by a transmitter, which can correctly display the tracker's position and orientation with respect to the transmitter's location [35]. Unlike optical tracking, electromagnetic tracking does not require a direct interface between the receiver and the transmitter to correctly locate the receiver in space. Such feature permits its use *in-vitro* or *in-vivo*. Having its own reference frame, the transmitter can record the position and orientation of its subsequent 6 degrees of freedom (DOF) following a Z, Y, X coordinate system (*Figure 1.9)*. The biggest disadvantage of electromagnetic tracking is its high susceptibility to error with the presence of ferromagnetic elements in the surrounding. Such disturbance can affect the performance of the system, degrading its precision quality.
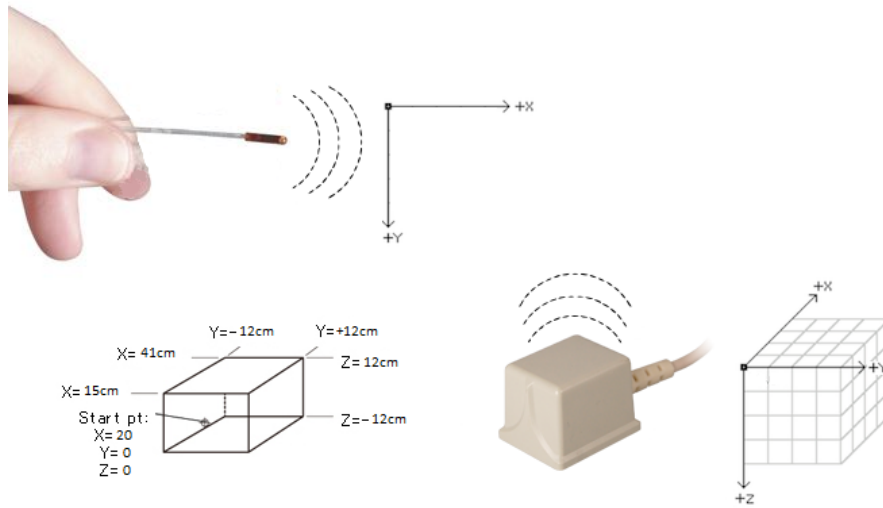
**Figure 1.9: Electromagnetic Tracking System**

*A magnetic field is induced by the EMG sensors (top) (M180, trakSTAR, ON) in three directions (x,y,z) and is translated by a transmitter (bottom right) in order to properly locate and estimate the position of the trackers in 3D space (bottom left) [36]*

## 1.8    State of the Art Designs

For advancement in surgical methods and techniques to ensue, proper understanding of the biomechanics and kinematics is considered crucial for the overall quality of the procedure. In terms of current clinical grounds, very little is known about how the severity of a tendon injury or a pulley rupture negatively affects the kinematics of the finger. Numerous studies in this area of research have been conducted; both *in-vitro* and *in-vivo*, analyzing the effects and changes on the finger joint ROM and tendon loads. There are two types of motion simulations in which these studies were carried under; passive motion and active-motor assist motion. Passive motion involves an external or a system to physically move the joints of the finger through its range of motion with no effort from the patient. Active-motor assistance motion involves the use of a motorized system to achieve flexion of the finger but requires some external help from a surgeon or a system.

### 1.8.1    Passive Motion Simulators

Passive motion of the finger involves the movement of the finger joints along its flexion and extension paths of motion without directly applying forces to the tendons or the use of surrounding muscles to achieve the motion. For instance, having a therapist physically bending and flexing the finger of a patient while the patient's hand is fully at rest is considered passive motion. While passive motion studies are very common in rehabilitation exercises, there are certain limitations to applying external forces to the joints such as accuracy of results and repeatability of motion. As the motion does not involve the engagement of the tendons or the muscles in the forearm, it does not correctly resemble or mimic the anatomical behavior of the hand; varying the end results of the study. Human engagement in the motion of a specimen can also result in unrepeatable movements thus, diminishing the quality of the results. Many rehabilitation exercises that follow post-tendon repair surgeries involve a therapist physically moving the joints of the finger, ensuring the smooth gliding of the tendons along its pathway. Whether performed *in-vivo* or *in-vitro*, most passive motion research studies of the hand are useful in the development of alternative and better configuration to normal synergistic motion in tendon rehabilitation.

Tanaka et al. [37] conducted studies on cadaveric arm specimens with the use of a transducer, optical tracking, and an external fixator (*Figure 1.10)*. Different wrist positions were achieved and optical trackers were attached along the right side of the finger to measure the joint angles. The proximal phalanx was cut at the distal edge of the A2 pulley and

replaced by small cantilever beam transducer, which was secured to the remaining proximal phalanx. Through the use of a suture, the FDP was connected to the transducer and force data was collected. All motions of the finger were passively generated to achieve full flexion and extension of the joints.
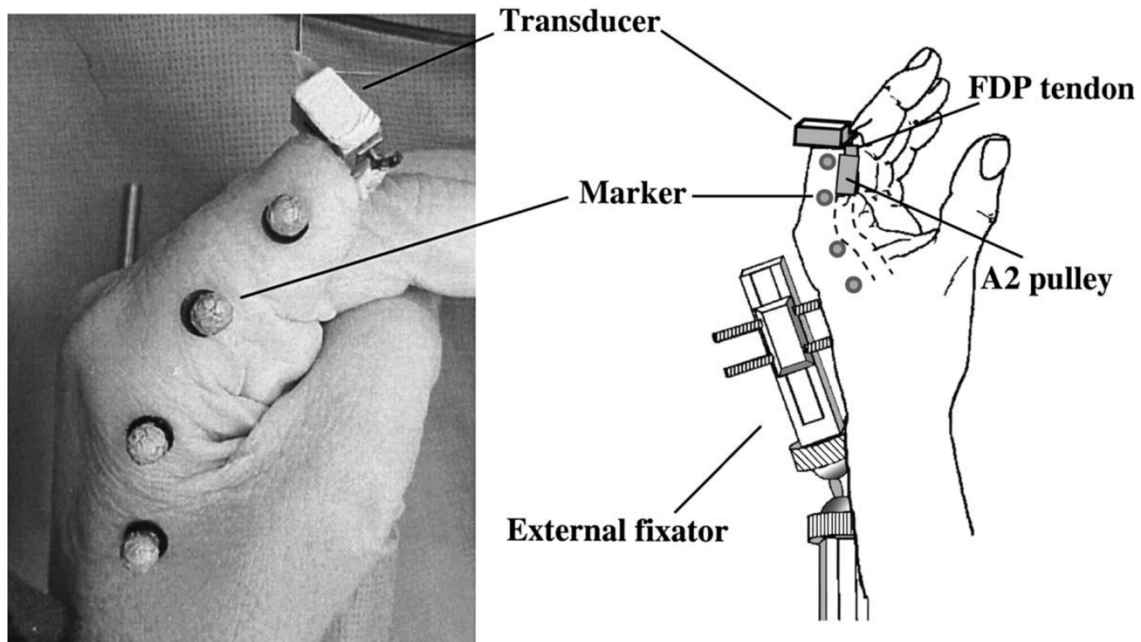


**Figure 1.10: Specimen Preparation**

*Cadaveric specimen setup for testing and measuring loads experienced by the FDP tendon using a transducer and joint angles experienced by the MCP joint using optical trackers [37]*

Human interaction is not the only approach to achieving passive motion of the finger. For example, an actuator attached at the tip of the distal phalanx intended to simulate finger flexion would still be considered passive motion. However, unlike human interface, electrical actuators are considered more accurate as their motions are repeatable and concise with previous motion runs; providing more reliable results. Nonetheless, they are still subjected to errors if the line of action of the force applied is not aligned with the anatomy.

### 1.8.2    Active-Motor Assist Motion Simulators

Active-motor assist is a similar methodological approach to passive motion. However, it incorporates the use of an electrical motor or actuator to help assist the finger on its pathway to full flexion, as opposed to applying an external force to simulate the motion. For example, having a patient exert a small amount of effort through their muscles and tendons to flex their finger joints while a motor manually assists the patient into achieving full flexion is considered an active-motor assist motion. Such simulators are deemed more accurate than passive motion as they incorporate the use of the tissues and the surrounding muscles in the movement of the joints therefore, partially mimicking the anatomy of hand.

Greenwald *et al.* [38] conducted a study on cadaveric hands amputated at the wrist joint and simulated under an active-motor assist system. All specimens were mounted onto a flat base using Kirschner wires, which are smooth stainless-steel pins that are commonly used in orthopedics and other types of medical and veterinary surgery, and the flexor tendon to be tested was sutured to a fixed force transducer for force data collection. A counterweight of 500g was applied onto the extensor tendon of the finger test and the lines of action of both flexor and extensor tendons were parallel to the finger when fully extended. A linear variable differential transformer (LVDT) was used to measure the excursion of the tendon as the finger moved along its flexion path. The platform in which the hand was fixed on was driven along a slide by a screw mechanism powered by a high-torque, variable speed motor (*Figure 1.11)*. Having the motor externally pulling on the hand and the flexor tendon internally pulling on the finger, flexion of the joints was achieved through the assistance of the motor system.
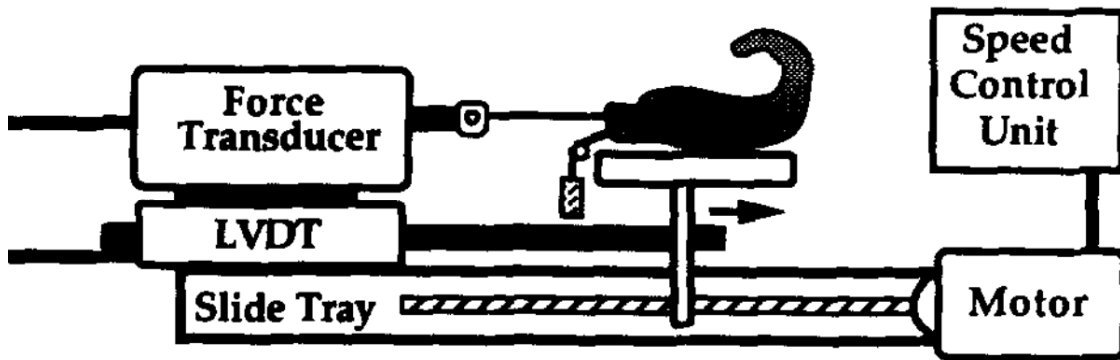
**Figure 1.11: Active Motor-Assist Setup**

*The active motor assist simulator setup from Greenwald et al's study where loads experienced by the flexor tendons were measured using a force transducer while the LVDT measured excursion of the tendon throughout linear motion achieved by a high torque motor [38]*

There are two types of actuators that are commonly used in biomechanics experiments, linear and servo. Both motors serve the same purpose and function however, servo motors are commonly selected as the more favorable choice due to its ability to output position whereas linear actuators tend to lack such feature. Although servo motors are more expensive and require excessive coding and tuning to sync the motor with the simulator, they are useful for measuring tendon excursions and are not subjected to position error.

## 1.9    Thesis Rationale

Research into the development of an accurate and reliable *in-vitro* finger motion simulator to properly mimic true *in-vivo* conditions will provide the means to enhance current clinical methods and procedures towards tendon repairs, pulley reconstructions, and rehabilitation protocols. While advancement in finger simulators have occurred in recent years, as outlined previously, the lack of simulating proper *in-vitro* active motion of the finger joints using a reliable tendon load control feedback loop to mimic true motions remains undone.

The purpose of this thesis is to design and develop a highly reliable and accurate simulator for testing active finger flexion and extension motion while analyzing tendon forces and joint rotations using a load and position controlled feedback loop under the influence of several clinical injury conditions.

## 1.10   Objectives

The primary objective was to develop an *in-vitro* finger motion simulator with closed-loop control of tendon load, and to evaluate its performance. A secondary objective was to use the simulator in cadaveric trials with clinically relevant injury conditions, in order to validate that the simulated biomechanics produce expected results compared to the clinical literature. The third objective was to establish the simulator with known statistical effect sizes and samples sizes, in order to have predictable statistical power for it to be useful in future studies.

## 1.11   Hypotheses

1. Tendon load repeatability will be better than ±5 N.

2. Tendon load control error will not exceed ±2 N.

3. Tendon load statistical effect size will be smaller than 0.5 N.

4. Finger joint ROM statistical effect size will be smaller than 0.5º.

## 1.12  Thesis Overview

The structure of the following chapters is as follows:

**Chapter 2**: Development of active motion simulator, process of PID tuning, and system validation.

**Chapter 3**: Wrist study: Cadaveric study where flexor tendon loads and finger joint ROM are evaluated under different wrist positions and tendon loading conditions. Injury was induced to the extensor tendon to simulate a mallet finger scenario. Load and ROM was compared pre- and post-injury.

**Chapter 4**: Pulley Study: Cadaveric study where the A2 and A4 pulleys are excised to observe the effects of sequential cuts on tendon load and joint ROM. Reconstruction of pulleys to regain intact state of the finger at different wrist positions.

**Chapter 5**: Summary, conclusions, and future work.

# Chapter 2

## 2 Development of a Finger Active Motion Simulator

*OVERVIEW: This chapter covers the design processes and steps taken to develop an active motion finger simulator that can achieve full flexion/extension of the finger joints. Load cell calibration and proper PID tuning was achieved to produce a more accurate and repeatable system. Using different performance tests, a comparative force analysis within the tendons at different velocities was conducted. In addition, repeatability trials between runs were tested to further validate the performance and reliability of the system.*

## 2.1 Introduction

*In-vitro* motion simulators can provide basic science biomechanics data and clinically relevant evaluations of surgical procedures, which can be translated into patient care. Although *in-vitro* passive motion studies are more common, due to their simplicity, they lack the intrinsic musculoskeletal forces that are characterized by *in-vivo* motion. One of the most critical drawbacks of passive motion simulators is their low repeatability, due to the limb being moved manually by an operator. When passively handling a limb or joint, the pathway in which the motion is simulated is poorly replicated.

Within the hand, all forces applied internally along the tendons should remain true to its accurate line of action and each tendon should be simulated individually based on its function and insertion point. Yang et al. [39] developed an *in-vitro* passive system that involves the manual manipulation of flexor tendons within cadaveric hand specimens amputated slightly proximal to the wrist. An external fixator was attached to the radius on one end and the metacarpals on the other end. This fixed the cadaveric specimens in the neutral position. The proximal ends of the FDS and FDP tendons were looped and linked through a mechanical pulley. This pulley system allowed for the tendons to balance through different excursion changes as forces were applied manually through human manipulation. A 25-lb load cell was connected to the mechanical pulley to record the acquired force and a 200g weight was applied to the extensor tendons to maintain full extension of the finger at rest. The system was capable of achieving full flexion of the fingers but there was no guarantee that successive trials would follow the same motion trajectory or loads within the tendons due to manual simulation of motion.

To correctly model a system that is capable of simulating full ranges of finger joint motion under *in-vitro* conditions, a synchronized and reliable simulator that runs solely by active motion to limit the errors associated with passive motion must be devised. Therefore, the objective of this study is to develop a more advanced simulator that is capable of achieving proper and accurate motion of the finger with the use of a well synchronized and tuned force and position feedback actuator system and model. With the use of actuators or motors within a system, desired flexion and extension motions can be achieved and mimicked in a highly precise and repeatable manner; resulting in more reliable and desirable outcomes.

## 2.2    Pilot Study

A pilot study using cadaveric specimens was conducted to determine ranges of tendon loads and excursion. This data would later be used to design the active motion simulator.

### 2.2.1    Specimen Preparation and Methods

Cadaveric specimens (age: 70±10.4 years; sex: 2 females, 3 males) were amputated through the midline of wrist joint and were firmly secured onto the base. To ensure further stability within the hand, 2.5 mm K-wires were inserted through all four metacarpals and a 600g mass hanging over a mechanical pulley was secured to the end of the extensor tendon as a counterforce. With the use of single degree of freedom (1DOF) in-line load cells (MDN 34, Honeywell, OH) and optical tracking, tendon forces, excursion, and joint ranges of motion data was collected for analysis. 0-braided Vicryl (ETHICON®) suture were used to suture each flexor tendon to an individual load cell that was firmly mounted onto handles (*Figure 2.1)*
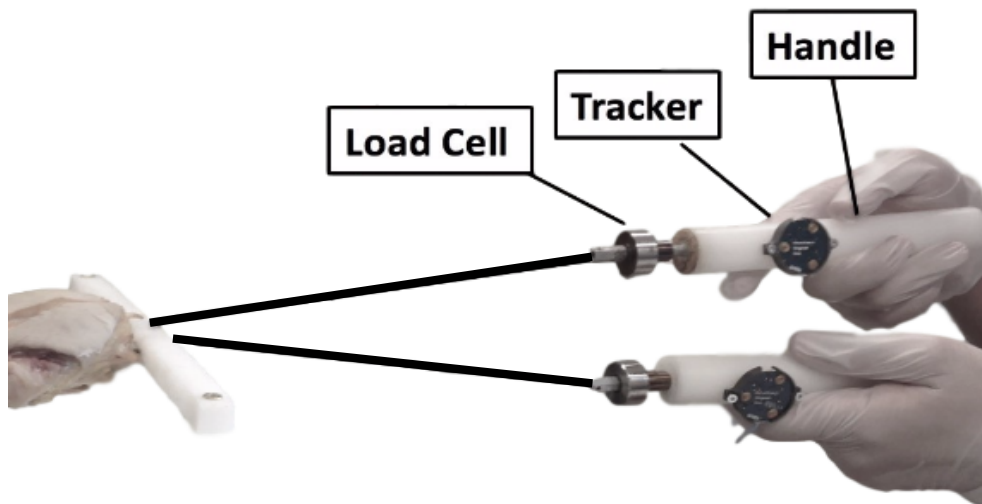


**Figure 2.1: Pilot Study Setup**

*The load cells are used to record forces within the tendons and trackers are used to record tendon excursion*

Range of motion (ROM) and tendon excursion data was collected through an optical tracking system. As explained in chapter one (section 1.5.2), a camera was used to detect seven trackers within space. Four of the seven trackers gathered ROM data while the other three collected tendon excursion data. To properly evaluate the ROM of the DIP, PIP, and MCP joints, each tracker was firmly mounted onto the finger bone segments, distal to the joint of interest (*Figure 2.2a*). The fourth tracker however was mounted to one of the static metacarpal bones and used as a fixed frame of reference for the remaining trackers to rotate about. Due to the size of the trackers, aluminum plates of various dimensions were used to isolate each tracker and ensure that no contact between the trackers is established during flexion (*Figure 2.2b*).
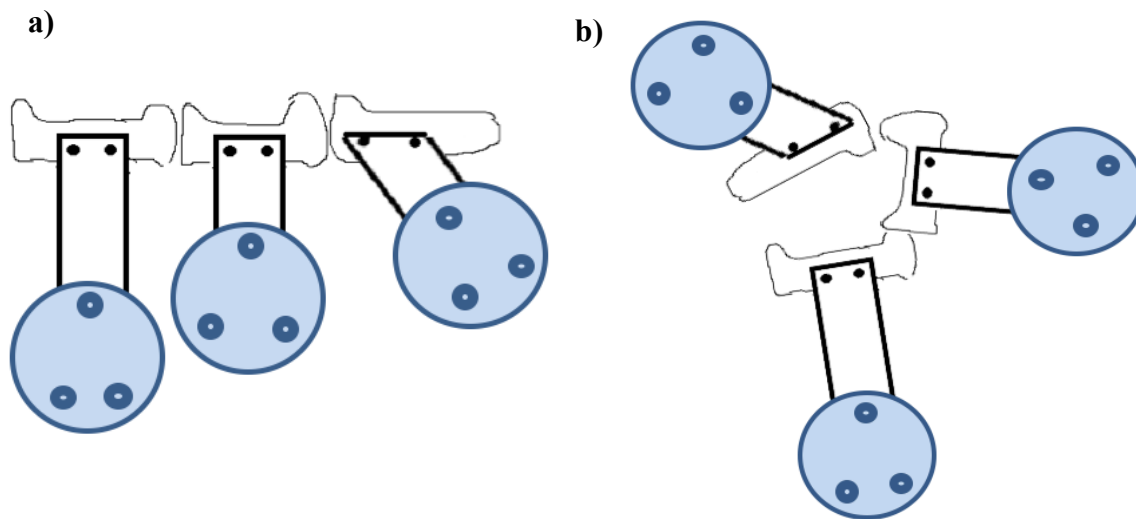


**Figure 2.2: Optical Trackers**

*Arrangement of the optical trackers on the finger segments where a) represents the finger in the neutral position and b) when fully flexed showing the arrangement of trackers and their different orientations along the finger.*

The remaining three trackers were used to measure overall excursion of the tendon. Two trackers were mounted onto the handles (*Figure 2.1*) and the third was on the 600g mass hanging over the

pulley. With such distribution, the overall maximum distance travelled by the flexor and extensor tendons were recorded and analyzed.

## 2.2.2    Results

The average peak force experienced within the tendon was 15N with forces as high as 20N. Excursions within the tendons ranged between 43mm and 50mm, with an overall average of 45mm. The average range of motion of the DIP, PIP, and MCP joints were 65º, 135º, and 60º respectively.

## 2.2.3    Discussion

The increase in peak load experienced by the tendon was mainly due to human error. Since the flexor tendons were manually simulated using muscle force, it is very likely that varying forces were applied within the suture line between trials, thus, increasing chances of irregularities within the data. Nonetheless, such results gave a better understanding on the limitations of the tendon in terms of the maximum forces required to achieve full flexion of the finger (20N). In regard to excursion and ROM of joints, data obtained were consistent between trial runs and more significantly, within literature [40]–[42]. Although optical tracking is known for its accuracy and reliability, the weight of the individual trackers triggered as a significant limitation. It was hypothesized that the weight applied onto the finger segments could have contributed to the rotation of the finger joints by passively flexing the joint past 90 degrees; jeopardizing the integrity of the study.

## 2.2.4    Conclusion

The results obtained from this study were of great significance as they provided data and insight on the true motion of the joints and the loads associated with the movement of the finger. All data collected was strongly taken into consideration when selecting material properties for the new active motion simulator.

## 2.3    Design of the Active Motion Simulator

### 2.3.1    Simulator Components

A computer tomography (CT) compatible simulator was constructed through CAD software (SolidWorks®, MA) to successfully achieve active flexion and extension of a finger at various wrist position (*Figure 2.3*). The simulator is comprised of two main components: a front base and a back base. The front base is the site where the cadaveric specimen is fixed and maintained, whereas the back base held most of the mechanical and electrical components of the system.
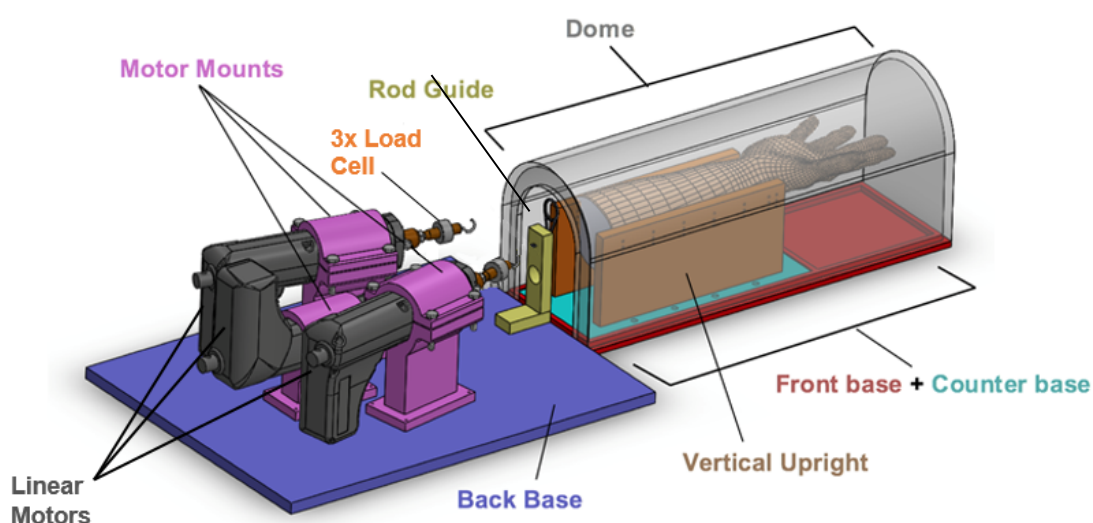


**Figure 2.3: Simulator Assembly**

*Full assembly of the active motion simulator viewing the different structural components that make up the system*

#### 2.3.1.1    Front Base

Designed from a combination of Delrin® (DuPont) and acrylic, four different components were used to develop the front base; a main platform, rigid vertical uprights, and an enclosing dome. Each component served a different purpose within the system. An acrylic platform was designed and constructed to serve the purpose of enclosing all of its sub components within its parameters. Dimensions selected for the base were chosen based on the average size of the hand, for both

sexes to ensure that all soft tissue was constrained within the chosen size of the base. Two vertical uprights, mounted to a counter-base were used to rigidly fix the cadaver onto the platform. Brass screws were inserted horizontally along the midline of the arm through the ulna and radius; ensuring proper fixation of the specimen during testing. This sub-component sat perfectly flushed within the main platform.

To guarantee that the cadaveric specimen is contained within the system, an acrylic dome was used to enclose the perimeters of the front base. The dome allowed for the manipulation of full finger movement at different wrist positions without the risk of obstruction.

## 2.3.1.2    Back Base

As the site of motion control, the back base contained most of the mechanical and electrical components of the simulator. Other than the technical aspect of the system, the back base was made up of three different components; the base itself, three 3D print motor mounts, and a suture guide rail. To secure and stabilize each motion actuator in position, 3D custom-made motor mounts were developed and built from Acrylonitrile-Butadiene-Styrene (ABS) sheets (*Figure 2.4)*. The motor mounts were designed specifically to allow each motor to sit comfortably and rigidly without the possibility of free motion within the enclosure. Since extensor tendons are only accessible at a lower elevation when a specimen is rigidly fixed in a neutral-palmar orientation, one of the three motor mounts designed varied in elevation in order to maintain the appropriate anatomical lines of actions of the tendons. The mount designed for the extensor motor was shorter in height in comparison to the two-flexor motor mounts.
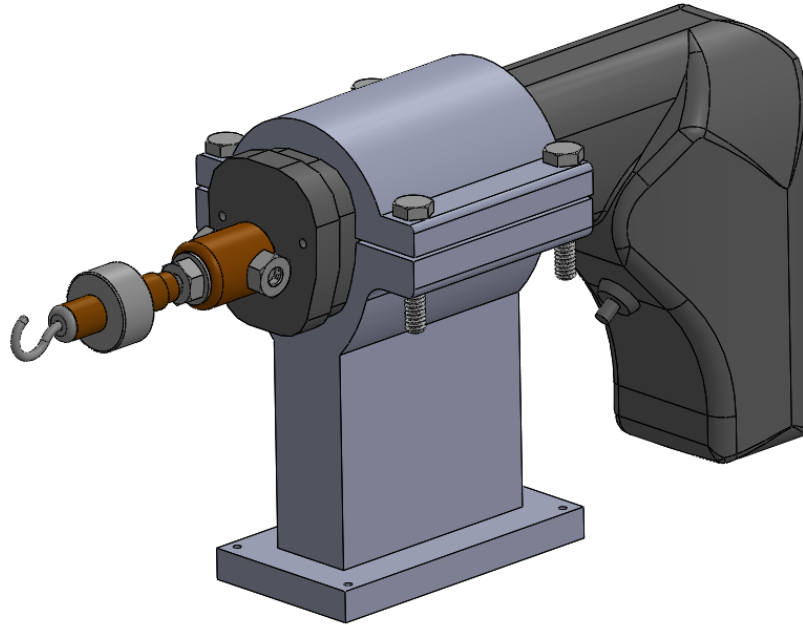
**Figure 2.4: Motor Mounts**

*Flexor mount holding one of two flexor motors*

To allow for motion to occur within the finger, forces within the three long tendons; flexor digitorum profundus (FDP), flexor digitorum superficialis (FDS), and the extensor tendon (ET) are required as mentioned in Chapter 1 (Sections 1.3.2, 1.3.3, and 1.3.4). For such forces to be applied, three 12V linear motion servo actuators (E050, Thomson Linear, TX) were used each with a stroke length of 4 inches; long enough to fulfill full flexion requirements based on the data collected from the pilot study. They also are equipped with a 10kΩ potentiometer to allow for accurate position feedback control. Such feature within the actuator permitted ease of monitoring excursions, as the position of the stroke along its pathway is constantly being read and recorded throughout each finger flexion run. All three motors were fitted into their corresponding 3D printed motor mounts and then rested onto the back base of the simulator using brass screws to correctly position and fix each motor mount in place. 0-Braided Vicryl (ETHICON®) sutures were used to connect the tendons from the forearm to their analogous motor and all controls were synced and driven through a LabVIEW interface software. Proper PID tuning of the controllers was necessary for outputting positive and reliable results between motions. Three 1DOF 25lbs in-line load cells (MDN 34, Honeywell, OH) were rigidly fixed onto the tip of each actuator's

shaft, or stroke, using custom designed fitted caps. All load cells were properly calibrated using the NI SCXI software for accurate force feedback data collection and were connected to a LabVIEW program where they were read and collected. Lastly, a rod guide was used to direct the suture line travelling from the ends of the tendons to the actuators, along its true line of action. As a result, the simulator more closely resembles the anatomical behaviour and properties of the tendons in the forearm as all lines of actions were maintained within the system. The use of a fishing rod guide proved beneficial by minimizing any frictional forces experienced by the suture line as it passes through the channel. Such properties allow for a smoother pathway of motion at the end effector, increasing the quality of the results obtained. The rod guide consists of an L-shaped bracket with a rod guide channel mounted at the top for the flexor tendons, and a lower circular cut out within the bracket for the extensor tendons.

## 2.3.2    Electromagnetic Tracker Installation

As discovered during the pilot study, optical trackers were found to be too bulky and heavy compared to the weight of the fingers. Consequently, to overcome this limitation, 2mm electromagnetic trackers were used instead to collect joint ROM. To install the trackers, incisions were made along the side of the finger to expose the different bone segments of interest. Pilot holes (2.1mm) were then drilled at approximately the center of each phalange and trackers were inserted laterally into each hole using a friction fit (*Figure 2.5*). The thickness of the holes ensured that each tracker sat flushed within the bone, restricting it from moving in place.
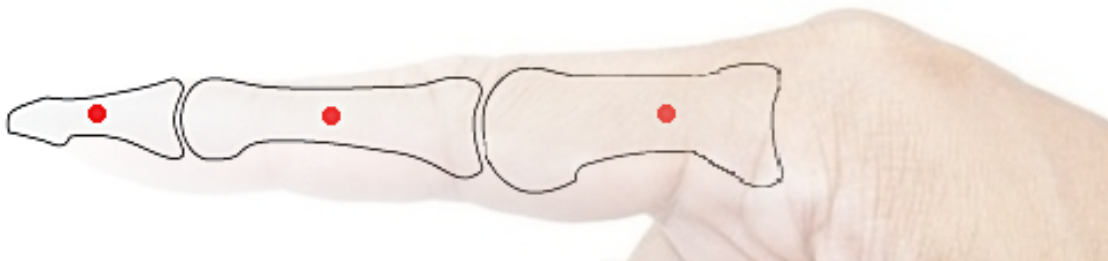


**Figure 2.5: Electromagnetic Tracker Installation**

*Finger diagram illustrating the location of the trackers' insertion points within bone*

## 2.3.3    Software Development

## 2.3.3.1    Closed Loop Tendon Load Controller

A Proportional-Integral-Derivative (PID) control scheme (*Figure 2.6*) was utilized for its easy implementation and straight forward tuning methods. Such feedback loop is capable of achieving both load and position control. Load control is attained by using a set target load and the position of the piston along the shaft as input to the controller; allowing the system to then output a relative step value that is fed to the motor to compensate for any errors experienced in load.
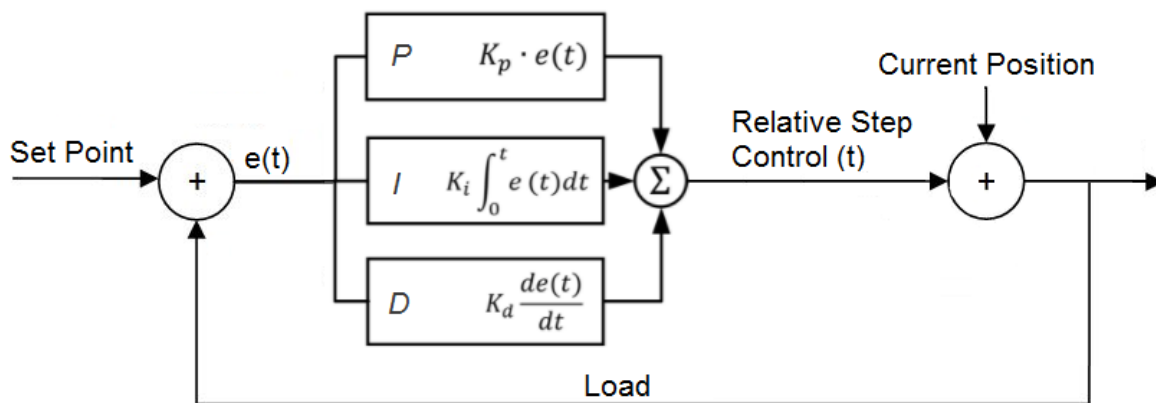


**Figure 2.6: Closed Loop PID Schematic**

*PID controller system to achieve and maintain target loads using a negative feedback loop*

However, there are two common approaches in which a controller can output position commands: absolute-time or relative-time conditions. The significant difference between both conditions is the lack of proper communication between the controller and actuator. The biggest drawback of absolute-time condition is that the output of the PID is based solely on the force signal outputted by the load cell, resulting in absolute position commands that are constantly sent to the actuator without proper knowledge of where the actuator currently is within its pathway. Relative-time however, has the ability to send position commands to its actuator, relative to the current position that is constantly being inputted through the position feedback feature of the actuator, along with the force signal obtained from the load cells. This is achieved by having the LabVIEW software constantly requesting for the actuator's current position, and feeding it to the

controller as an input signal (*Figure 2.7)*. Once the position of the actuator is supplied, the resultant PID output would calculate a command based on the force data from the load cell and then adding the command output to the actuator's current position as the new target position. For instance, assuming that the PID output range was manually selected to fall between -50 to 50, the target load was set to 5N, and the current position of the motor is at 250 (0 representing full retraction and 1000 representing full extension as previously mentioned).

 In the case where the target load has not been reached yet, based on the tuning of the PID, the controller would calculate the appropriate position that allows for the forces to settle around the target load goal, and then add the computed value to the current position value of the motor (250 + (-50) = 200). Once the motor reaches its new position, the PID controller would then constantly check the system to see if the target load has been achieved. In cases where it fails, the controller would then re-compute a new command value and the process would continue until the target load is reached and the system is stable. This approach is deemed far more accurate than the absolute condition as errors such as overshoot and settling time are better maintained and corrected.
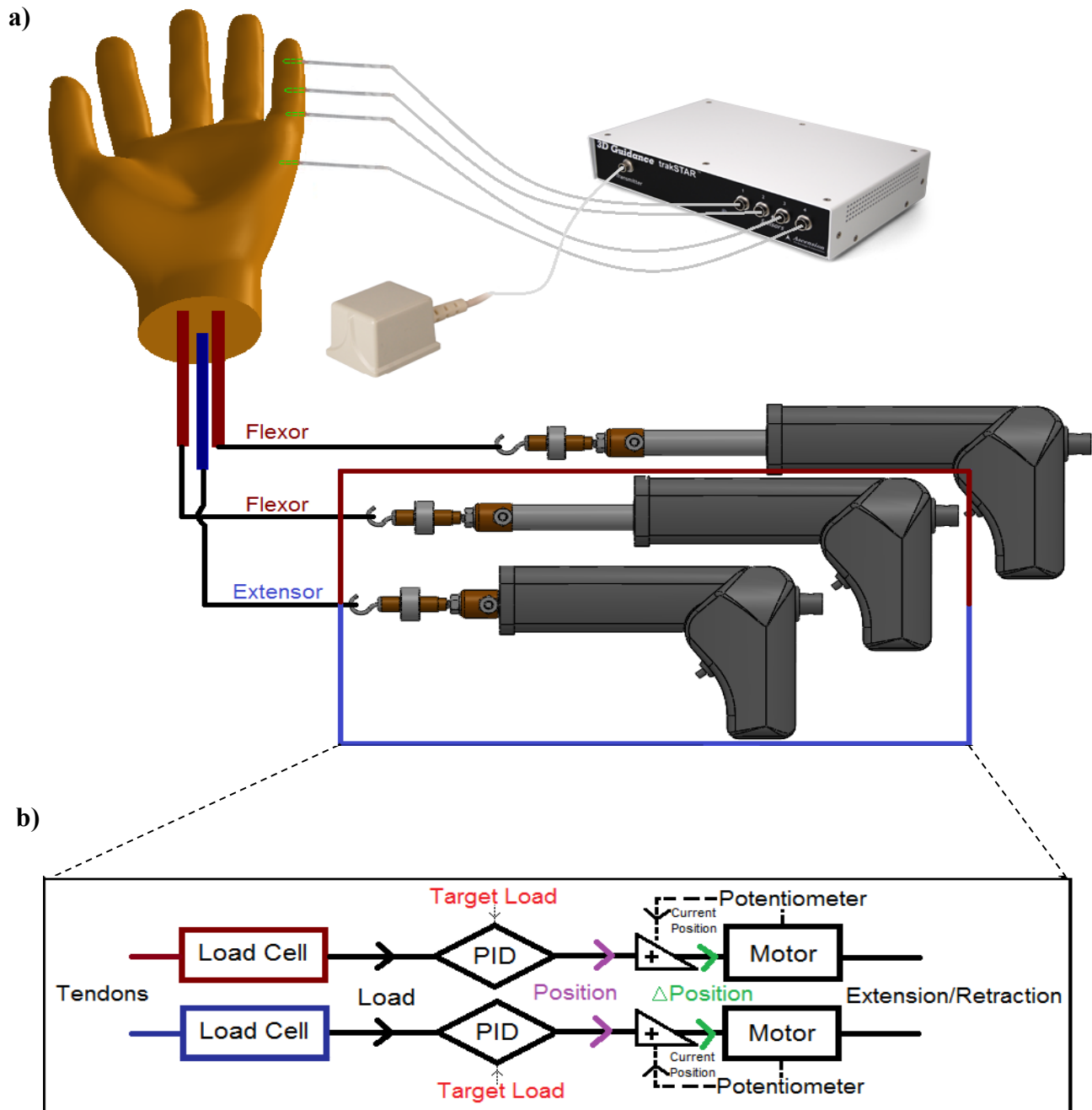
**Figure 2.7: Experimental Setup and System Flowchart**

*Design setup of the system demonstrating a) the application/wiring of the EMG (M180, trakSTAR, ON) tracking system and b) the layout of the flexor (red) and extensor (blue) motors with a detailed flow chart illustrating the function of the system*

## 2.4 Tuning and Validating the Simulator's Performance

A quarter amplitude damping (QAD) tuning process was used to efficiently eliminate any errors between the target load and the load measured by the load. The controller was designed to respond quickly to changes with little-to-no overshooting and a smaller settling time [43]. The steps taken to validate the performance of the system and ensure that the PID is well tuned for its objective involved multiple strain tests on the load cell using a spring, a pulley system, and a cadaveric finger. All three simulations involved the use of the force and position feedback feature of the system to output repeatable and reliable data that can be used to validation the quality and performance of the simulator. An operating range was set within the LabVIEW program to allow for an acceptable ±2N range in which the PID can safely stabilize within. Application of such dead band within the system increases the precision and reliability of the data being outputted by the controller throughout performance trials.

### 2.4.1 Spring Mechanism

The first setup involved the use of an extension spring (k=2.83N/mm) attached to a rigid body on one end and directly connected to an actuator on the other end through a suture. A target load was manually set and the PID controller would output a desired position command to the motor to attempt to reach the target load within minimal error. This was attained by feeding the PID set-point a static or dynamic load value, whether through a step response graph or a sinusoidal curve, and observing the behaviour of the motor in regard to achieving the set load within minimal error.

The step response diagram ranged from 0N to 15N with 5N increments while the sinusoidal curve ranged from 5N to 15N with 5N amplitude. Each trial was run three times for repeatability measures and all force data was collected and plotted accordingly. Although a spring does not fully mimic the elastic properties of a tendon, it allows the motors to be tuned in a way that at least closely resembles the tuning required when a tendon is applied.

## 2.4.2   Pulley Mechanism

The purpose of this setup was to evaluate the performance of the PID controller after incorporating a control algorithm that regulates the extensor motor's operating parameters when trying to maintain a set load against a dynamic antagonistic force. With such algorithm, the system is ensured to never result in a state of tug of war between both motors when flexion or extension is conducted. The set up involved the use of a mechanical pulley and two motors, an extensor motor and a flexor motor with their corresponding load cells. Both motors were connected to one another through a 0-braided Vicryl (ETHICON®) suture line over a frictionless pulley system. Run under position control, the flexor motor was ordered to retract to a specific position set by the user; increasing the tension within the cable and evidently forcing the PID controller to extend the extensor motor forward to compensate for the increase in load. An increase in error between the target load and the load measured is directly proportional to an increase in the motor's speed and sensitivity; ensuring that the target load is constantly maintained throughout the motion of the antagonistic force. This system was evaluated under set target loads of 5N, 10N, and 15N on the extensor motor.

## 2.4.3   In-vitro Test

This performance experiment was conducted on the fifth finger digit, or the pinky finger, of a freshly frozen cadaver specimen amputated at mid-forearm (64 years, male) and attached to the simulator via the vertical uprights. A foam block was used to support and maintain the wrist in the neutral position. The flexor and extensor tendons of the pinky finger were individually isolated and 0-braided Vicryl (ETHICON®) sutures were used to suture the ends of the tendons (*Figure 2.8)*. To avoid the possibility of tissue desiccation, all soft tissue within the forearm was left intact. All sutures were passed under the skin and each tendon was connected to its corresponding motor though the rod guide; maintaining their true and proper lines of action. Similar to the pulley test protocol, the *in-vivo* test involved the use of both types of motors, the flexor and the extensor motors. The distance traveled by the flexor motors during motion allowed for full flexion of the finger to occur and extensor motors slowly followed the path of the flexors while attempting to maintain loads of 5N, 10N and 15N. All motion trials were

performed through the full range of flexion-extension of the finger at velocities of 0.5in/s, 0.6in/s and 0.8in/s.
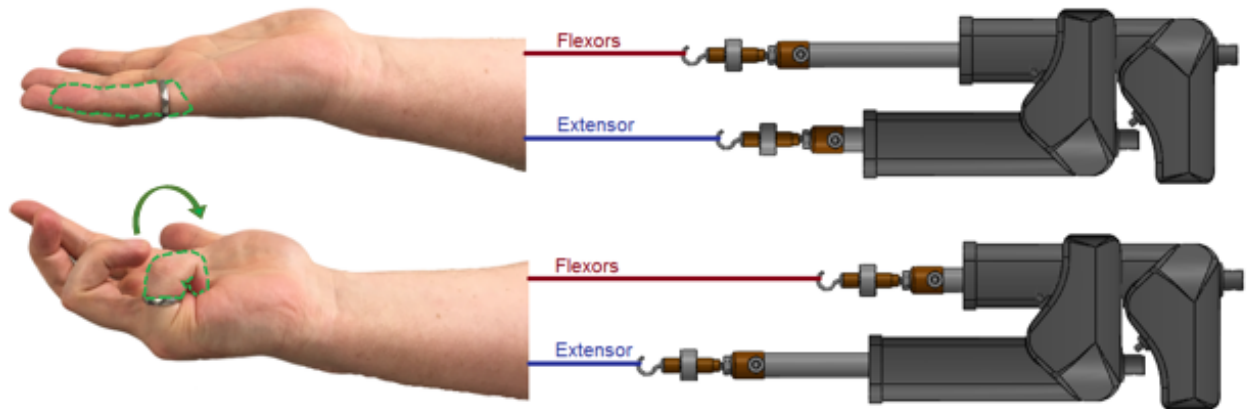


**Figure 2.8:** *In-Vitro* **Test Setup**

*The setup of the performance test illustrating the flexor motors in red and the extensor motors in blue*

## 2.5   Results

### 2.5.1     Step Response Test

The root means square error (RMSE) in load before tuning of the PID was as high as 3.71 N while the error after proper tuning of the PID was as low as 0.38N (*Figure 2.9*). Within the velocity tests conducted, the average RMSE when the motors were travelling at 0.8in/s (*Figure 2.10*), 0.6in/s (*Figure2.11*) and 0.5in/s (*Figure 2.12*) were 1.3 N, 1.0 N, and 1.1 N respectively. Repeatability of the simulator travelling at 0.8in/s, 0.6in/s and 0.5in/s were 0.5 N, 0.6 N, and 0.6 N respectively.
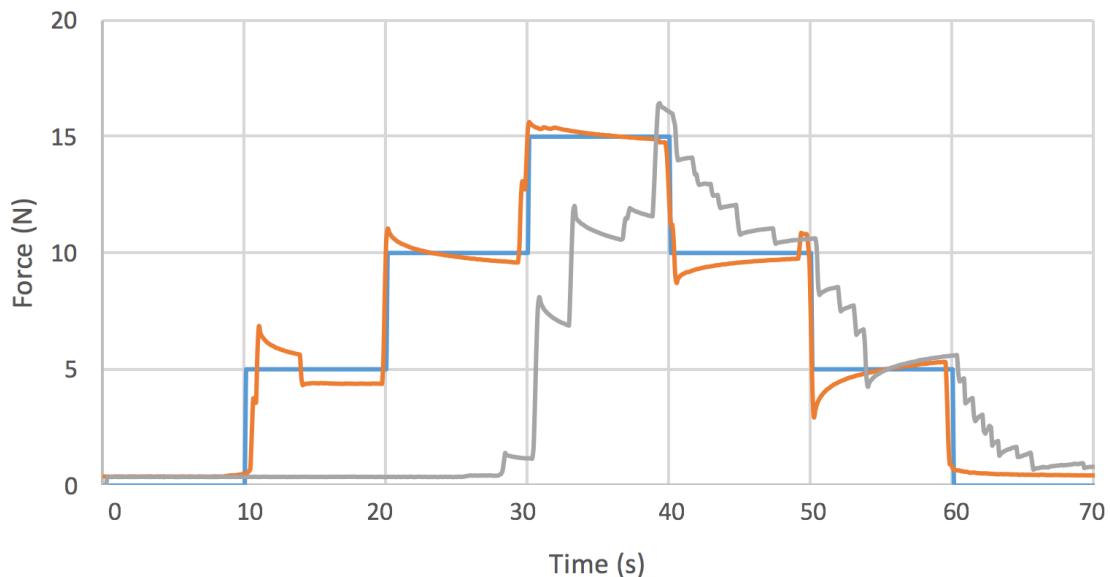


**Figure 2.9: Pre vs. Post Tuning of PID**

*The plot above demonstrates the behaviour of the PID controller when attempting to follow a step response graph (blue) before proper tuning (grey) [k=0.1, I=0.01, d=0.1] and after tuning (orange) [k=1.2, I=0.001, d=0.005]*
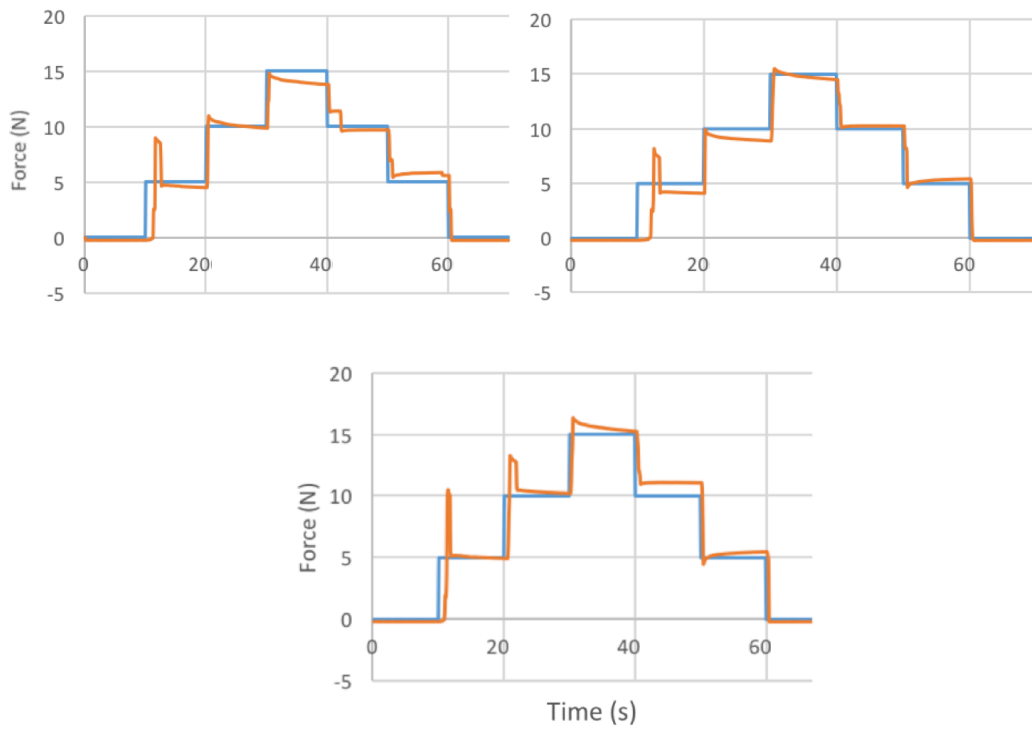
**Figure 2.10: Step Response Test (0.8in/s)**
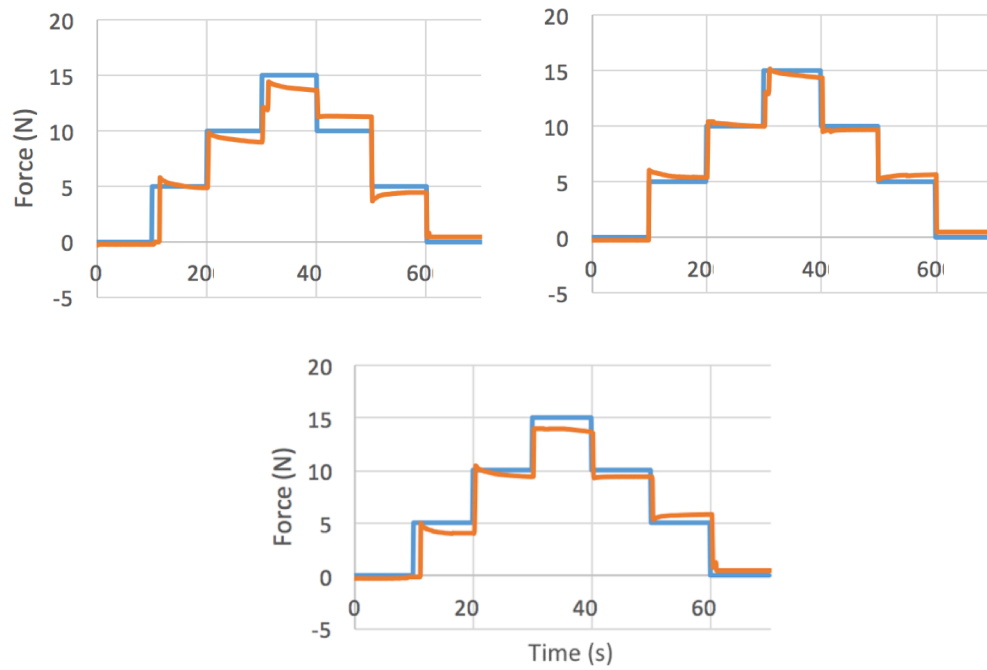


**Figure 2.11: Step Response Test (0.6in/s)**
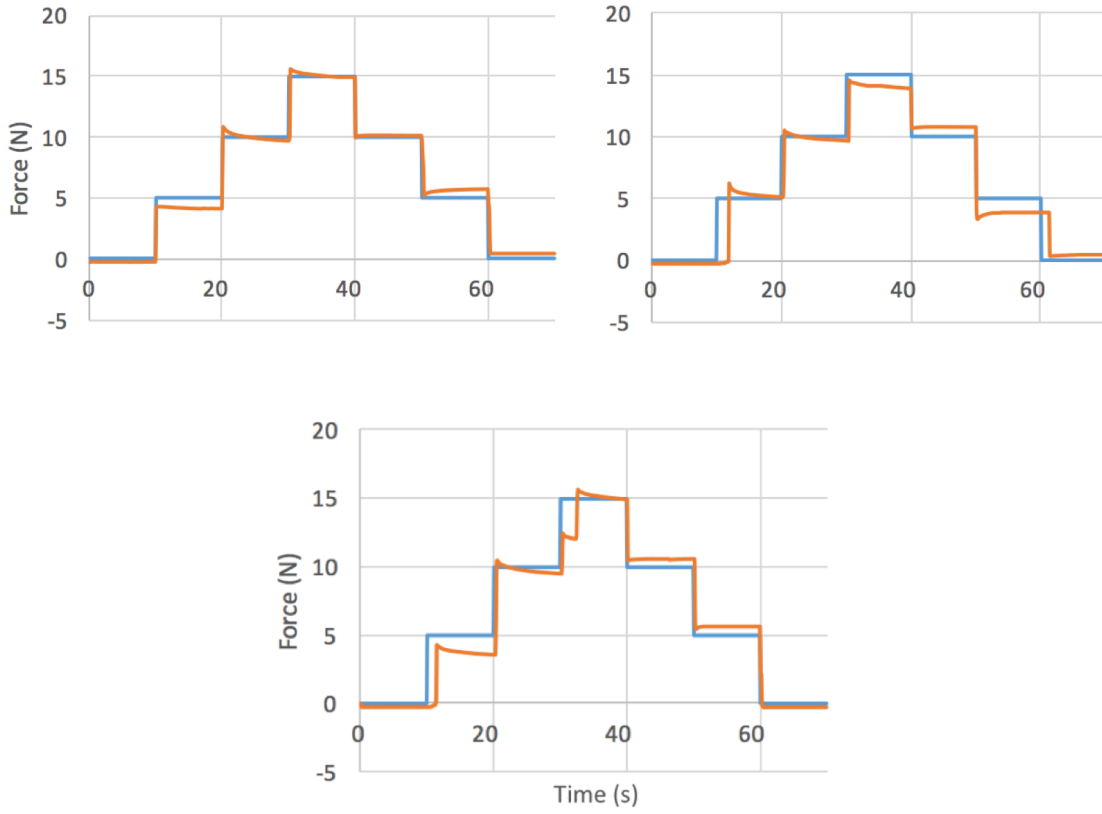
**Figure 2.12: Step Response Test (0.5in/s)**

## 2.5.2    Sinusoidal Curve Test

Within the velocity tests conducted, the average RMSE when the motors were travelling at 0.8in/s (*Figure 2.13)*, 0.6in/s (*Figure 2.14)* and 0.5in/s (*Figure 2.15)* were 1.9 N, 1.6 N, and 1.6 N respectively. Repeatability of the simulator travelling at 0.8in/s, 0.6in/s and 0.5in/s were 1.4 N, 0.9 N, and 1.0 N respectively. All PID metrics were kept constant with the calibrated values derived during the step response test.
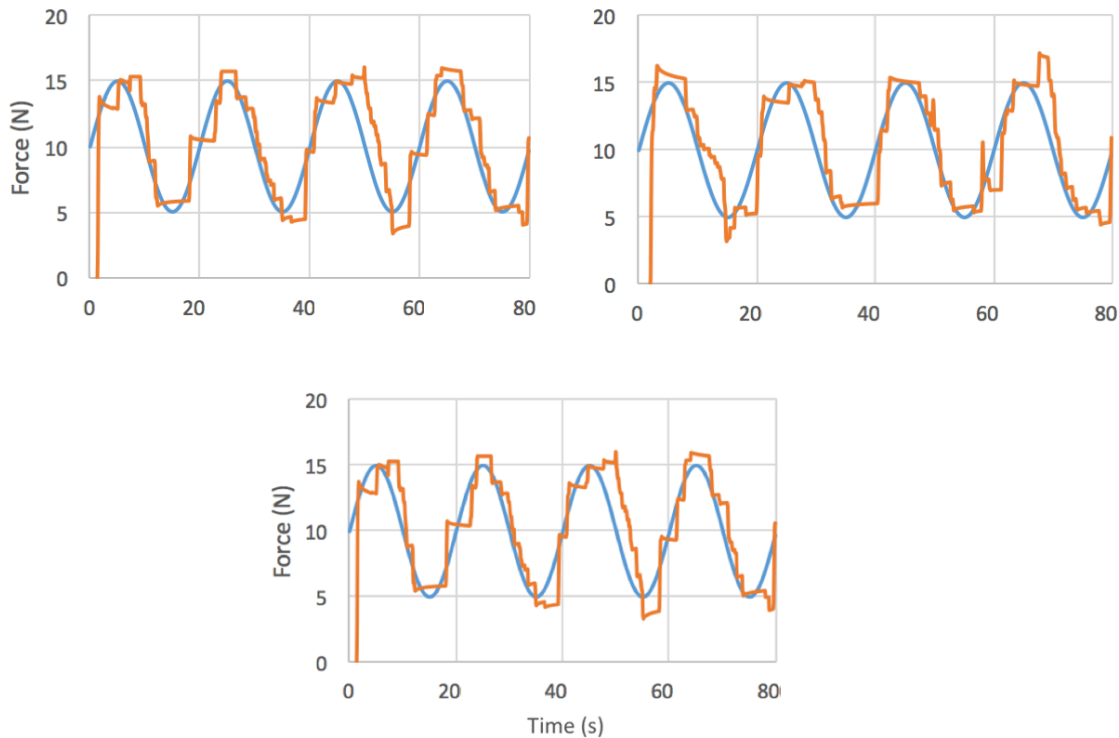


**Figure 2.13: Sinusoidal Curve Test (0.8in/s)**

*All plots illustrated above were run at 0.8in/s. The three plots demonstrate the behaviour of the PID controller (orange) when attempting to follow a sine curve (blue)*
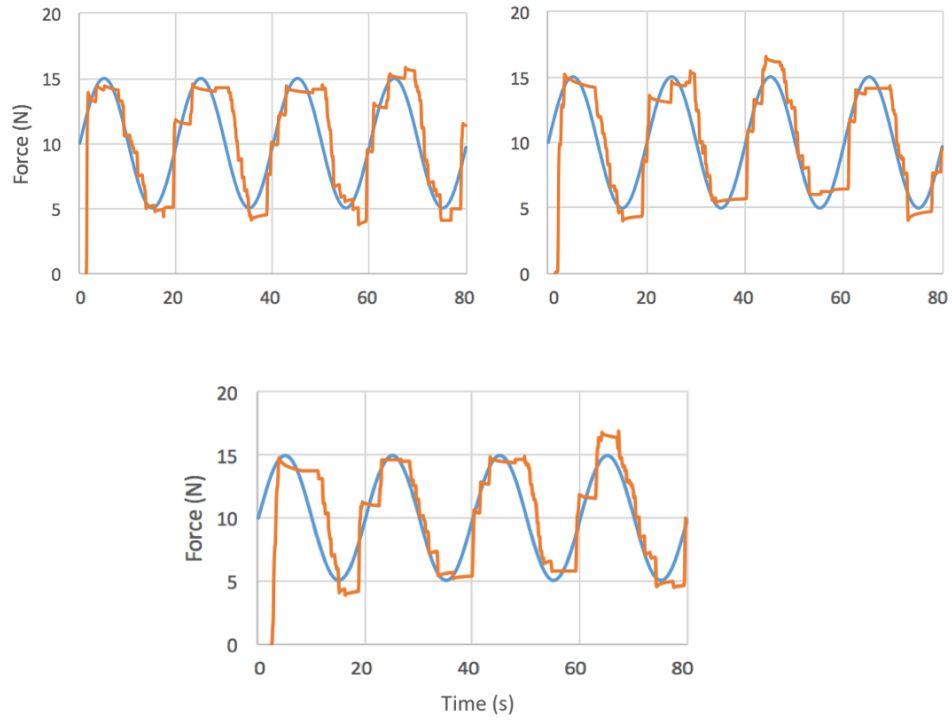
**Figure 2.14: Sinusoidal Curve Test (0.6in/s)**
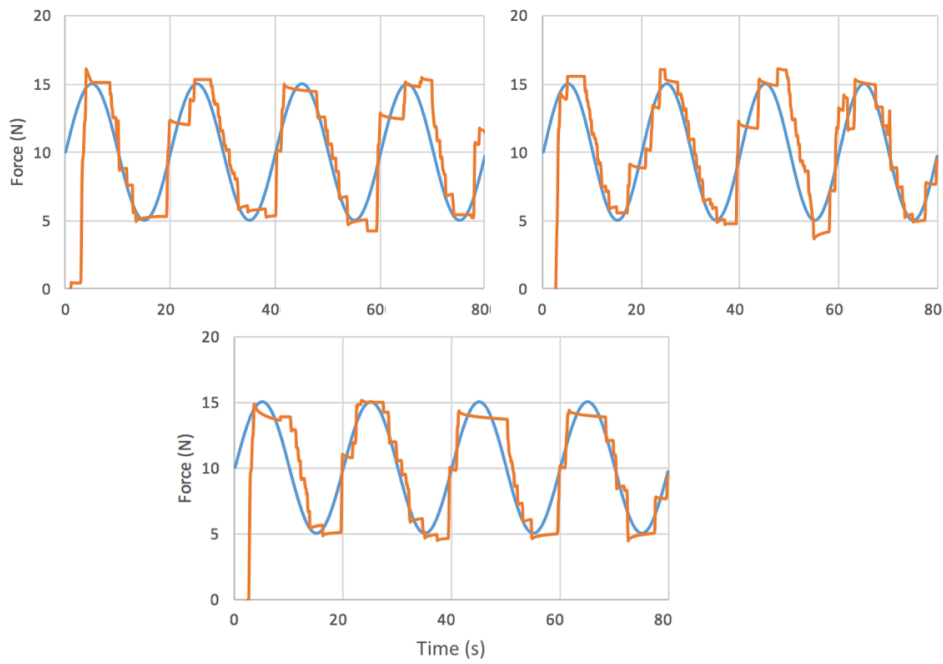


**Figure 2.15: Sinusoidal Curve Test (0.5in/s)**

### 2.5.3 Antagonist Model Performance

Using the antagonist pulley model, the RMS errors were 1.6, 1.3 and 1.2 N with simulated extensor loads of 5, 10 and 15 N, respectively (*Figure 2.16*).
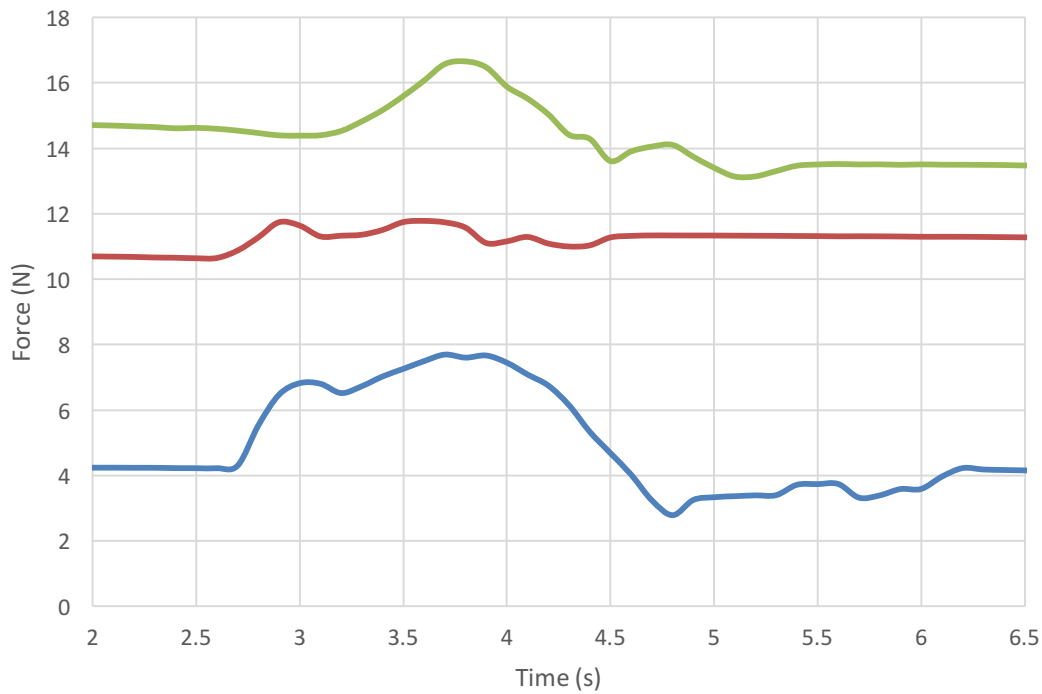


**Figure 2.16: Antagonist Performance Test**

*These graphs demonstrate the performance of the PID controller when attempting to maintain a constant load of 5N (blue), 10N (orange), and 15N (grey) within a 50mm excursion against an antagonistic force*

## 2.5.4    In-vitro Test

Performance results from the cadaveric test are illustrated below. Three different extensor loads were maintained throughout the test. The RMSE when the extensor target load is at 5N, 10N and 15N are 2.2N, 1.5N, and 2.1N respectively (*Figure 2.17*).
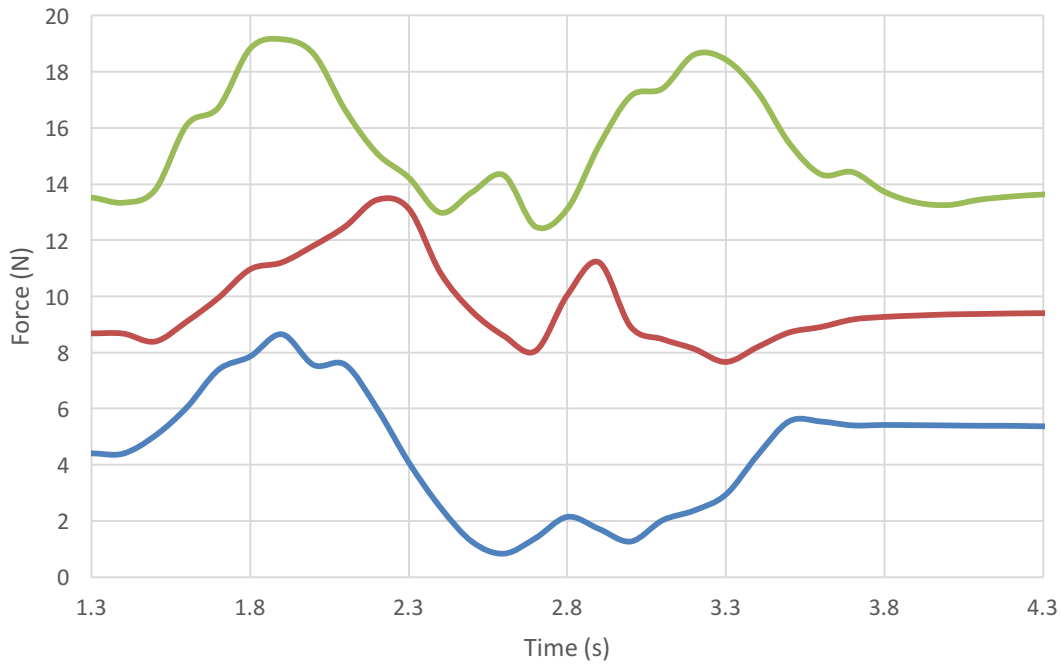


**Figure 2.17:** *In-vitro* **Performance Test**

*These graphs demonstrate the performance of the PID controller when attempting to maintain a constant load of 5N (blue), 10N (orange), and 15N (grey) within the tendons of a cadaveric specimen*

## 2.6   Discussion

Based on the step and sine performance tests conducted, there appears to be an increase in overshoot of the system as speed is amplified; negatively affecting the performance of the controller. However, the repeatability of the simulator managed to lie within the ±5N error hypothesized in Chapter 1 (Section 1.9). The increase in the repeatability of the motion trials provides a clear indication of the benefits to using active manipulation methods to achieve motion. In addition, the PID managed to correctly stabilize a target load within a ±2N error during the step response, sinusoidal response and the antagonist performance test; further validating the performance of the simulator. Some of the results obtained within the in-vitro test however surpassed the threshold error set by 0.1N - 0.2N. Although the errors obtained were slightly higher than what was initially aimed for, this excess in error was considered not large enough to signify a compromise in the simulator's performance.

## 2.7   Conclusions

Performance evaluations showed that the accuracy and repeatability of the PID controller was within acceptable ranges of error. Thus, the finger motion system was suitable for further *in-vitro* motion biomechanics studies.

# Chapter 3

## 3 Effect of Wrist Position and Distal Extensor Rupture on Finger Kinematics and Tendon Loads: An In-Vitro Study

*OVERVIEW: This chapter presents an in-vitro study conducted using two cadaveric upper limb specimens (4 fingers) under varying extensor loads, different wrist positions, and a simulated injury to the extensor tendon, which can lead to a 'mallet finger' deformity. Repeatability tests were also conducted to further validate the performance of the active motion simulator (developed in chapter 2).*

## 3.1 Introduction

### 3.1.1 Literature Review

According to current literature on wrist biomechanics, varying wrist positions can have a clinically significant effect on the finger kinematics and tendon loads required to achieved full flexion. Several in-vivo wrist studies have evaluated the maximum power grip strength at different wrist positions, as opposed to individual finger loads. Li *et al.* [44] and Lee *et al.* [45] both conducted active motion tests on healthy subjects in-vivo to assess the effect of wrist position on the maximum grip force achievable. Li *et al.* reported the effects of both wrist flexion/extension and radial/ulnar deviation on grip force using force sensors to record finger force production, and one biaxial ergometer to measure wrist position. They showed a significant trend on total force production with peak forces produced at 20° wrist extension and 5° ulnar deviation. However, Lee *et al.* focused solely on the effects of wrist flexed and extended positions. Grip strength and grip endurance were quantified using a hydraulic hand dynamometer *(Figure 3.1)* and results showed significant maximum grip strength at 15° and 30° extension for the dominant hand and 15°, 30°, and 45° extension for the non-dominant hand.
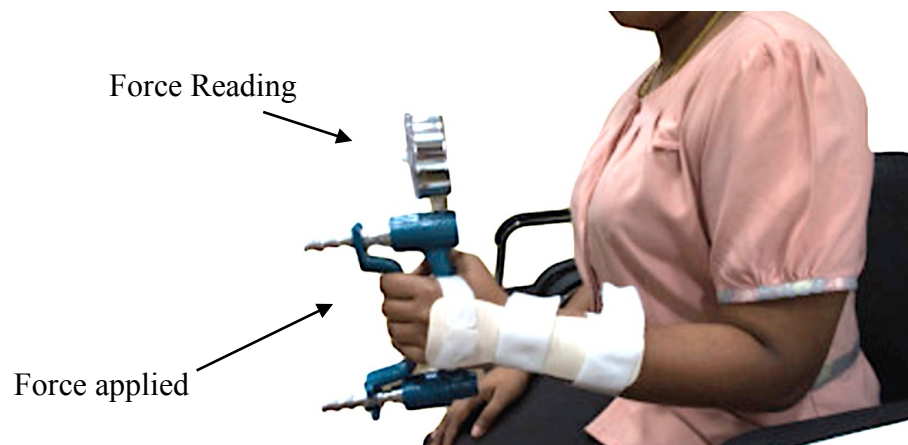


**Figure 3.1: Dynamometer**

*Tool used to measure grip strength*

Another in-vivo study conducted by Pryce *et al.* [46] concentrated on the effect of wrist combination positions (neutral, ulnar deviation, flexion, extension) on the maximum power grip strength. Results revealed that the differences in power grip strength were not significant for 0° ulnar deviation and 15° wrist extended, 15° ulnar deviation and 15° wrist extended, 15° ulnar deviation and 0° wrist flexed, and 0° ulnar deviation and 0° flexed/extended wrist positions.

The common conclusion derived by most wrist studies is that the largest possible grip force is achieved with the wrist in extension, followed by ulnar deviation. However, there are certain limitations within these studies. The majority of the literature focuses on the total external force produced by the fingers, instead of analyzing the load of each tendon alone internally. While external loads are usually important in understanding the total amount of work achieved by a person, internal loading is also vital in determining the amount of work required to directly translate and attain that load achieved at the finger in both intact and post-surgical repair conditions [47]. Due to the anatomical arrangement and complexity of the tendon-wrist mechanism, it is evident that internal forces exerted along the tendons are often minimized due to mechanical advantage and therefore, never equivalent to the load measured using a force grip measuring device [48]. The active motion simulator developed and used in this study has the ability to measure and record real-time loads experienced within tendons, FDP and FDS, and the extensor tendon within the forearm during full flexion of each finger individually at different wrist positions. Both external and internal loads have value for further understanding the biomechanics of the hand. This information is clinically relevant to surgical repairs and post-operative rehabilitation therapy protocols.

## 3.1.2 Mallet Finger Injury

Mallet finger is one of the most common injuries of the hand and is caused by a tear in the extensor tendon insertion point at the distal interphalangeal (DIP) joint (*Figure 3.2)* [49]. They are often induced in the workplace or by intense physical activity such as sports, most commonly in basketball. Due to the impairment of the extensor tendon mechanism, active extension of the distal phalanx is constrained and can be unachievable based on the degree of the laceration. The resulting imbalance between the flexor and extensor tendon mechanism can eventually lead to an early or late swan-neck deformity, a deformed condition where the DIP joint becomes permanently flexed with the PIP joint in hyperextension, which can result in further loss of finger function [50]. Therefore, once induced, it is crucial for the integrity of the extensor tendon mechanism at the DIP joint to be restored.



**Figure 3.2: Mallet Finger Injury**

*Tear of the extensor tendon at the DIP joint representing a mallet finger*

Depending on the severity of the laceration, a patient can suffer from acute loss of extension (0-10°), to severe loss of extension (>25°) [51]. There are several surgical repair techniques clinically used to correct chronic mallet finger deformity. Splint therapy is also a common approach to help restore finger function and regain any loss of range of motion experienced at the joint [52]. Nakamura *et al.* [53] conducted a study comparing the long-term effects of

surgical intervention on the quality of care of patients (n=15), in comparison to splint therapy (n=62). The surgical procedure involved making a lazy-S incision over the dorsal distal interphalangeal joint for exploration of the ruptured terminal extensor tendon and then fixing the joint in the extended position with a K-wire (*figure 3.3*).
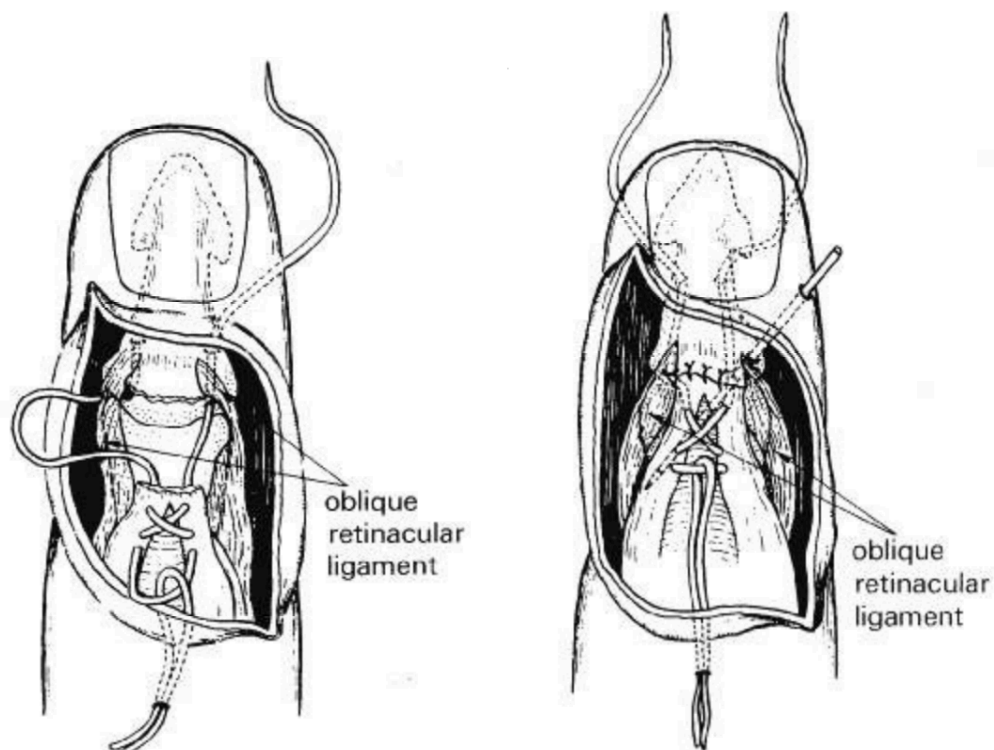


**Figure 3.3: Surgical Reconstruction of Extensor Tendon**

*Surgical mallet finger repair procedure as conducted by Nakamura et al. [53]. A stainless-steel wire is passed through the proximal tendon in a figure-of-eight configuration (left) and pulled distally towards the distal tendon and tied firmly as the K-wire held the distal phalanx in an extended position (right)*

They reported that 86.7% of patients that underwent surgery experienced more than 10° of improvement in extension, with an average improvement up to 34° at the DIP joint, as opposed to only 62.9% of patients with splints experiencing the same outcome. In addition, patients treated by surgical intervention expressed greater satisfaction with the outcome than did a conservatively treated group; concluding that surgery is a better option than conservative therapy

in treating fresh mallet finger [53]. Although the effects of mallet finger on joint ROM is well understood, it is still unclear whether evulsion or rupture of the distal tendon attachment has an effect on the extensor tendon load.

The purpose of this in-vitro study was to measure the effects of wrist position on individual finger flexor tendon loads, FDP and FDS, as well as the joint ranges of motion (DIP, PIP, and MCP). In addition, this study aims to analyze and compare the changes in loading experienced by the extensor tendon after simulating a mallet finger injury to the DIP joint.

## 3.2   Methods

### 3.2.1     Protocol

Tendons, FDP, FDS, and the extensor, were tested and analyzed per finger. Each flexor tendon of the same finger was simulated together under three extensor-loading conditions: 5N, 10N, and 15N (*Figure 3.5)*. Six combined sets of wrist positions were tested in the coronal (0° and 30° of ulnar deviation) and sagittal plane (0° and 30° of wrist flexion and extension) (*Figure 3.4*).
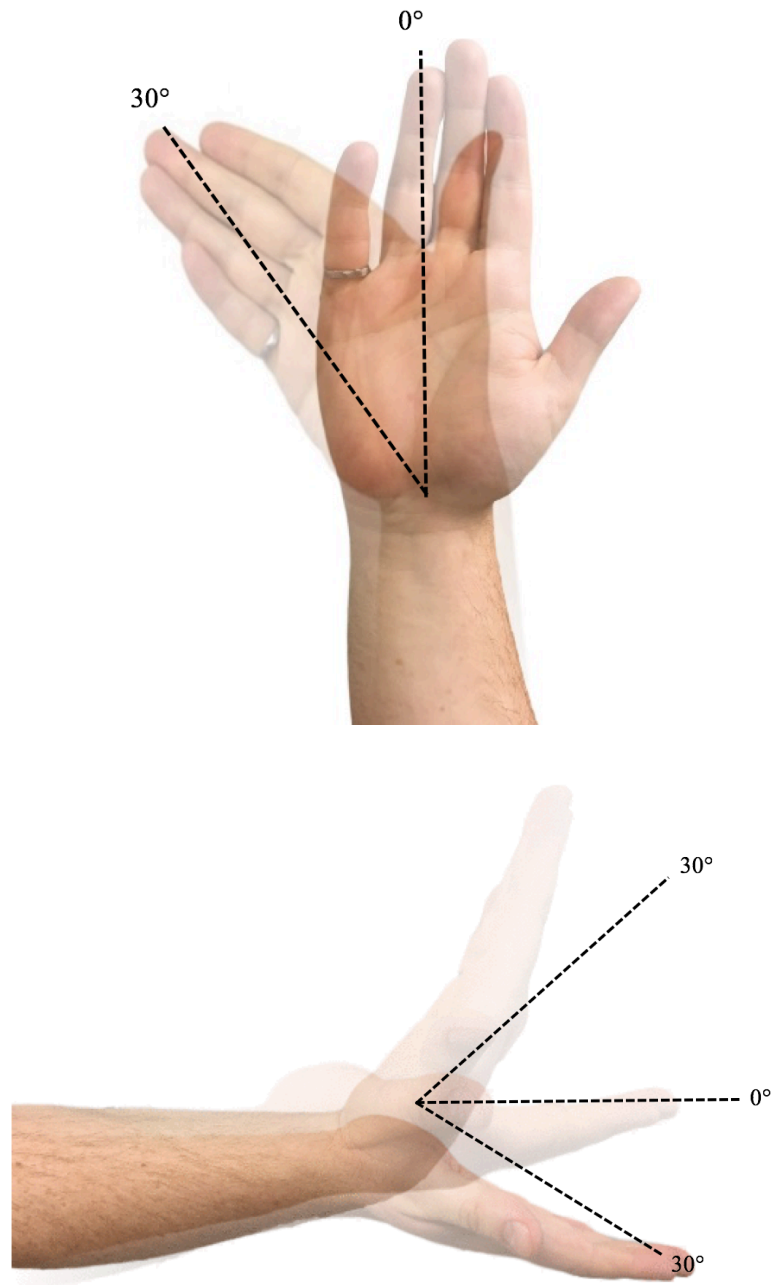
**Figure 3.4: Wrist Combinations**

*Diagram illustrating the different positions (neutral, flexed, extended, and ulnar deviated) and angles (0° and 30°) in which the wrist was fixed at along the coronal plane (top) and the sagittal plane (bottom)*
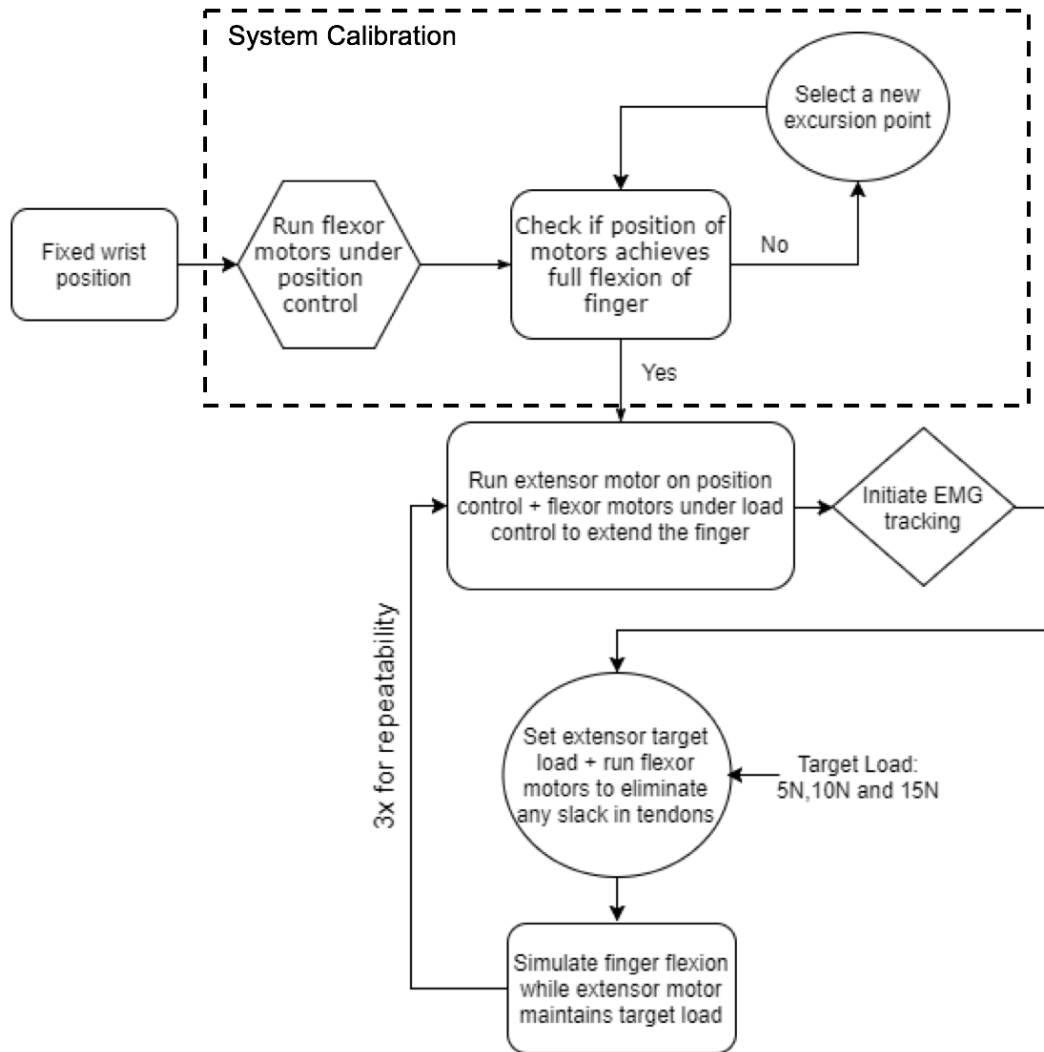
**Figure 3.5: Testing Protocol Flowchart**

*Diagram outlining the steps taken to run the simulator through the experimental protocol*

Before initiating data collection, a trial run denoting the amount of tendon excursion required to allow the finger to actively achieve full flexion and extension once the wrist was fixed was executed. Once obtained, the extensor and flexor linear actuators were automated to eliminate any slack in the corresponding tendons before simulating motion. During flexion, the flexor motors were designed to retract under position control to achieve the target excursion point while the extensor motors were programmed to always extend allowing the finger to constantly move through its full active range of motion and ensuring that the target load is maintained throughout. Once flexion is complete, the system reverts allowing the extensor motors to retract to a target position while the flexors extend to fully extend the finger to its initial joint orientation. This step was replicated with the hand in every wrist position. The performance of the simulator was evaluated by examining each condition three times through the full flexion/extension range of the finger to ensure that accuracy and repeatability of the outcome measures are maintained.

## 3.2.2    Specimen Preparation

Four digits, comprised of the index, long and middle fingers, were tested from two fresh-frozen cadaveric specimens amputated at mid-forearm (age: 71±9.8 years; sex: male). Flexors, FDP and FDS, and the extensor tendon of interest were isolated and sutured using 0-braided Vicryl (ETHICON®). K-wires were inserted through the metacarpals of the second to fifth digit to ensure proper fixation of the hand once tendons are pulled. The specimen was then placed onto the front base of the simulator using multiple screws inserted horizontally through the ulna and radius, as explained in section 2.2.1.1 of Chapter 2. All isolated tendons within the forearm were accessible by rolling over the layer of skin proximal to the wrist (*Figure 3.6*). Each tendon was coupled to its appropriate servo motor through the suture line. All tissues within the specimen was left intact and monitored for dryness. Saline solution was used to maintain proper hydration of the tissues
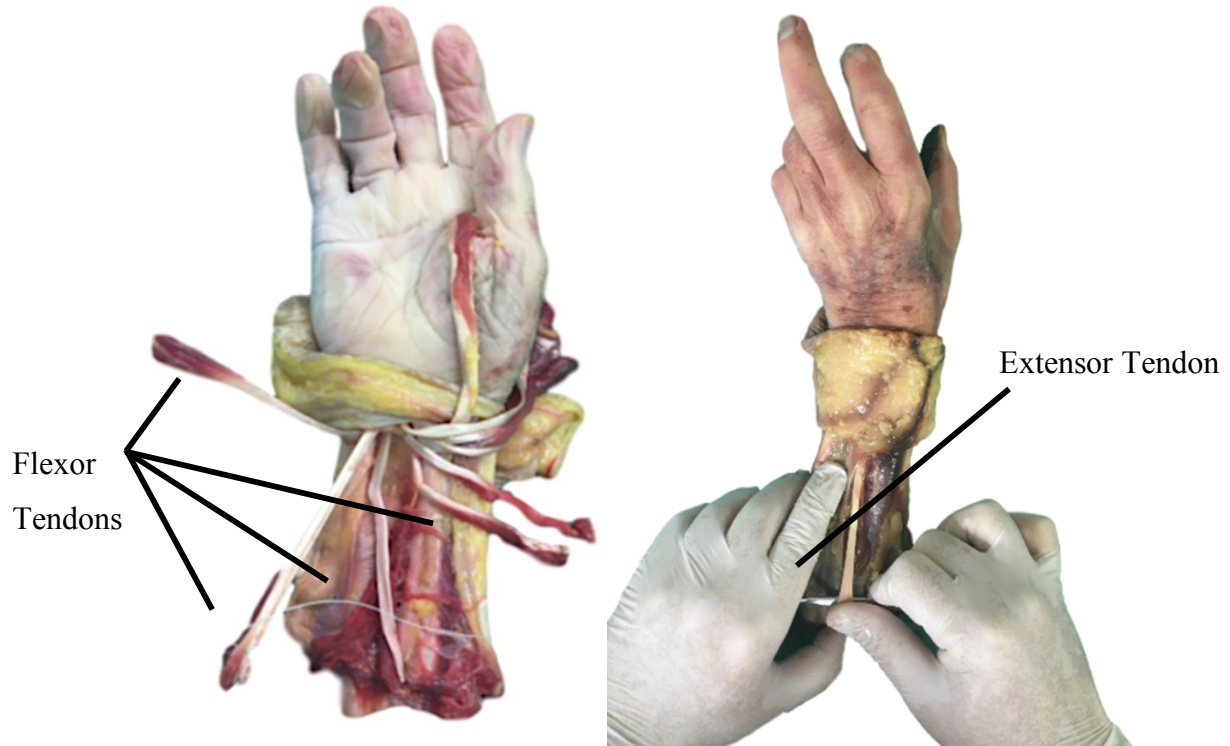
**Figure 3.6: Flexor and Extensor Tendon Isolation**

*Separation of flexors (left) and extensors (right) within the forearm*

All tendon lines were passed underneath the forearm and retained proper anatomical lines of action. 2mm electromagnetic trackers (M180, trakSTAR, ON) were then inserted into each finger joint (DIP, PIP, MCP) to analyze proper joint kinematics and range of motion (ROM) throughout the study. A tracker was also inserted within the metacarpal of the second digit to ensure fixity. All load cells were properly zeroed and calibrated within a custom LabVIEW program for accurate tendon load measurement and data collection. Rigid foam wedges were used to adjust the wrist at varying positions (*Figure 3.7*). The hand was stabilized against each foam wedge using a Velcro strap.

(a)

(b)

(c)
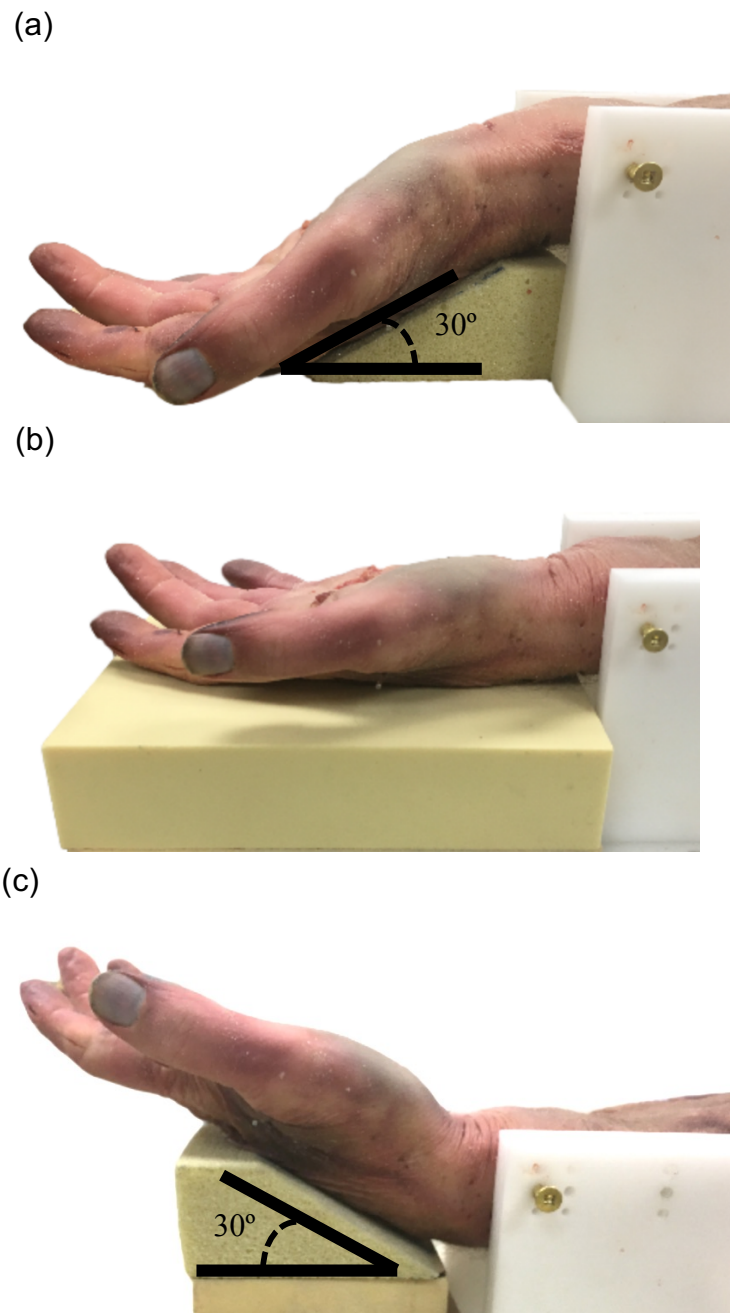
**Figure 3.7: Wrist Position Angles using Foam Blocks**

*Using blocks to achieve wrist extended (a), neutral (b), flexed (c) positions*

### 3.2.3    Statistical Analysis

Both 2-way and 3-way Repeated Measures ANOVA (RM-ANOVA) were performed with significance set at $p < 0.05$. The 3-way RM-ANOVA compared the range of motion and tendon load of the healthy intact subjects under 3 factors: wrist position, extensor load, and repeated trial number. The 2-way RM-ANOVA compared the healthy intact subjects to the injured subjects in the wrist neutral position under 2 factors: extensor tendon condition (intact/injured) and repeated trial number. All RM-ANOVAs were examined for significant trends within-subject effects and pairwise comparisons between factor levels. The repeatability of motion for the simulator was reported using the average standard deviation (ASD) throughout the range of motion.

## 3.3　Results

### 3.3.1　Repeatability of Tendon Forces

The average standard deviations were computed between consecutive trials for all motions in each position. The repeatability of the simulator between load trials was quite high with average standard deviations of 0.48 N for neutral (*Figure 3.8)*, 0.74 N for flexion, 0.98N for extension (*Figure 3.9)*, 0.27 N for neutral-ulnar deviation, 0.36 N for flexion-ulnar deviation, and 0.69 N for extension-ulnar deviation (*Figure 3.10)*.
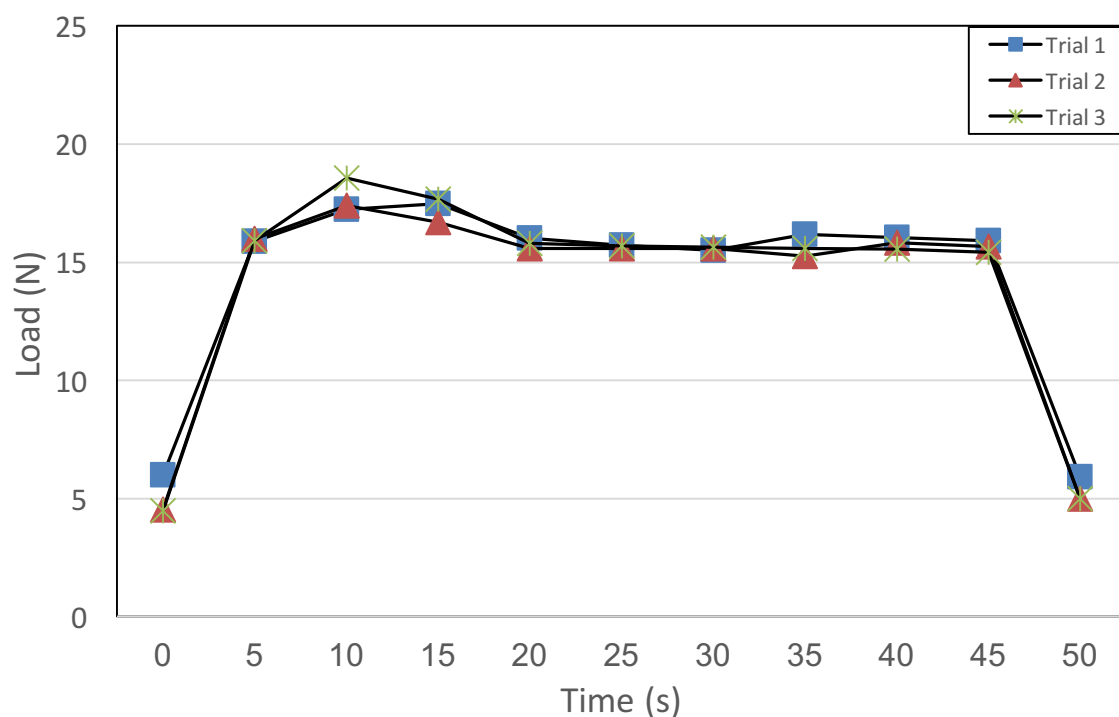


**Figure 3.8: Load Repeatability in Wrist Neutral**

*Repeatability of flexor tendon FDP under 10 N extensor load in the wrist neutral position, showing the overall behaviour of all three motion trials of load with respect to time*
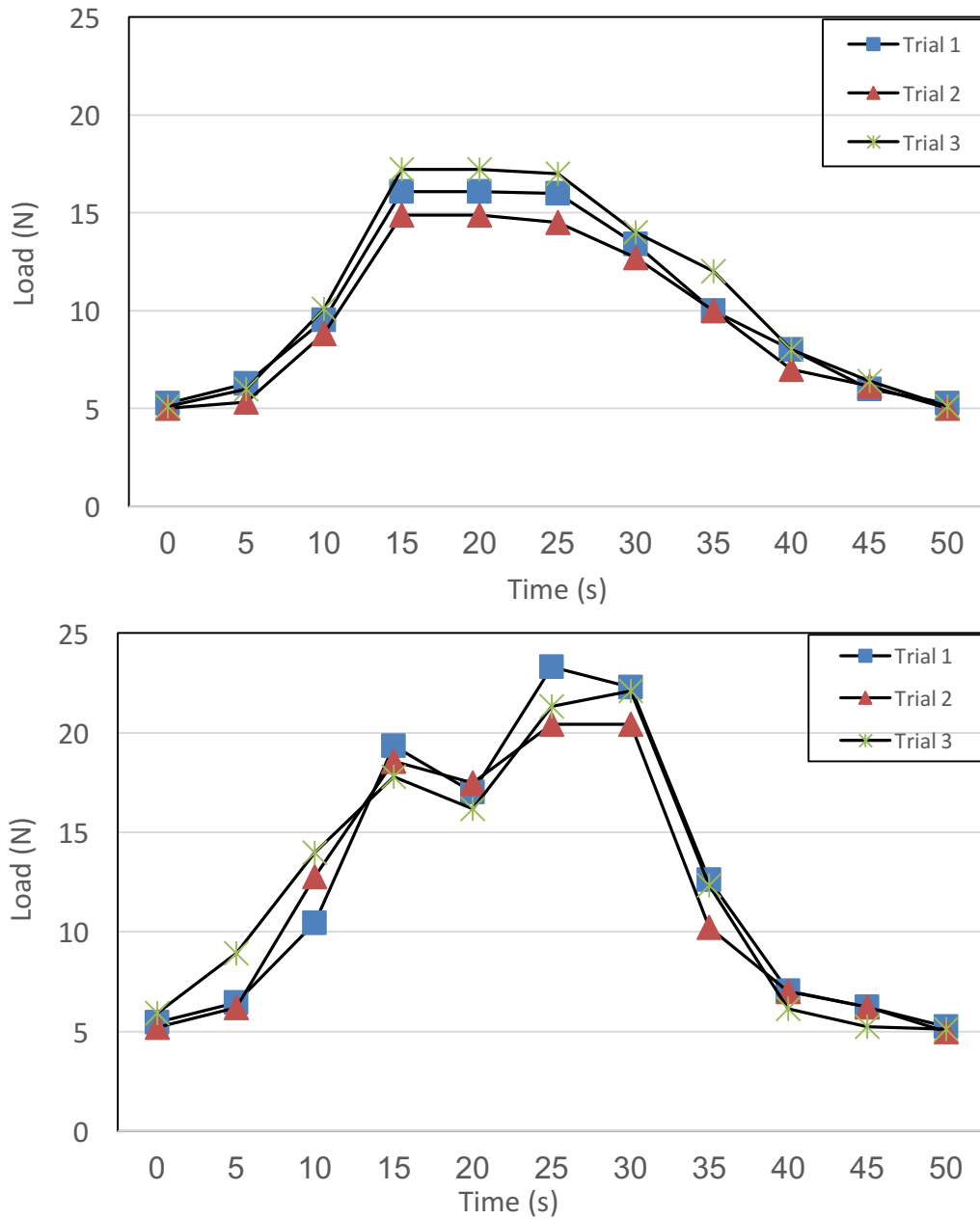
**Figure 3.9: Load Repeatability in Wrist Flexed/Extended**

*Repeatability of flexor tendon FDP under 10 N extensor load in the wrist flexed position (top) and wrist extended position (bottom), showing the overall behaviour of all three motion trials of load with respect to time*
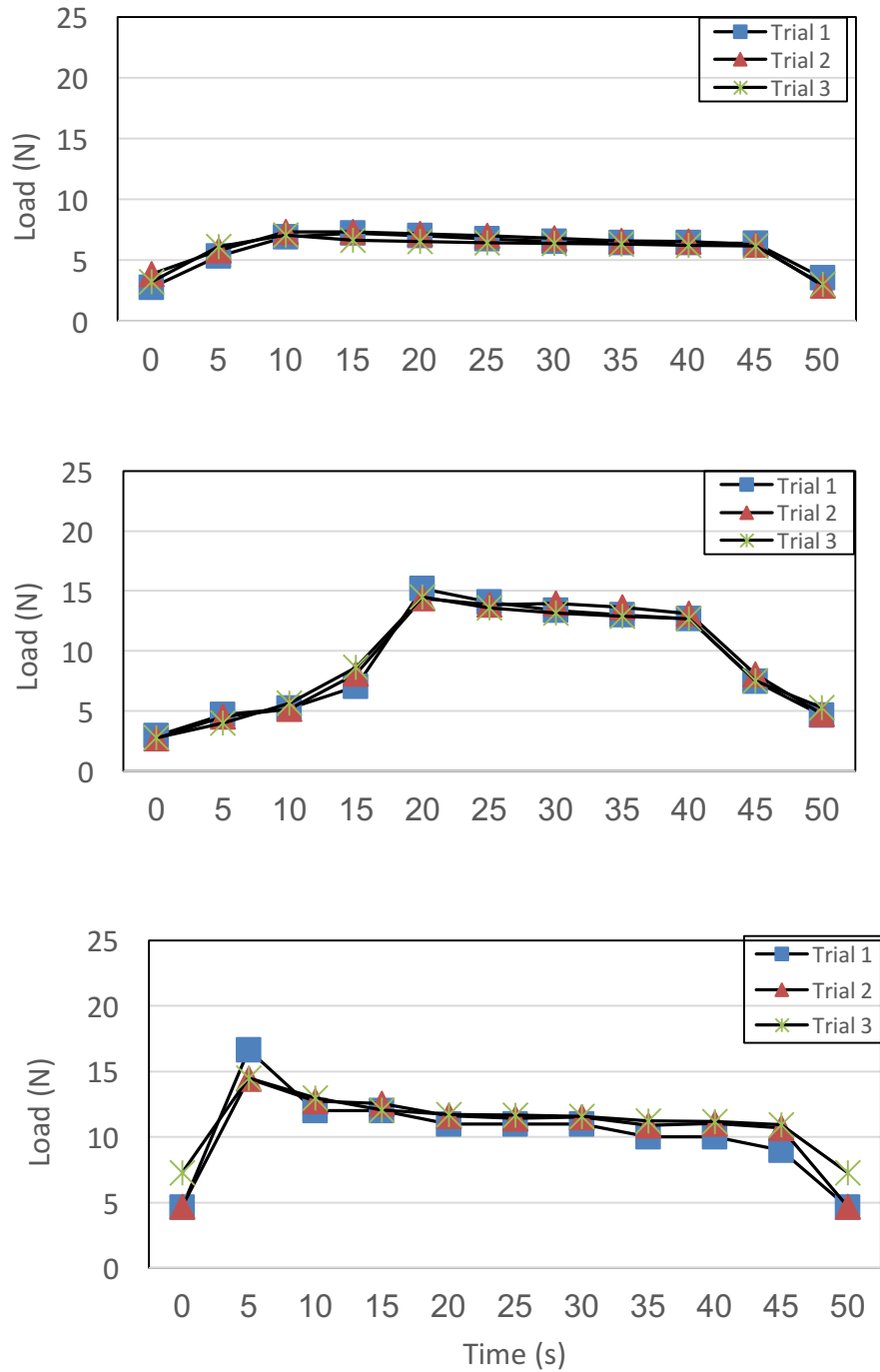
**Figure 3.10: Load Repeatability in Wrist Ulnar Deviated-Neutral/Flexed/Extended**

*Repeatability of flexor tendon FDP under 10 N extensor load in the wrist ulnar deviated– neutral position (top), wrist ulnar deviated – flexed position (middle), and wrist ulnar deviated– extended, showing the overall behaviour of all three-motion trial*

The peak force magnitudes and standard deviations achieved by both flexor tendons, FDP and FDS, to actively flex the finger under different wrist positions were collected and averaged between all 4 digits (*Figure 3.11*). The forces behaved as expected where pure extension of the wrist displayed the largest peak magnitude in FDP, followed by ulnar deviation with extension. Nevertheless, FDS did not abide by the same trend as ulnar deviation-extension managed to have a greater effect on load than pure extension in the neutral plane. Moreover, both positions, pure extension and extension with ulnar deviation, revealed to have the largest effects on flexor loads, as established in the literature. Furthermore, an increase in the extensor load resulted in a significant within-subjects' effects increase in both flexor tendon loads FDP (p=0.025) and FDS (p=0.008), as they are rather directly proportional.
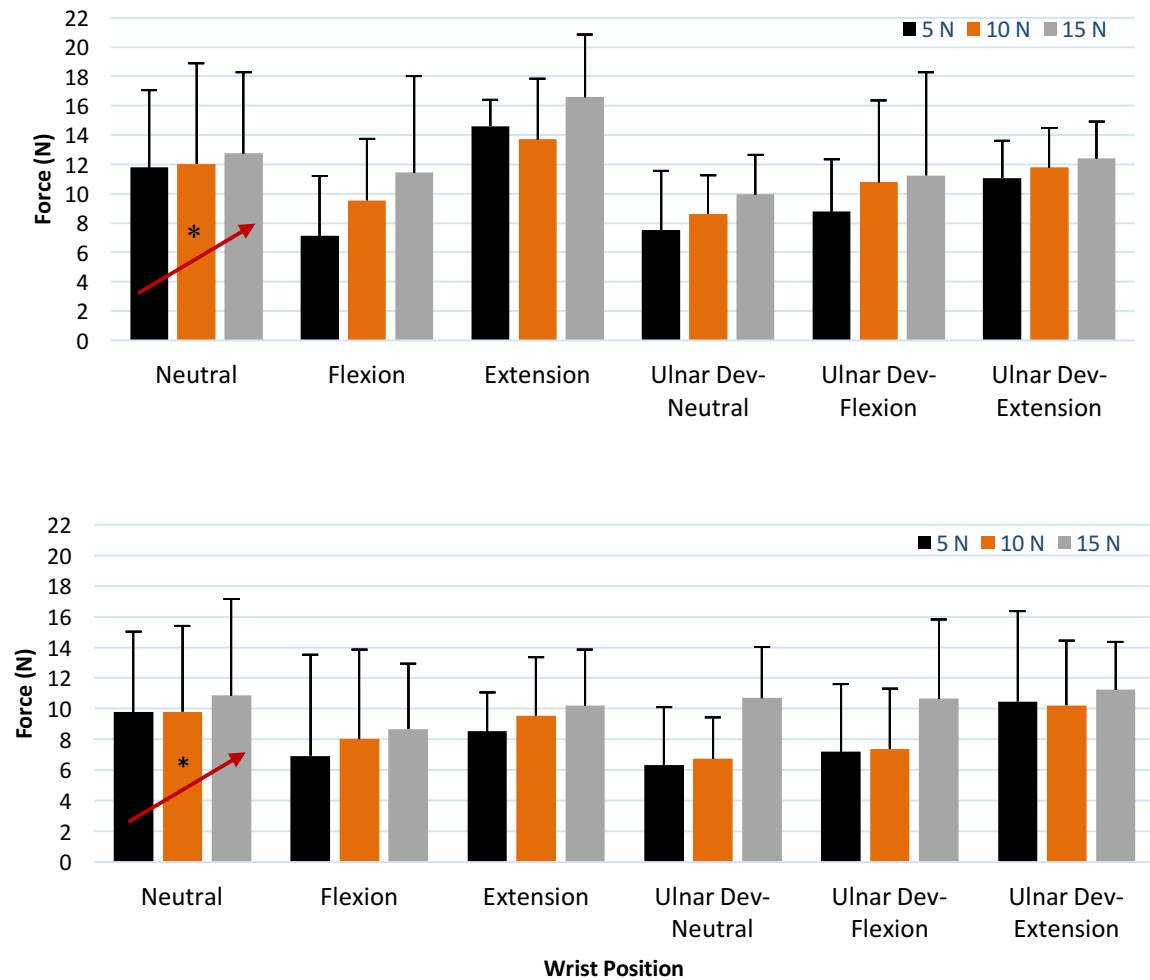
**Figure 3.11: Peak Loads of FDP and FDS**

*Average peak magnitudes and standard deviations of FDP (top) and FDS (bottom) loads required to achieve full active flexion of the finger in different wrist position for four digits. The arrow and asterisk represent statistical significance within-subject effects in flexor load as extensor load increases (FDP (p=0.025) and FDS (p=0.008)).*

## 3.3.2    Repeatability of Joint Kinematics

The repeatability measures of range of motion trials was also quite high with average standard deviations of 2.14° for neutral *Figure 3.12)*, 2.45° for flexion, 3.97° for extension (*Figure 3.13)*, 2.55° for neutral-ulnar deviation, 2.42° for flexion-ulnar deviation, and 2.58° for extension-ulnar deviation (*Figure 3.14)*.
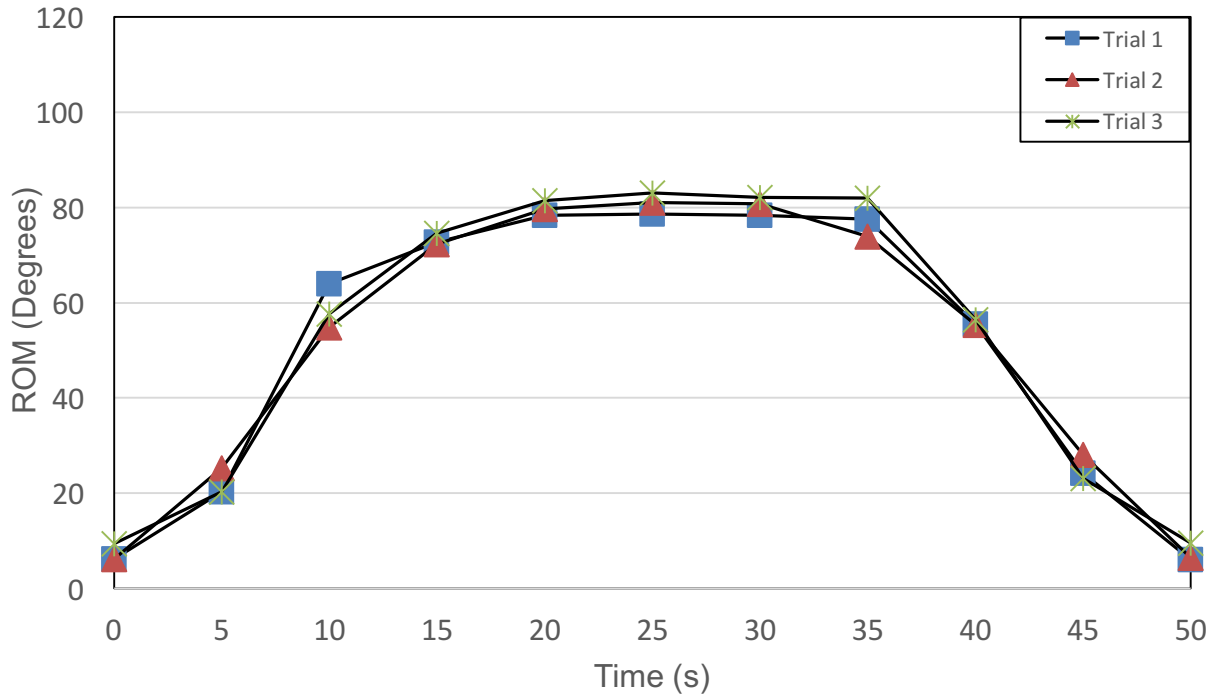


**Figure 3.12: ROM Repeatability in Wrist Neutral**

*Repeatability of the MCP joint under 10N extensor load in the wrist neutral position showing the overall behaviour of all three motion trials of load with respect to time*
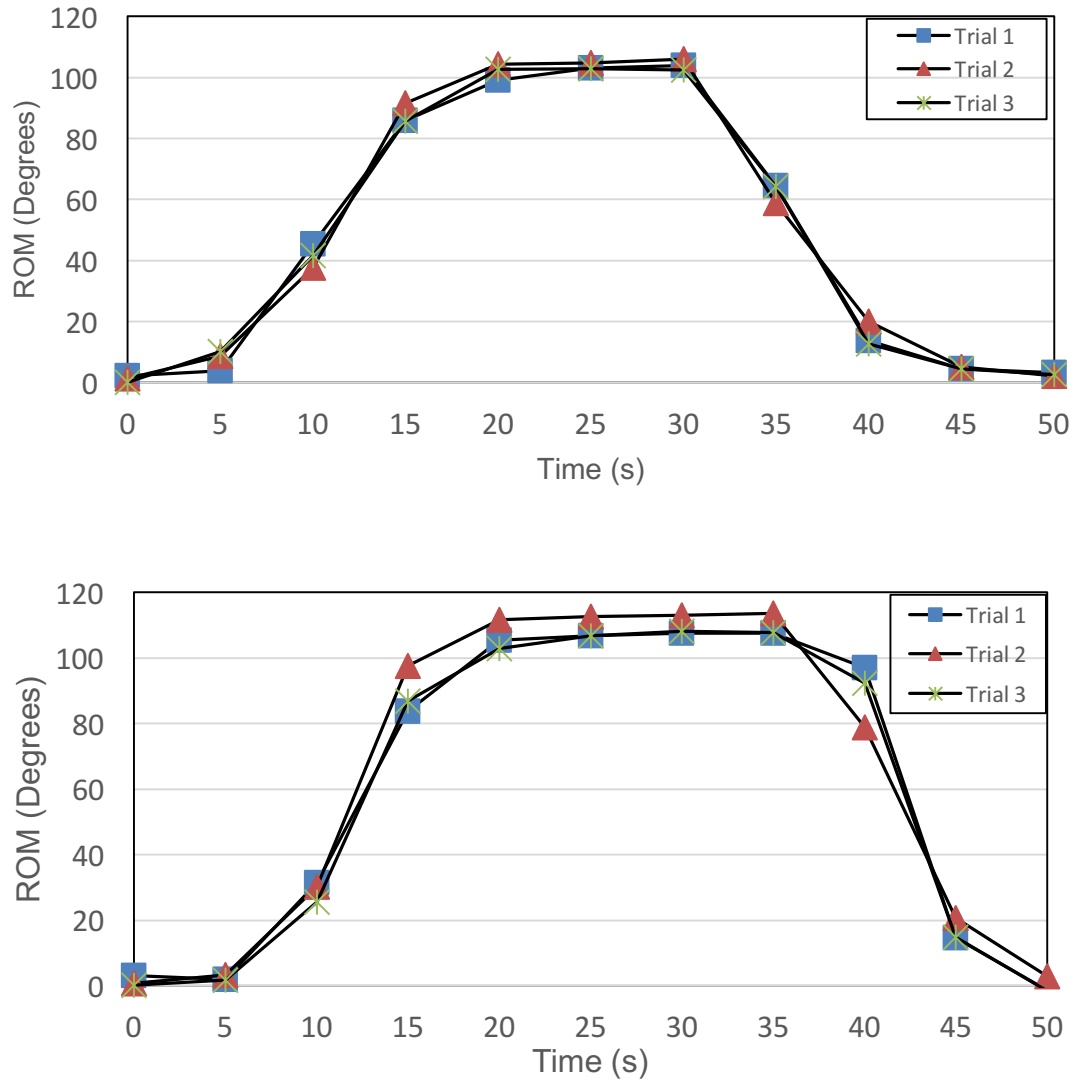
**Figure 3.13: ROM Repeatability in Wrist Flexed/Extended**

*Repeatability of the MCP joint under 10N extensor load in the wrist flexed position (top) and wrist extended position (bottom) showing the overall behaviour of all three motion trials of load with respect to time*
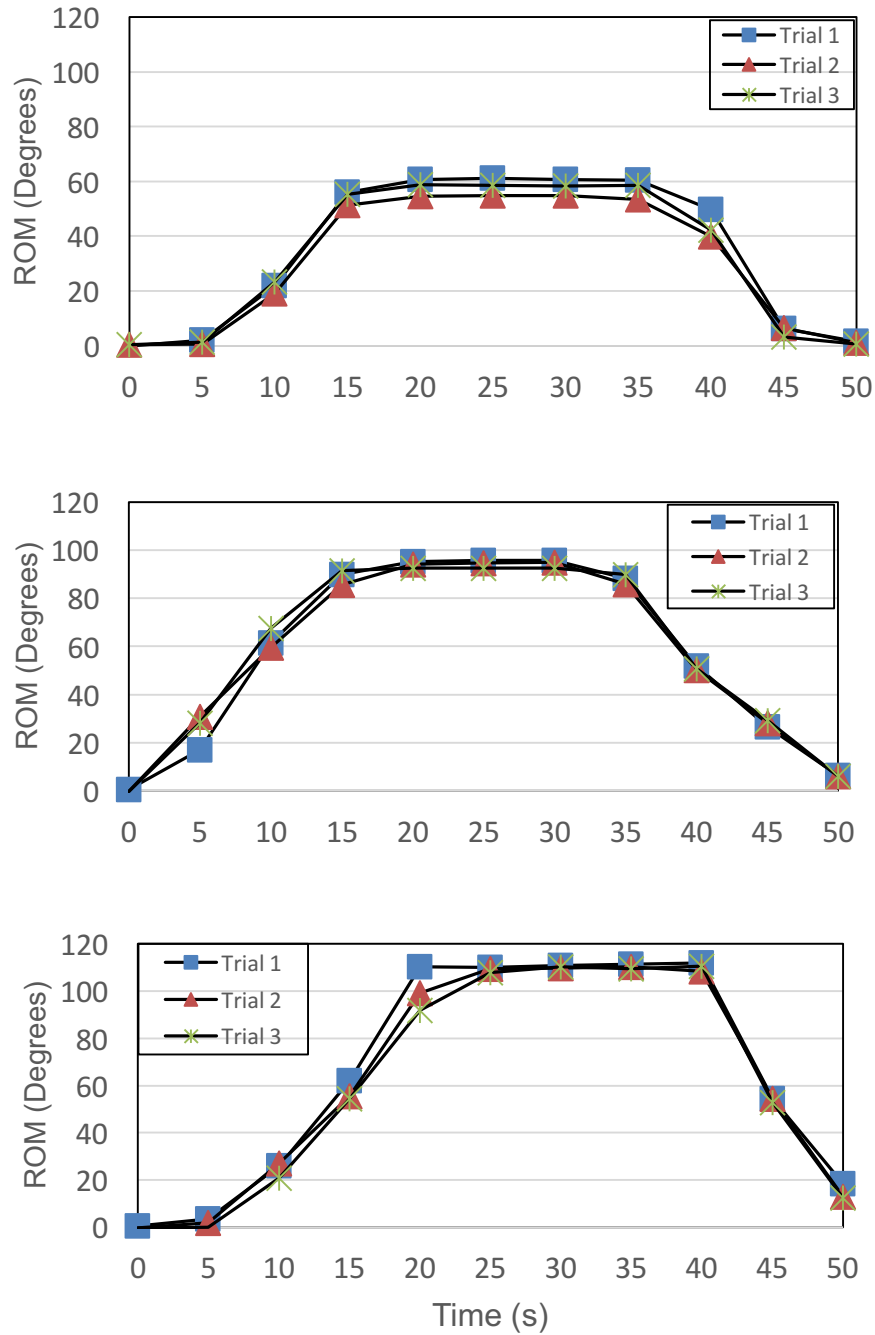
**Figure 3.14: ROM Repeatability in Wrist Ulnar Deviated-Neutral/Flexed/Extended**

*Repeatability of the MCP joint under 10N extensor load in the wrist ulnar deviated– neutral position (top), wrist ulnar deviated – flexed position (middle), and wrist ulnar deviated– extended showing the overall behaviour of all three motion trials of load with respect to time*

### 3.3.3      Wrist Position Analysis

A three-way RM-ANOVA was computed comparing the effects of all 6 wrist positions and the repeated trial runs on joint range of motion and flexor tendon loads for all 4 specimens tested. There were no statistical significant differences found (p=0.034) in all three joint's ROM (DIP, PIP, and MCP) under different wrist positions, extensor loadings, and repeated trial runs. Unlike ROM, both flexor loads, FDP and FDS, achieved significance in trends (p=0.025 and p=0.008 respectively) when comparing within-subject effects of varying extensor loads. In addition, PW comparisons between the three-extensor loading conditions displayed significance in FDS between 5N and 15N loadings (p=0.040) whereas FDP was close to significance between the same loading conditions, but never reached true significance (p=0.056). Finally, there was no significance due to changes in wrist positions for trial runs.

### 3.3.4      Injury Condition

Forces of the extensor tendons were used to analyze the effect of a simulated mallet finger injury on the kinematics of the finger during active extension of the finger. The peak force magnitudes and standard deviations were collected and averaged between all 4 specimens (*Figure 3.15*).
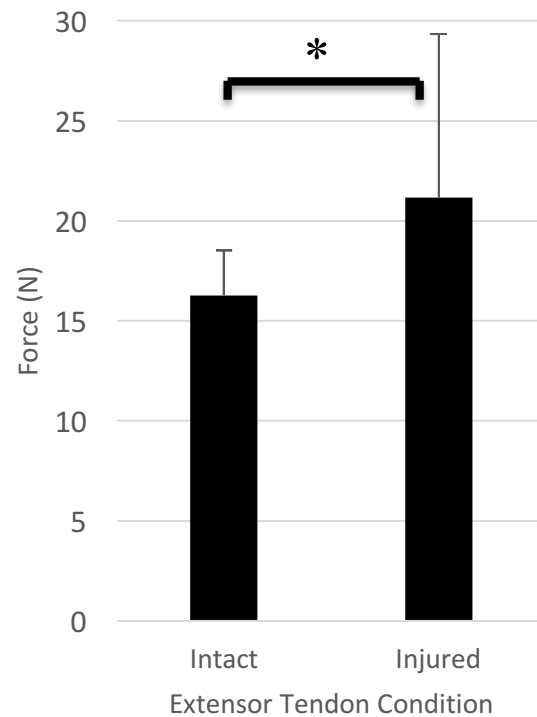
**Figure 3.15: Extensor Load Pre and Post Injury**

*Average peak magnitudes of extensor loads required in achieving full active extension of the finger pre-and-post mallet finger injury simulation for all 4 specimens. The asterisk illustrates statistical significance between both conditions (p<0.05)*

A two-way RM-ANOVA was computed comparing the effects of pre-and-post injury simulation on the extensor load, as well as finger joint ranges of motion during active extension of the finger in the neutral wrist position (n=12). Similar to the healthy state conditions, each motion trial was repeated three times and compared as a separate factor within the statistical analysis. Both MCP and PIP experienced no significant trends or changes in their range of motion between both conditions (intact vs. injured). However, the DIP managed to achieve significance in trend within-subject effects (p<0.01) and a significant PW comparison of 32° between the intact and the injured states. In terms of the extensor tendon load, a significant within-subject effects trend

was achieved (p=0.040) with a significant gain in the load by 4.9N post injury. No significance was computed for the difference in trial runs between conditions.

## 3.4   Discussion

The results obtained from the simulator achieved high accuracy and repeatability in its data output, confirming the system's precision and reliability. Not only were the computed average errors low, but also were all within the hypothesized PID error range of ±2N in Chapter 1 (section 1.9). Additionally, there were no significant differences between any repeated trials.

Since the integrity and mechanics of the fingers tested were left unaltered throughout the wrist study, it was expected that variations in the wrist position and extensor loading would have little to no effect on the joint ROM. Once a tendon is loaded to the finger's maximum allowable flexion angle, any further increase applied to the extensor load should not, and as established in this study, does not have an effect on the joint range of motion, providing that the magnitude of the load does not overcome the load applied on the flexor tendons. Such outcome was ultimately displayed within this study, further validating the accuracy and reliability of the system.

However, unlike ROM, increase in extensor load should cause an increase in the flexor loads, as they are proportional. This trend was in fact also observed with a significant within-subjects' effects trend in both flexor tendons FDP (p=0.025) and FDS (p=0.008).

Although the statistical analysis failed to reveal any significances or effects of wrist position on tendon load, the peak load data distributed in *Figure 3.11* in the results section clearly demonstrates that the largest loads were reached with wrist in extension, which agrees with the literature [44], [45]. Interestingly however, FDS did not follow the same trends as FDP, experienced greater loads with an ulnar deviated and extended wrist.

Loss of extension ROM at the DIP joint has been established within the literature [51]  and the degree of range lost can vary between 10-25° based on the severity of the tendon injury [51]. ROM results obtained from this study revealed a significant loss of 32° (p<0.01) in the range of the DIP joint with no significant losses in either PIP or MCP during active extension. In addition, there was an increase in the extensor load after injury simulation compared to the intact state. In

other words, more force is required by the extensor tendon to actively extend the finger with a mallet finger injury, as opposed to an intact finger.

Although losses in DIP's range of motion after mallet finger simulation is expected and therefore not clinically relevant, the current gap in literature regarding forces of the extensor tendon and the correlation between the degree of the injury and the load experienced by the tendon is highly ambiguous and has not been clinically investigated prior to this study.

Limitations to this study arise from the use of elderly cadaver specimens for kinematic analysis, and the limited small sample size used. King *et al.* [54] reported significant degradation of cyclic peak loads in dense connective tissues of 8.6±4.6% over an 18 hour period (p<0.0001) at room temperature (23±2°C) for in-vitro testing. This finding might also have an influence on the elasticity of the tendons and the overall laxity of the joints over time.

## 3.5   Conclusion

The overall accuracy and repeatability of the simulator was validated as all force and ROM data collected complimented the literature. In addition, the effect of tissue degradation and stiffness on the simulator's ability to produce repeatable motion was negligible as no major differences in the average standard deviations of repeated trials were detected. Overall, the repeatability of the simulator was met with the objective outlined in Chapter 1 (Section 1.9).

# Chapter 4

## 4 Sequential A2 and A4 Pulley Sectioning and Reconstruction: Cadaveric Kinematics Study

*OVERVIEW: This chapter presents a pulley study conducted using five cadaveric upper limb specimens (14 fingers) looking at the effect of sequential pulley cuts of the A2 and A4 pulley on the ROM of joints and flexor tendon loads. In addition, lacerated pulleys were then surgically repaired to restore full ROM of joints and tested with the wrist in three positions; neutral, flexed, and extended. A detailed discussion of the results obtained is also included to validate the relevance and significance of the results within clinical grounds.*

## 4.1 Background

The A2 and A4 pulleys have been clinically acknowledged from previous studies to be very important in maintaining proper finger biomechanics [55]–[57]. Anatomically, these pulleys shield a proportionally large area of the flexor tendons. As discussed in Chapter 1 (Section 1.2.4), they function by transmitting tensile load within flexor tendons to rotational torque at the joints. Therefore, any minor disruption to the A2 and A4 pulleys can jeopardize range of joint motion and negatively affect the kinematics of the finger.

Chow *et al.* [12] conducted a cadaveric study examining the effects of partial distal/proximal incisions of the A2 and A4 pulleys on the ring and index finger's flexion kinematics and biomechanics (n=32). The experimented protocol involved separating the specimens (8 fingers/group) into four groups; A2 proximal 50% partial incision, A2 distal 50% partial incision, A4 proximal 50% partial incision, and A4 distal 50% partial incision. All measurements were compared to the intact state as the control group. The FDP tendon was loaded by a computer driven servo-motor and the angular rotations of the finger joints were measured by micro-potentiometers (Honeywell Clarostat Model 586) (*figure 4.1*).
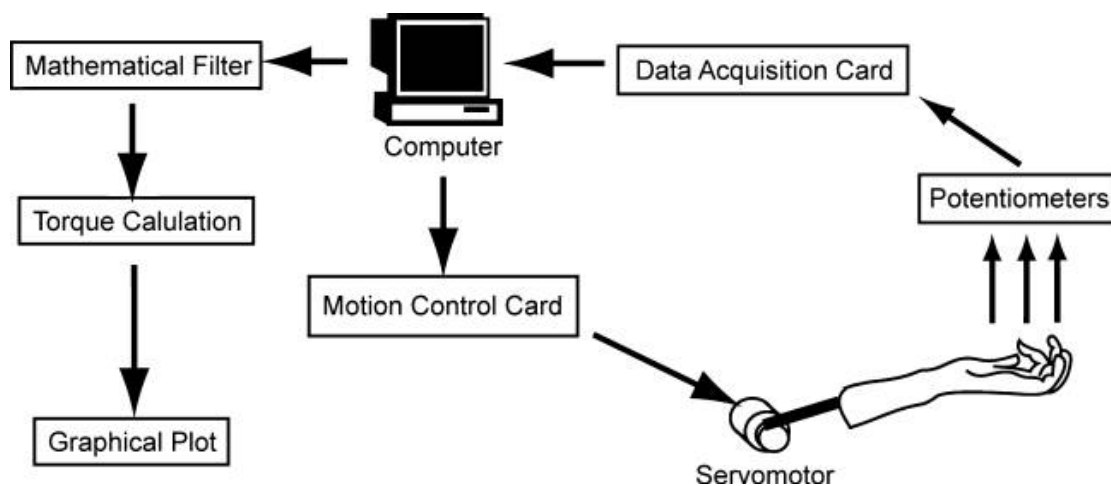
**Figure 4.1: Experimental Setup**

*Flowchart illustrates the step by step process taken during the study [12]*

Results from this study revealed an overall significant loss in finger motion after proximal 50% incisions of either the A2 or the A4 pulleys were made, 6.6% and 8.6% respectively. This effect

was greatest seen in the MCP joint with a decrease in joint rotation. No significant changes in joint inertial torques were shown.

Tomaino *et al.* [58] conducted another cadaveric study investigating the effect of sequential excisions (25%-75%) of the A2 and A4 pulleys on digital angular rotation and the energy required to flex the finger. Results from this study revealed a 3% and 5% significant loss in angular rotation due to 50% and 75% excision of the A2 pulley, respectively. However, unlike Chow *et al's* results, partial excision of the A4 pulley failed to reveal any significant losses in joint rotation. 50-75% excision of both pulleys however resulted in 5-8% loss, respectively. In terms of forces within the flexor tendons, significant difference was only noticed after 75% of the A2 pulley had been cut. Mitsionis *et al.* [59] however, demonstrated different outcome results following similar experimental procedures. Their results concluded that a minimal length of 50% of either A2 or A4 pulleys must be maintained for ideal finger kinematics.

Finally, Lu et al. [60] conducted a study where excursion and moment arms of flexor tendons FDP and FDS with respect to the MCP joint were evaluated under the effects of different pulley conditions of cadaveric specimens (n=8). The experimental protocol involved measuring each specimen under four pulley states; intact, A2 intact with A1 fully cut, 50% proximal cut of A2 with A1 fully cut, both A1 and A2 fully cut. Linear position sensors (LP-100F; Midori America Corporation, Fullerton, CA) were attached to the FDS, FDP, and EDC to measure the tendon excursions simultaneously. A 3D motion capture system with eight cameras (Eagle; Motion Analysis Corporation, Santa Rosa, CA) was also used to measure joint rotation. Excursion of the tendon was measured by applying a 7N weight onto the tendon of interest to achieve full finger flexion, whereas the other tendons were supplied with a 1N weight to simulate passive tendon tension. Results obtained from this study failed to reveal significant differences in excursion of FDP and the moment arms of FDP and FDS with A1 fully cut and A2 50% cut. These results further strengthen the conclusion made by other studies as it implies that both A2 and A4 pulleys can undergo 50% cuts without significantly affecting the kinematics of the finger.

The development of active motion simulators to reanimate cadaver specimens has opened many doors to attaining reliable data for the investigation of joint kinematics. The biggest and most common limitation seen within these pulley studies mentioned above is the lack of a proper

integrated system that is capable of controlling a finger while measuring tendon load and excursion in all tendons simultaneously during simulated active motion. As research is limited in its ability to properly model and mimic true in-vivo behaviours of specimens, the simulator developed in Chapter 2 has the capability of overcoming those limitations faced within the studies due to its ability of proper loading and excursion control of all tendons. In addition, its high resolution allows it to detect any small changes in load and joint kinematics after sequential pulley excision, as well as following reconstruction. Surgical pulley reconstruction procedures are very common and aid in restoring normal finger function after laceration [61]. Yet, there is a current literature gap regarding the effects of different wrist position on the internal tendon loads and joint ROM of the finger following each sequential pulley cut and reconstruction made. Therefore, the purpose of this study was to investigate the effects of sequential A2 and A4 pulley sections and reconstruction on the DIP, PIP, and MCP joint ranges of motion, as well as, the loads required to achieve full active flexion of the finger prior and post laceration. In addition, outcome measures following surgical reconstruction of the pulleys was explored under three different positions; neutral, flexed, and extended.

## 4.2　Methods

### 4.2.1　Protocol

Tendons, FDP, FDS, and the extensor, were tested and analyzed per finger. Each flexor tendon was pulled with a 10N applied onto the extensors in three different wrist positions; wrist neutral, 30º wrist flexion, and 30º wrist extension. An initial trial run was first executed to denote the amount of tendon excursion required for the finger to actively achieve full flexion/extension. Once obtained, the linear actuators were automated to automatically achieve the target position through position control once instructed to. Baseline tendon forces and ROM of each joint in the intact pulley state was measured and recorded. This step was replicated with every wrist position.

Before initiating any pulley cuts, an incision was first made on the palmar surface of each tested finger to identify and measure the A2 and A4 pulleys clearly. The incisions were 1–2cm in length and were made 1cm distal to the MCP joint and 1cm proximal to the DIP joint. The lengths of the pulleys were recorded using a Vernier caliper to the nearest mm (A2: 17.7±

2.1mm, A4: 6.4± 1.0mm) and increments of 25% and 50% were marked on the A2 and A4 pulley respectively with a thin sharpie pen (*Figure 4.2)*.
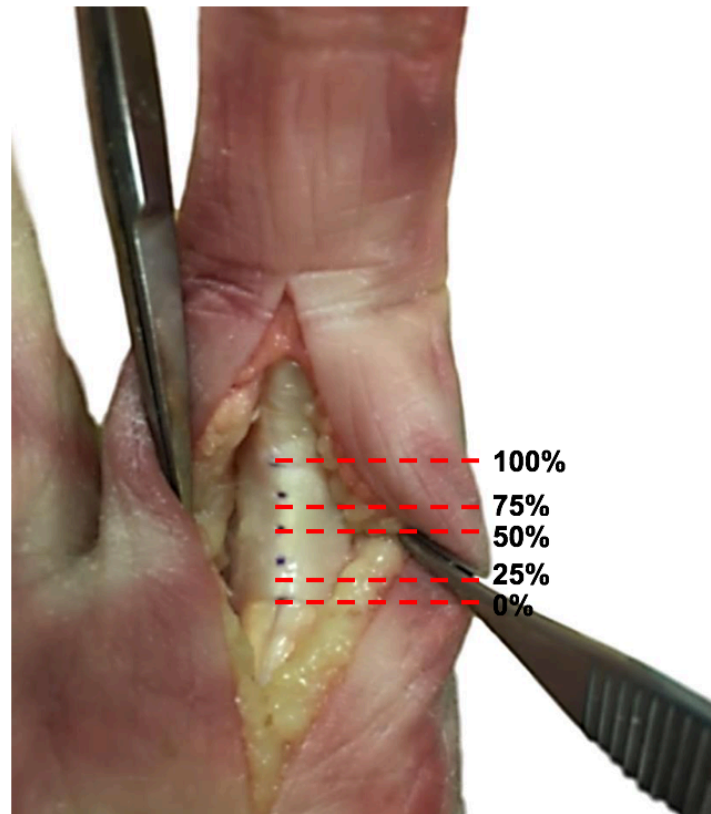


**Figure 4.2: 25% Sectioning of the A2 Pulley**

*The black dots on the pulley represents every 25% mark as illustrated by the red dashed lines*

The surgical excision protocol proceeded as follows:

1. A2 25% sequential cuts until 100%; A4 intact
2. A2 reconstruction; A4 intact
3. Release of A2 reconstruction; A4 50% sequential cuts until 100% (fully cut)
4. A2 reconstruction; A4 100% cut
5. A2 reconstruction; A4 reconstruction (full reconstruction)
6. A2 release; A4 reconstruction;

Excursions of flexor tendons were always referenced back to the intact excursion and all tendon load and joint ROM measurements were recorded and analyzed between each cut/reconstruction.

All sequential pulley excisions following the intact state were conducted only in the wrist neutral position where as full excision and reconstruction were analyzed in all three wrist positions. Tendon grafts isolated from forearm were used for the reconstruction of the pulleys in a double loop technique where the tendon was looped twice around the flexor tendon and adjacent bone (*Figure 4.3*). The skin was never removed and was sutured together after each sequential cut or reconstruction.
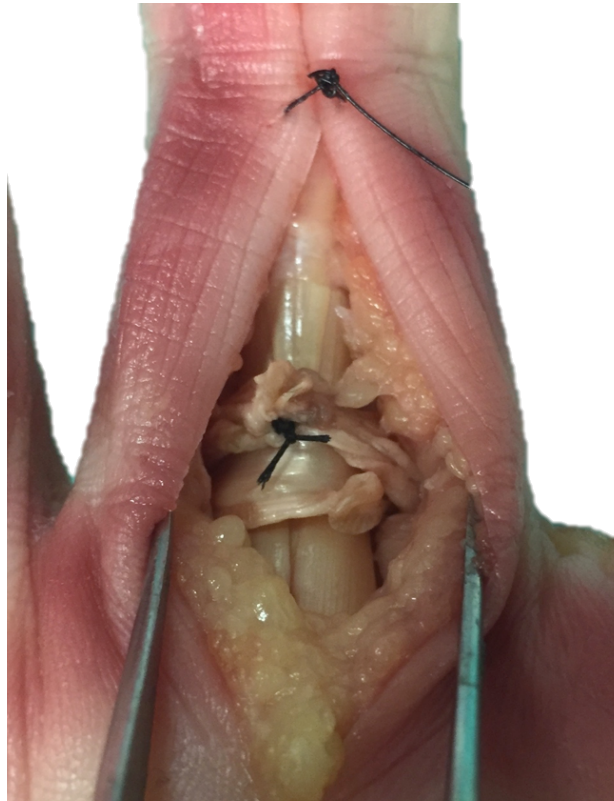


**Figure 4.3: Pulley Reconstruction**

*Reconstruction of the A2 pulley using tendon grafts*

## 4.2.2    Specimen Preparation

Fourteen digits, comprised of the index, long and ring fingers, were tested from five freshly frozen cadaveric specimens amputated 10cm proximal to the wrist (age: 71.8±9.9 years; sex: 2 males, 3 females). All CT scans of specimens were screened prior to testing for signs of osteoarthritis disease (OA) at the joints. The flexor digitorum profundus (FDP), flexor digitorum

superficialis (FDS), and the extensor tendon (ET) of the three fingers were isolated for testing. The involved tendons were sutured using 0-braided Vicryl (ETHICON®) in order to be loaded onto the linear actuators. All tendon lines retained proper anatomical lines of action and electromagnetic trackers were inserted into each finger joint (DIP, PIP, MCP) to analyze proper joint kinematics and range of motion (ROM) throughout the study. The metacarpals were fixed by K-wires to avoid unnecessary motion and an electromagnetic tracker was inserted within the metacarpal of the second digit to ensure fixation. Similar to the wrist study, the specimen was then securely fixed to the front base of the simulator for testing and self-designed foam blocks were also used to adjust the wrist at varying positions. The wrist was also restricted using 2mm Dacron fishing wire to prevent movement of the wrist in the sagittal and coronal plane between runs. All remaining tissues within the specimen were left intact and saline solution was used to maintain proper hydration of the tissues to preserve the natural function of the hand.

## 4.2.3    Statistical Analysis

Multiple 1way, 2-way, and 3-way Repeated Measure ANOVAs were executed to establish significant trends within subject effects ($p < 0.05$). The 1-way RM-ANOVAs compared the difference flexor loads, FDP and FDS, under different pulley conditions in the wrist neutral position. The 2-way tests focused more on the effect of different pulley conditions and finger flexion/extension runs on the individual joint angular rotations. Lastly, the 3-way RM-ANOVA compared the effect of all 3 factors, pulley condition, wrist position, and finger flexion/extension on tendon loads and joint ROM to piece together an understanding of the true influence that these factors have on the outcome measures of interest.  All RM-ANOVA simulations were examined for trend significances within-subject effects and pairwise comparison (PW) significances between individual variables. In addition, a G*Power software (Appendix F) was used during this study to quantify the minimum sample size (n=12) required for achieving significant trends within 80% statistical power based on metrics such as the effect size that is obtained from results of completed specimen tests.

## 4.3   Results

### 4.3.1     Tendon Forces

With the wrist in neutral, sequential sectioning of the A2 and A4 pulleys revealed significant trends in both FDP (p=0.001) and FDS (p=0.003) tendon loads with a significant reduction of 2.3±1.9N (p=0.029) load in the FDP load after complete A2 and A4 excision (*Figure 4.4*).
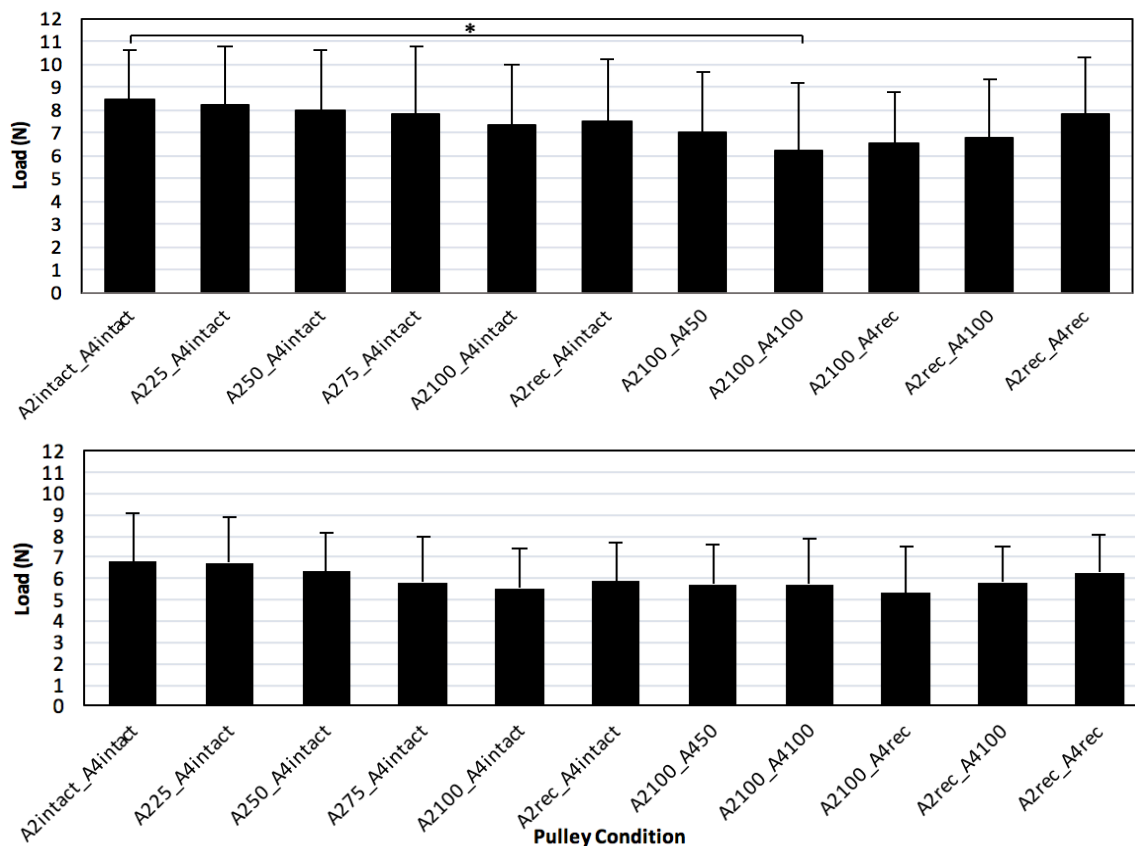


**Figure 4.4: FDP and FDS Load following Pulley Sectioning/Repair**

*FDP (top) and FDS (bottom) tendon loads are illustrated where the asterisk highlights PW comparison significances. Error bars represent the standard deviations between specimens (n=14)*

As seen in *Figure 4.5,* with the wrist flexed, cutting both A2 and A4 pulleys also revealed significant trends in both FDP (p=0.006) and FDS (p=0.002) loads. FDP was reduced by 3.6±3.5 N (p=0.034) when both pulleys were excised, and restored to within 0.5 N of the intact state by their subsequent reconstruction (p=0.034).  Lastly, with the wrist extended, cutting both pulleys

revealed significances in both FDP and FDS tendon loads (p=0.001, p=0.046 respectively). FDP was significantly reduced by 3.5±1.7 N (p<0.001).
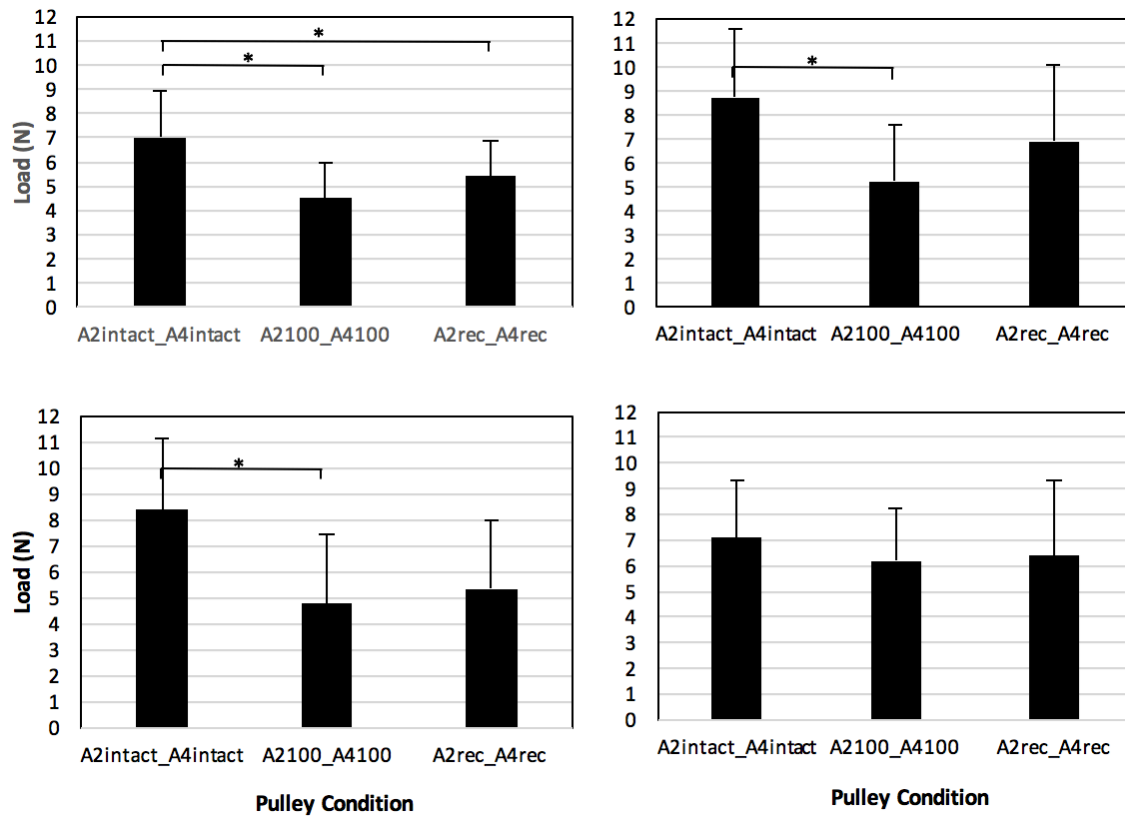


**Figure 4.5: Influence of Wrist Position on FDP Load Post Sectioning/Repair**

*FDP load with wrist flexed (top left), wrist extended (top right), and FDS with wrist flexed (bottom left), wrist extended (bottom right). The asterisk highlights PW comparison significances between conditions. Error bars represent the standard deviations between specimens (n=11).*

As demonstrated in *Figure 4.6*, with both pulleys reconstructed, the wrist position had a significant effect on tendon load (p=0.030). The flexed wrist position resulted in a reduction of FDP load compared to the neutral wrist position (p=0.010). Wrist extension also produced an apparent reduction, though not statistically significant.
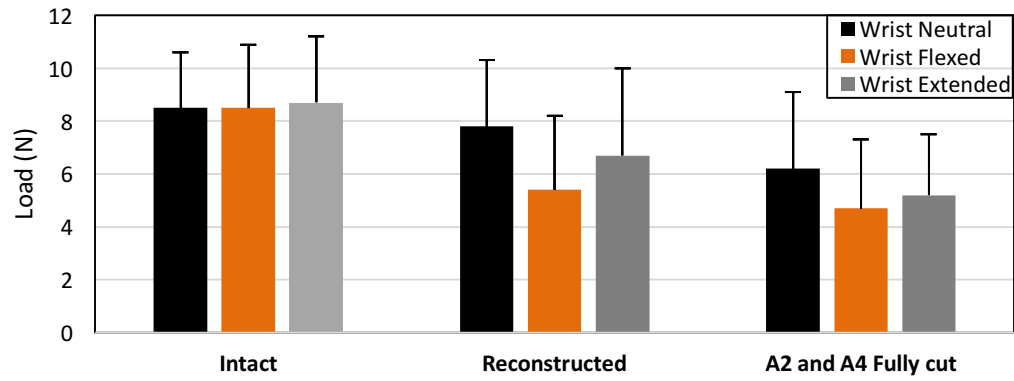
**Figure 4.6: Maximum FDP Loads intact, sectioned and reconstructed pulleys as a function of wrist position.**

## 4.3.2 Joint ROM

With the wrist in neutral, sequential sectioning of the A2 pulley alone from 50%–100% with A4 still intact significantly reduced the MCP ROM by 2.2±1.9° (p=0.015), 2.7±2.5° (p=0.019), and 4.8±4.2° (p=0.014). Full sectioning of both pulleys resulted in a significant MCP ROM loss of 9.1±7.1° (p=0.016), and restored to within 0.7° of the intact state by reconstruction (p=0.040) (*Figure 4.7*). The DIP and PIP joints did not experience similar significance.
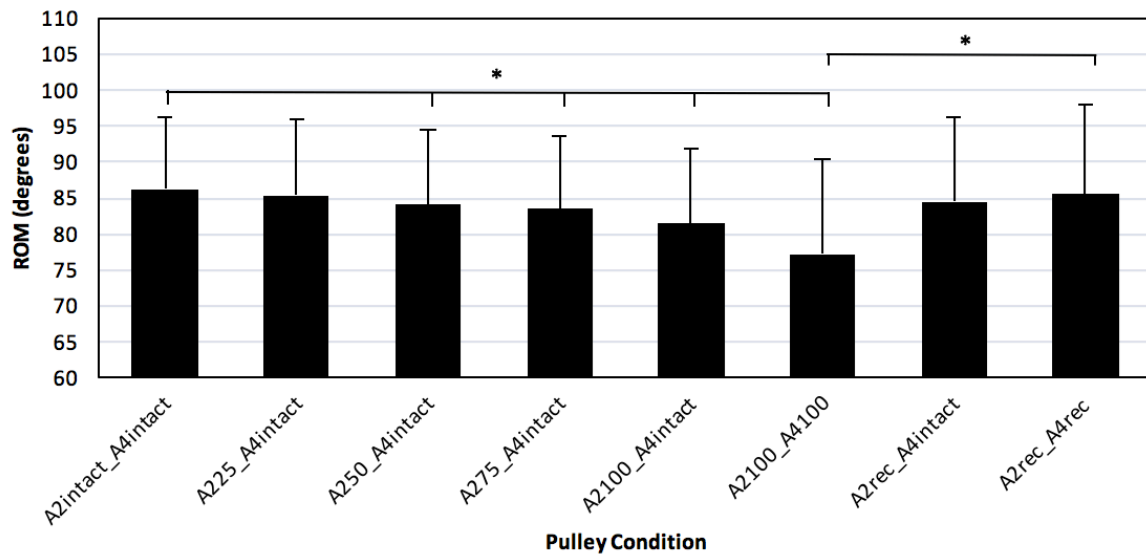


**Figure 4.7: Influence of Pulley Sectioning/Repair on MCP's ROM**

*The asterisk highlights PW significances between conditions. Error bars represent the standard deviations between specimens (n=14)*

With the wrist flexed, cutting both A2 and A4 reduced MCP ROM (p=0.002) by 7.4±6.3° (p=0.009). With the wrist extended, cutting both A2 and A4 reduced MCP ROM (p=0.006) by 7.2±7.3° (p=0.024) and reconstruction restored ROM to within 2° of the intact state (p=0.014). DIP and PIP ROM were not significantly altered. When both pulleys were fully reconstructed, there was a loss of 12±16.1° (p=0.049) in MCP ROM in wrist neutral compared to wrist flexed, as well as a 17.5±16°(p=0.004) loss in wrist neutral compared to wrist extended. In addition, there was a loss of 9.7±10.8° (p=0.015) in PIP ROM in wrist neutral compared to wrist flexed and a 10.8±14°(p=0.039) loss in wrist neutral compared to wrist extended.
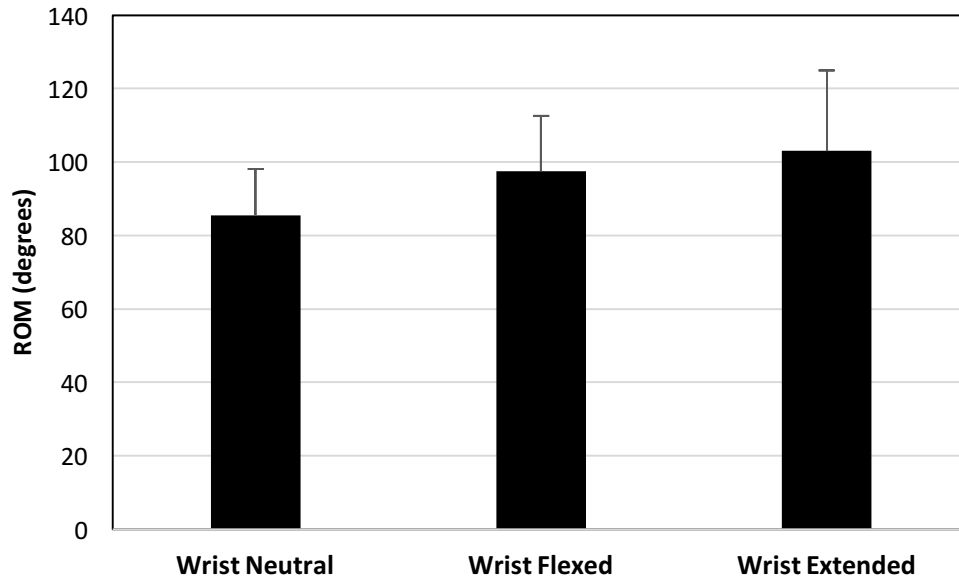
**Figure 4.8: Maximum MCP ROM following reconstructed pulleys as a function of wrist position**

## 4.4 Discussion

### 4.4.1    Effect of sequential cuts/reconstruction on Kinematics

Partial excision of the A2 pulley had the largest effect on MCP's angular rotation. With the wrist in neutral, the MCP experienced a 3%, 3%, and 6% significant reduction in its range of motion with every sequential 50%, 75%, and 100% A2 cut made compared to the intact state. In addition, each sequential cut resulted in an average significant reduction of 2% between each state. However, partial excision of the A4 pulley failed to reveal similar trends within our sample size.

Full sectioning of both pulleys also revealed significant losses not only on the joint ROM, but also in tendon load. With the wrist in neutral, MCP suffered an 11% loss in its ROM while the FDP suffered a 27% loss compared to the intact state. Furthermore, MCP and FDP metrics were reduced by 8% and 43% respectively with the wrist in flexion, and 8% and 40% respectively with the wrist in extension. Such significant losses in both ROM and load due to partial and full excisions of the pulleys signify the true importance of having a functional A2 and A4 pulley on the kinematics of the finger.

Surgical reconstruction of the pulleys is clinically common and valuable in reinstating proper kinematics of the finger. Following sequential A2 and A4 pulley reconstruction, MCP ROM and FDP loads were restored to within 0.7° (10% increase) and 0.7N (19% increase) of the intact state respectively with the wrist in neutral, 2° (5% increase) and 3N (7% increase) with the wrist in flexion, and 2° (5% increase) and 1.8 N (19% increase) with the wrist in extension. As justified by the results of this study, sequential reconstruction of the pulleys restored normal kinematics to within no significant difference of the intact state; thus, supporting the decision to reconstruct.

### 4.4.2    Effect of Wrist Position on Kinematics following Reconstruction

With both pulleys reconstructed, the wrist position had a significant effect on tendon load and ROM. The flexed wrist position resulted in a 31% reduction of FDP load compared to the neutral wrist position. Wrist extension also produced an apparent reduction, though not statistically significant. However, ROM did not seem to follow the same trends when comparing wrist

positions. Full reconstruction of the pulleys resulted in a 14% and 20% increase in MCP ROM with the wrist in flexion and extension respectively compared to the wrist neutral position. Although both ROM and load did not follow the same tendencies, the most important clinical approach when considering rehab is the management of strain that is applied onto the pulley reconstructions. Since minimizing strain is prioritized, these results may suggest that rehabilitation of surgically reconstructed flexor tendon pulleys should be carried out with the wrist flexed, as opposed to wrist in neutral as conducted in current day clinics.

This study had two limitations. Firstly, the cadaveric specimens were previously frozen and of advanced age and secondly, amputating each digit after testing it to make room for the trackers could have altered the biomechanics of the subsequent digit. However, despite the limitations, an important strength of this study is its sample size. As previously mentioned in the Methods section, a G*Power software was used to identify the number of specimens required to achieve significant trends in results and therefore, with proper computation, the sample size chosen for this study was sufficient enough to detect important trends and changes between conditions; highlighting the importance of the software when examining a study. In addition, with the sample size used, the effect sizes of the individual tendon and ROM metrics were averaged to be 0.3N and 0.2° respectively, complementing the initial hypothesis made in Chapter 1 (section 1.9).

## 4.5   Conclusion

The in-vitro finger motion simulator managed to detect significant changes in both load and ROM caused by the sectioning of A2 and A4 pulleys. As established within current clinical grounds, a patient can undergo a 50% cuts to both the A2 and A4 pulleys without significantly affecting the kinematics of the finger. These results were further strengthened within our research as the simulator was capable of detecting minor changes that occurred between each sequential cut made, with an exception for the PIP and DIP joint ROMs as they were not significantly affected by these conditions. However, the current gap in literature regarding the effect of pulley sectioning/reconstruction on tendon load has been resolved, providing additional tendon load information that compliments the state of knowledge on joint ROM. Placing the wrist in 30° of flexion has shown to result in decreased tension in the reconstructed FDP tendon compared to a neutral wrist. These results may suggest that rehabilitation protocol should be carried out with the wrist flexed in order to reduce strain on pulley reconstructions. In addition,

pulley reconstructions restored both metrics, load and ROM, with no significant difference compared to the intact state, increasing their function by not only reducing bowstringing, but by restoring natural joint.

# Chapter 5

## 5  Discussion and Future Work

*OVERVIEW: This chapter reviews the work done in previous chapters and highlights the strengths and weaknesses developed throughout this research. In addition, an outline for future work to further improve clinical research using the simulator is proposed.*

## 5.1   Summary

In order to provide the highest quality of care to a patient suffering from any trauma to the hand, fine understanding of the kinematics using appropriate instruments is vital when enhancing the treatment and rehabilitation protocols of severe injury cases. In Chapter 2, the process behind the design and development of an active finger motion simulator, as well as the method of actuation, PID tuning, and tracking was outlined. Two flexor tendons, flexor digitorum profundus and flexor digitorum superficialis, and one extensor tendon were each directly sutured onto load cells that were calibrated (Appendix A) for precise force measurements and mounted onto the shafts of the linear actuators, proper position and force feedback control. Objective 1 and Hypothesis 1 & 2 outlining the performance requirements of the simulator in Chapter 1 were satisfied in Chapter 2 as the simulator was successful in producing repeatable motions managed to yield accurate and reliable under the influence of a well-tuned PID control system during several performance tests, including an *in-vitro* test.

Chapter 3 summarized a wrist study conducted on four fingers with the sole purpose of satisfying the second objective; the system's ability to produce expected results compared to current literature. Within this study, six different wrist positions were achieved to examine the effect they have on the kinematics of the finger and loads within the flexor tendons during active flexion and extension of the finger. In addition, the effect of a simulated tear in the extensor tendon at the DIP joint was also investigated. Complimentary to literature, the largest effects in load were found with the wrist in extension and ulnar deviation, and the lacerated extensor tendon resulted in a 32° loss at the DIP joint during extension. Overall, the simulator was able to actively produce repeatable flexion/extension motion of four finger to within 0.6±0.2N between trials; surpassing the ±2N error margin constraint set.

Once the performance of the system was properly validated, Chapter 4 focused on a clinical investigation into the effects of sequential sectioning and reconstruction of the A2 and A4 pulley on the loads within the tendons, and range of motion of the finger joints. A simulated loss of the both pulleys resulted in reductions of tendon load. A reduction in joint range of motion was also observed, which is consistent with the known tendon bowstringing effect. In addition, subsequent reconstruction resulted in a near complete restoration of intact function. Wrist position in 30° of flexion caused a decrease in FDP tendon loads compared to the wrist

in neutral. This is a clinically relevant result, as it supports the clinical decision to reconstruct the pulleys. These results also suggest that post-operative rehabilitation should be carried out with the wrist flexed in order to reduce strain on the repaired pulleys. In addition, this chapter satisfied the remaining hypothesis (3 & 4) by investigating the influence of effect size on achieving significant trends within an 80% statistical power.

## 5.2   Strengths and Limitations

The active motion finger simulator developed within this work is one of the more advanced systems that is used for *in-vitro* testing. Its performance in terms of its repeatability and accuracy increases its credibility as an optimum testing tool within clinical and research grounds.

A noteworthy strength observed during the pulley study conducted in Chapter 4 is the amount of time taken for full completion of the testing protocol (t=8hrs) as opposed to Chapter 3's protocol (t = 20hrs). In light of King *et al.* [54] finding, chances of significant degradation of peak loads in tendons and the joints over time are lowered immensely during such short testing periods (<10hrs); increasing the integrity of the study.

A limitation is the use of previously frozen cadaveric specimens of advanced age. This limitation was mitigated by having an orthopedic fellow prescreen specimen CT scans for pathology.

## 5.3   Future Work

The simulator managed to satisfy every objective and hypothesis defined in Chapter 1, however further increasing of the tracking method of the joints can be achieved. Since the simulator is mostly comprised of Delrin, its compatibility to computerized tomography (CT) allows for more precise and advanced joint rotation measurements and therefore, higher accuracy when analyzing potential losses in the ranges of motion. In addition, the simulation of the lumbrical muscles of the hand along with the flexor tendon would be a valuable step to take in the advancement of the simulator. The lumbricals are intrinsic muscles of the hand that flex the MCP joints and extend the DIP and PIP joints. Their integration might be of clinical significance when carrying out future cadaveric studies.

However, the current design of simulator never failed to produce desirable outcomes, strengthening the motive to allow it to tackle further clinical studies that can be explored to achieve relevant clinical outcomes within research grounds. A specific study of clinical interest would involve examining different joint implant properties and how they each comply to the needs of a patient in terms of finger mobility and wearing of the joint. Implant development for joint arthroplasty is currently in its infancy, but is also a very interesting and draws many exciting clinical questions. Other studies might involve further dissecting and understanding the true effects and contributions of each individual carpal bone in the wrist to the tendon loads, if any. A study such as this would involve examining a pre-and post-injury and repair condition to understand the influence of trauma on the integrity of the hand.

# Bibliography

[1]    T. D. White, M. T. Black, and P. A. Folkens, *Human osteology*. Elsevier/Academic Press, 2012.

[2]    A. Kumar, T. S. Mundra, and A. Kumar, "Anatomy of the Hand," in *Encyclopedia of Biometrics*, Boston, MA: Springer US, 2015, pp. 19–28.

[3]    J. R. Doyle and M. J. Botte, *Surgical anatomy of the hand and upper extremity*. Lippincott Williams & Wilkins, 2003.

[4]    J. M. Hunter, L. H. Schneider, and E. J. Mackin, *Tendon Surgery in the Hand*. Mosby, 1987.

[5]    M. Griffin, S. Hindocha, D. Jordan, M. Saleh, and W. Khan, "An overview of the management of flexor tendon injuries.," *Open Orthop. J.*, vol. 6, pp. 28–35, 2012.

[6]    J. R. Doyle, "Anatomy of the finger flexor tendon sheath and pulley system," *J. Hand Surg. Am.*, vol. 13, no. 4, pp. 473–484, Jul. 1988.

[7]    B. Zafonte, D. Rendulic, R. M. Szabo, H. Inanami, N. Kuroshima, and S. Pechlaner, "Flexor pulley system: anatomy, injury, and management.," *J. Hand Surg. Am.*, vol. 39, no. 12, p. 2525–32; quiz 2533, Dec. 2014.

[8]    Mosby, Hunter, Macken, and Callahan, "Rehabilitation of the Hand: Surgery and Therapy," Mosby, 1995, p. Vol.1.

[9]    I. Schöffl, K. Oppelt, J. Jüngert, A. Schweizer, T. Bayer, W. Neuhuber, and V. Schöffl, "The influence of concentric and eccentric loading on the finger pulley system," *J. Biomech.*, vol. 42, no. 13, pp. 2124–2128, Sep. 2009.

[10]   I. Roloff, V. R. Schöffl, L. Vigouroux, and F. Quaine, "Biomechanical model for the determination of the forces acting on the finger pulley system," *J. Biomech.*, vol. 39, no. 5, pp. 915–923, Jan. 2006.

[11] O. Hauger, C. B. Chung, N. Lektrakul, M. J. Botte, D. Trudell, R. D. Boutin, and D. Resnick, "Pulley System in the Fingers: Normal Anatomy and Simulated Lesions in Cadavers at MR Imaging, CT, and US with and without Contrast Material Distention of the Tendon Sheath," *Radiology*, vol. 217, no. 1, pp. 201–212, Oct. 2000.

[12] J. C. Chow, J. Sensinger, D. McNeal, B. Chow, F. Amirouche, and M. Gonzalez, "Importance of proximal A2 and A4 pulleys to maintaining kinematics in the hand: a biomechanical study.," *Hand (N. Y).*, vol. 9, no. 1, pp. 105–11, Mar. 2014.

[13] J. R. Doyle, "Anatomy of the flexor tendon sheath and pulley system: a current review.," *J. Hand Surg. Am.*, vol. 14, no. 2 Pt 2, pp. 349–51, Mar. 1989.

[14] S. J. Heithoff, L. H. Millender, and J. Helman, "Bowstringing as a complication of trigger finger release.," *J. Hand Surg. Am.*, vol. 13, no. 4, pp. 567–70, Jul. 1988.

[15] C. E. de Putter, R. W. Selles, S. Polinder, M. M. Panneman, S. R. Hovius, and E. F. van Beeck, "Economic Impact of Hand and Wrist Injuries: Health-Care Costs and Productivity Costs in a Population-Based Study," *J. Bone Jt. Surgery-American Vol.*, vol. 94, no. 9, pp. e56-1–7, May 2012.

[16] J. P. de Jong, J. T. Nguyen, A. J. M. Sonnema, E. C. Nguyen, P. C. Amadio, and S. L. Moran, "The incidence of acute traumatic tendon injuries in the hand and wrist: a 10-year population-based study.," *Clin. Orthop. Surg.*, vol. 6, no. 2, pp. 196–202, Jun. 2014.

[17] Strickland, "Flexor Tendon Injuries: II. Operative Technique.," *J. Am. Acad. Orthop. Surg.*, vol. 3, no. 1, pp. 55–62, Jan. 1995.

[18] J. Strickland, "Results of flexor tendon surgery in zone II," *Hand Clin.*, no. 1, pp. 67–79, 1985.

[19] S. Bunnell, *Surgery of the Hand*, 2nd ed. Philadelphia : J.B. Lippincott Co., 1948.

[20] C. E. Verdan, "Primary repair of flexor tendons.," *J. Bone Joint Surg. Am.*, vol. 42–A, pp. 647–57, Jun. 1960.

[21] L. H. Schneider and S. B. Feldscher, *Tenolysis: Dynamic Approach to Surgery and Therapy*. Philadelphia, 2002.

[22] T. Pillukat, R. Fuhrmann, J. Windolf, and J. van Schoonhoven, "Tenolysis of the flexor tendons in the hand," *Der Orthopäde*, vol. 44, no. 10, pp. 767–76, Oct. 2015.

[23] M. Jaibaji, "Advances in the biology of zone 2 flexor tendon healing and adhesion formation," *Ann Plast. Surg.*, vol. 45, pp. 83–92, 2000.

[24] J. K. F. Wong, Y. H. Lui, Z. Kapacee, K. E. Kadler, M. W. J. Ferguson, and D. A. McGrouther, "The cellular biology of flexor tendon adhesion formation: an old problem in a new paradigm.," *Am. J. Pathol.*, vol. 175, no. 5, pp. 1938–51, Nov. 2009.

[25] J. Strickland, "Flexor tendon injuries: Foundations of treatment," *J Am Acad Ortho Surg*, vol. 3, pp. 44–45, 1995.

[26] D. Elliot and D. McGrouther, "The excursions of the long extensor tendons of the hand," *J. Hand Surg. J. Br. Soc. Surg. Hand*, vol. 11, no. 1, pp. 77–80, Feb. 1986.

[27] S. R. Bollen, "Soft tissue injury in extreme rock climbers," *Br. J. Sports Med.*, vol. 22, no. 4, pp. 145–7, Dec. 1988.

[28] V. Schöffl, T. Hochholzer, H. P. Winkelmann, and W. Strecker, "Pulley injuries in rock climbers," *Wilderness Environ. Med.*, vol. 14, no. 2, pp. 94–100, 2003.

[29] J. T. Rohrbough, M. K. Mudge, and R. C. Schilling, "Overuse injuries in the elite rock climber," *Med. Sci. Sports Exerc.*, vol. 32, no. 8, pp. 1369–72, Aug. 2000.

[30] A. Schweizer, "Biomechanical properties of the crimp grip position in rock climbers," *J. Biomech.*, vol. 34, no. 2, pp. 217–223, Feb. 2001.

[31] C. Norkin and D. White, *Measurement of joint motion : a guide to goniometry*, 5th ed. Jaypee Brothers Medical Publishers, 2009.

[32] R. L. Gajdosik and R. W. Bohannon, "Goniometry Emphasizing Reliability and Validity Clinical Measurement of Range of Motion: Review of Clinical Measurement of Range of

Motion Review of Goniometry Emphasizing Reliability and Validity," *PHYS THER*, vol. 67, pp. 1867–1872, 1987.

[33] T. Pillukat, R. Fuhrmann, J. Windolf, and J. van Schoonhoven, "Tenolysis of the flexor tendons in the hand," *Orthopade*, vol. 44, no. 10, pp. 767–776, Oct. 2015.

[34] K. Dorfmuller-Ulhaas and D. Schmalstieg, "Finger tracking for interaction in augmented environments," in *Proceedings IEEE and ACM International Symposium on Augmented Reality*, pp. 55–64.

[35] D. D. Frantz, A. D. Wiles, S. E. Leis, and S. R. Kirsch, "Accuracy assessment protocols for electromagnetic tracking systems.," *Phys. Med. Biol.*, vol. 48, no. 14, pp. 2241–51, Jul. 2003.

[36] A. T. Corporation, *3D Guidance trakSTAR*. 2013.

[37] T. Tanaka, P. C. Amadio, C. Zhao, M. E. Zobitz, and K.-N. An, "Flexor Digitorum Profundus Tendon Tension during Finger Manipulation A Study in Human Cadaver Hands."

[38] D. Greenwald, S. Shumway, C. Allen, and D. Mass, "Dynamic analysis of profundus tendon function," *J. Hand Surg. Am.*, vol. 19, no. 4, pp. 626–635, Jul. 1994.

[39] T.-H. Yang, S.-C. Lu, W.-J. Lin, K. Zhao, C. Zhao, K.-N. An, I.-M. Jou, P.-Y. Lee, L.-C. Kuo, and F.-C. Su, "Assessing Finger Joint Biomechanics by Applying Equal Force to Flexor Tendons In Vitro Using a Novel Simultaneous Approach.," *PLoS One*, vol. 11, no. 8, p. e0160301, 2016.

[40] F. Schuind, M. Garcia-Elias, W. P. Cooney, and K.-N. An, "Flexor tendon forces: In vivo measurements," *J. Hand Surg. Am.*, vol. 17, no. 2, pp. 291–298, Mar. 1992.

[41] J. T. Dennerlein, "Finger Flexor Tendon Forces Are a Complex Function of Finger Joint Motions and Fingertip Forces," *J. Hand Ther.*, vol. 18, no. 2, pp. 120–127, 2005.

[42] D. A. McGrouther and M. R. Ahmed, "Flexor tendon excursions in no-man's land," *Hand*,

vol. 13, no. 2, pp. 129–41, Jun. 1981.

[43]   W. K. Ho, O. P. Gan, E. B. Tay, and E. L. Ang, "Performance and gain and phase margins of well-known PID tuning formulas," *IEEE Trans. Control Syst. Technol.*, vol. 4, no. 4, pp. 473–477, Jul. 1996.

[44]   Z.-M. Li, "The influence of wrist position on individual finger forces during forceful grip," *J. Hand Surg. Am.*, vol. 27, no. 5, pp. 886–96, Sep. 2002.

[45]   J.-A. Lee and S. Sechachalam, "The Effect of Wrist Position on Grip Endurance and Grip Strength," vol. 41, no. 10.

[46]   J. C. Pryce, "The wrist position between neutral and ulnar deviation that facilitates the maximum power grip strength," *J. Biomech.*, vol. 13, no. 6, Jan. 1980.

[47]   S. L. Halson, "Monitoring training load to understand fatigue in athletes.," *Sports Med.*, vol. 44 Suppl 2, no. Suppl 2, pp. S139-47, Nov. 2014.

[48]   G. Salvendy, *Handbook of human factors and ergonomics*. John Wiley & Sons, 2012.

[49]   D. Oravcová, "Injury of the extensor mechanism in the zone I - mallet deformity," *Rozhl. Chir.*, vol. 93, no. 3, pp. 117–22, Mar. 2014.

[50]   B. Okafor, C. Mbubaegbu, I. Munshi, and D. J. Williams, "Mallet Deformity of the Finger," *Bone Joint J.*, vol. 79–B, no. 4, 1997.

[51]   G. P. Crawford, "The Molded Polythene Splint for Mallet Finger Deformities.," *J. Hand Surg. Am.*, vol. 9, no. 2, pp. 231–7, Mar. 1984.

[52]   R. A. Warren, S. H. Norris, and D. G. Ferguson, "Mallet finger: a Trial of Two Splints," *J. Hand Surg. Br.*, vol. 13, no. 2, pp. 151–3, May 1988.

[53]   K. Nakamura and B. Nanjyo, "Reassessment of surgery for mallet finger.," *Plast. Reconstr. Surg.*, vol. 93, no. 1, pp. 141-9–1, Jan. 1994.

[54]   G. J. King, C. L. Pillon, and J. A. Johnson, "Effect of in vitro testing over extended

periods on the low-load mechanical behaviour of dense connective tissues.," *J. Orthop. Res.*, vol. 18, no. 4, pp. 678–81, Jul. 2000.

[55] D. Rispler, D. Greenwald, S. Shumway, C. Allan, and D. Mass, "Efficiency of the flexor tendon pulley system in human cadaver hands.," *J. Hand Surg. Am.*, vol. 21, no. 3, pp. 444–50, May 1996.

[56] I. Kwai Ben and D. Elliot, "'Venting' or partial lateral release of the A2 and A4 pulleys after repair of zone 2 flexor tendon injuries.," *J. Hand Surg. Br.*, vol. 23, no. 5, pp. 649–54, Oct. 1998.

[57] G. Mitsionis, K. J. Fischer, J. A. Bastidas, R. Grewal, H. J. Pfaeffle, and M. M. Tomaino, "Feasibility of Partial A2 and A4 Pulley Excision: Residual Pulley Strength," *J. Hand Surg. Am.*, vol. 25, no. 1, pp. 90–94, Feb. 2000.

[58] M. Tomaino, G. Mitsionis, J. Basitidas, R. Grewal, and J. Pfaeffle, "The effect of partial excision of the A2 and A4 pulleys on the biomechanics of finger flexion.," *J. Hand Surg. Br.*, vol. 23, no. 1, pp. 50–2, Feb. 1998.

[59] G. Mitsionis, J. A. Bastidas, R. Grewal, H. J. Pfaeffle, K. J. Fischer, and M. M. Tomaino, "Feasibility of partial A2 and A4 pulley excision: effect on finger flexor tendon biomechanics.," *J. Hand Surg. Am.*, vol. 24, no. 2, pp. 310–4, Mar. 1999.

[60] S.-C. Lu, T.-H. Yang, L.-C. Kuo, I.-M. Jou, Y.-N. Sun, and F.-C. Su, "Effects of Different Extents of Pulley Release on Tendon Excursion Efficiency and Tendon Moment Arms," *J. Orthop. Res.*, vol. 33, no. 2, pp. 224–228, Feb. 2015.

[61] G. T. Lin, P. C. Amadio, K. N. An, W. P. Cooney, and E. Y. Chao, "Biomechanical analysis of finger flexor pulley reconstruction.," *J. Hand Surg. Br.*, vol. 14, no. 3, pp. 278–82, Aug. 1989.

# Appendices

## Appendix A: Load cell and PID calibration

## A.1 Validation of the Load Cell

To calibrate and validate the performance of the 1DOF in-line load cells (MDN 34, Honeywell, OH) used for providing reliable force data, a series of known masses were hung in 2g increments with the load cell in a vertical orientation. Initial zeroing of the load cell was necessary before applying the first load. This test revealed a strong agreement between the load cell and the applied mass with coefficient of determination of $R^2$ = 0.99997 and an average error of 0.2 $\pm$ 0.13g (*figure A.1*).
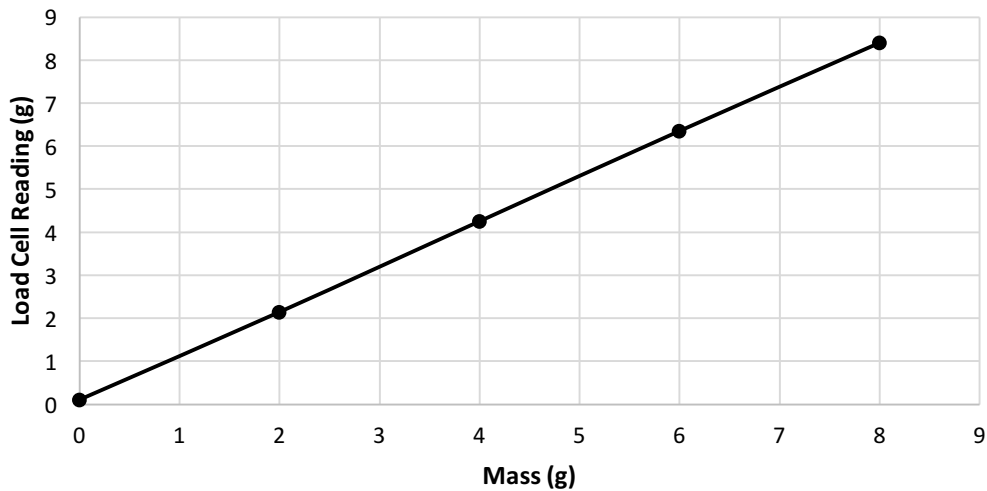


**Figure A.1: Load Cell Calibration**

*The load cell was validated by hanging masses of known quantities in 2g increments and had an $R^2$ value of 0.99997*

# A.2 PID Calibration

To validate the performance of the closed loop force feedback system, a PID was built and the individual gains (proportional, integral, and derivative) were tuned to minimize any errors within the system. Target forces ranging from 0-25N in 5N increments were set for the controller to achieve and gain values for each unit were individually varied between trial runs to denote their effect on the performance of the simulator as demonstrated in the graphs below.

## A.2.1 Effect of Proportional Gain (K)

As demonstrated in the figures below, an increase in the proportional gain causes an increase in noise in the system as the actuator becomes more over-responsive.
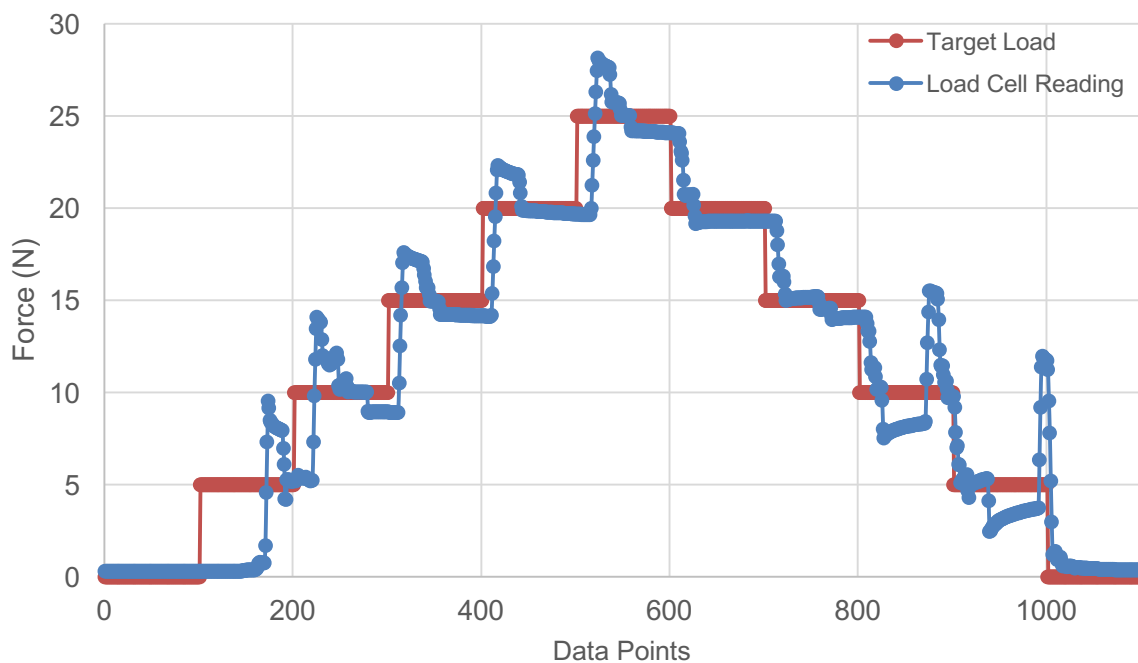


**Figure A.2.1.1: Response Graph for Proportional Gain K = 0.5**
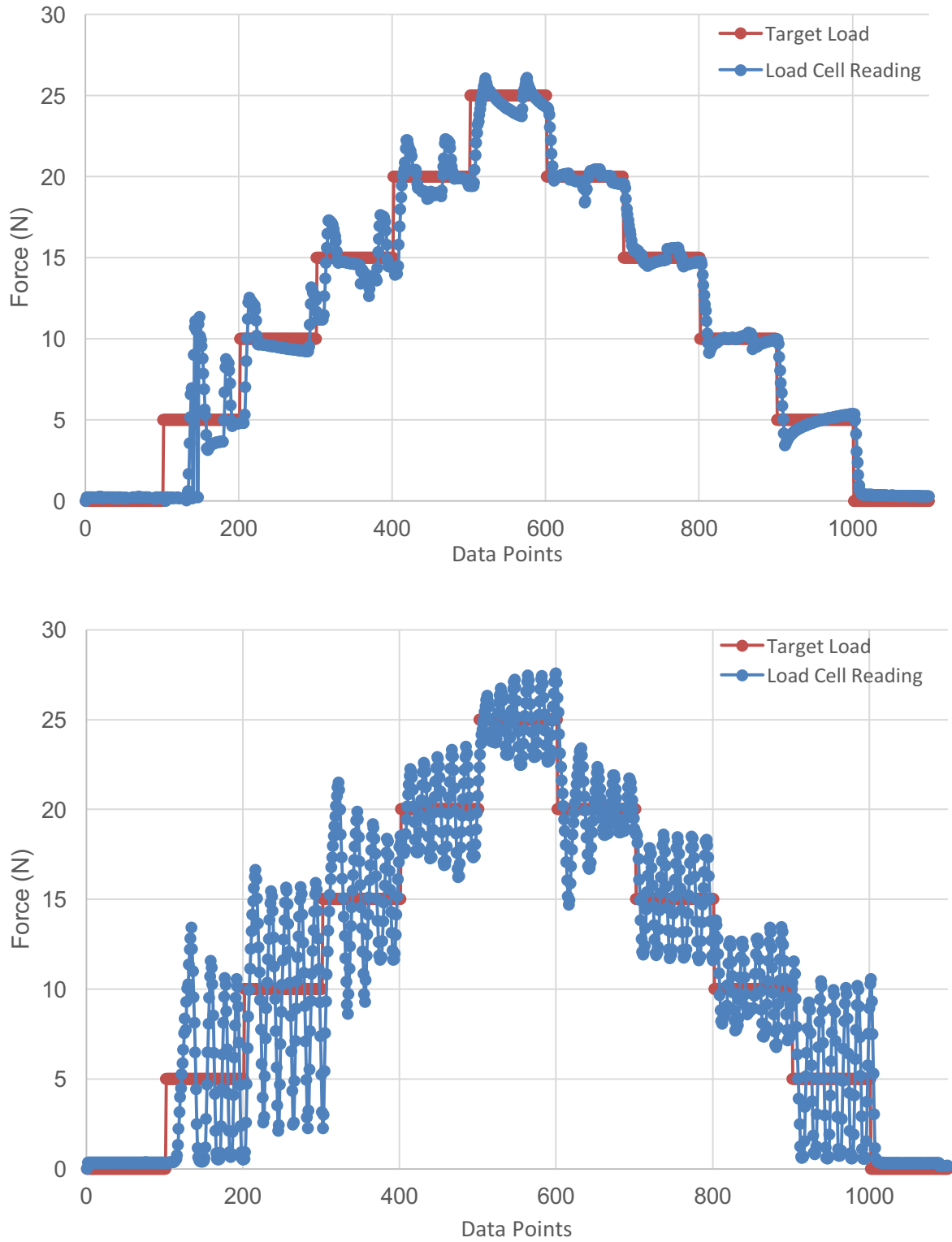
**Figure A.2.1.2: Response Graph for Proportional Gain K = 1.5 and K=5**

K=1.5(top), K=5 (bottom). *As gain increases, the motor becomes more aggressive to changes in load*

## A.2.2 Effect of Integral Gain (I)

As demonstrated in the figures below, an increase in the integral gain causes the simulator to be overall less responsive to changes in load; increasing error.
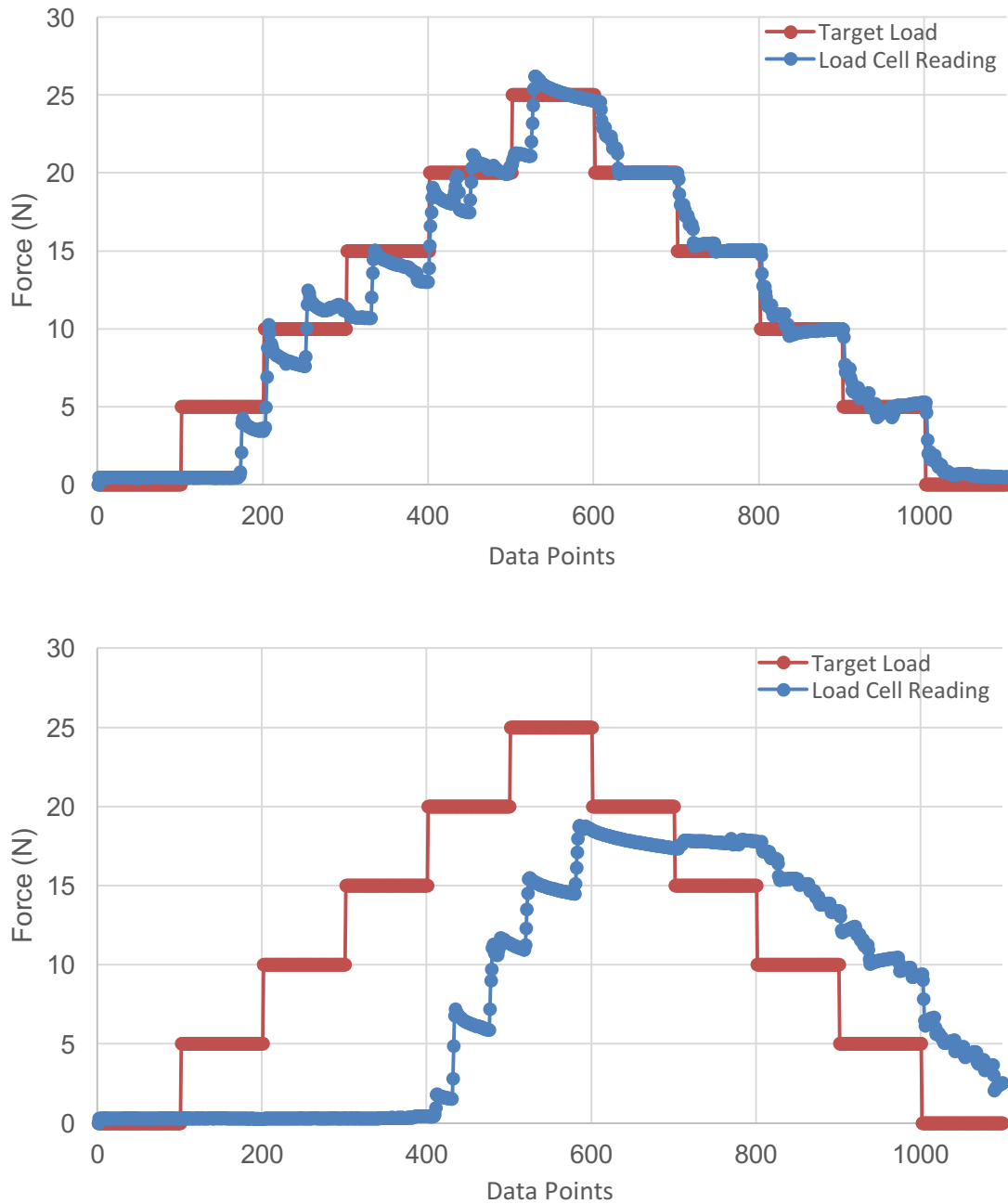


**Figure A.2.2.1: Response Graph for Integral Gain I = 0.01 and I= 0.05**

*I = 0.01 (top) and I= 0.05 (bottom)*
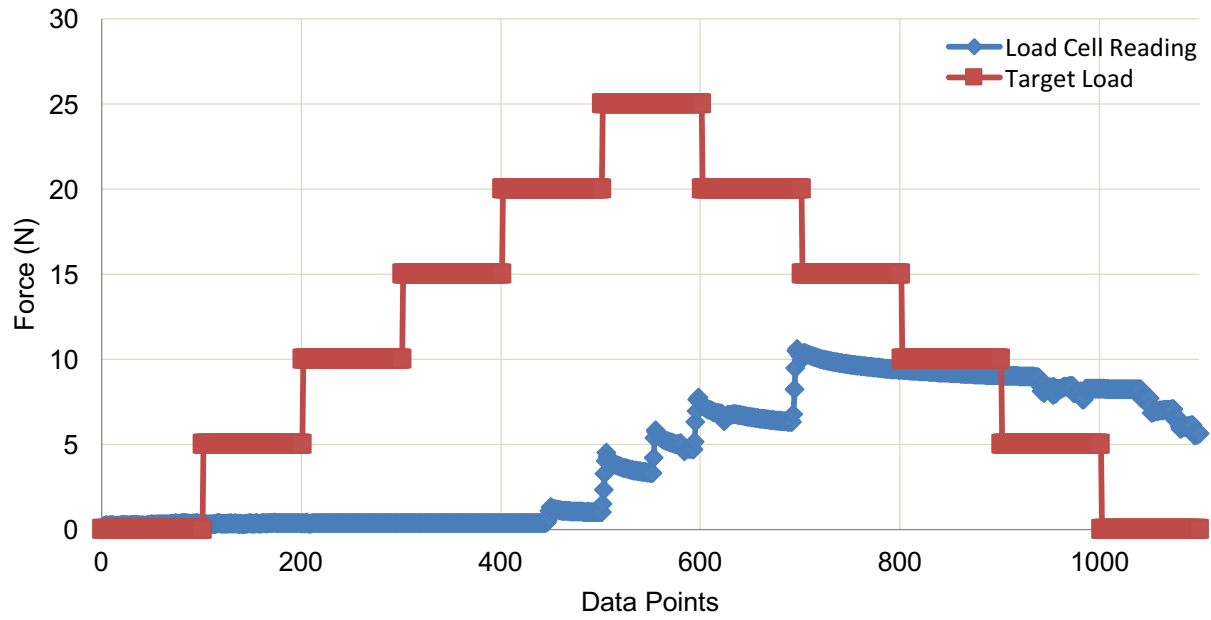
**Figure A.2.2.2: Response Graph for Integral Gain I=0.1**

*As the gain increases, the motor becomes less sensitive to load.*

## A.2.3 Effect of derivative Gain (D)

An increase in the derivate gain did not seem to demonstrate as big of an effect on the simulator's performance as do other metrics. However, similar to other gains, an increase in the derivative metric resulted in more noise in the system.
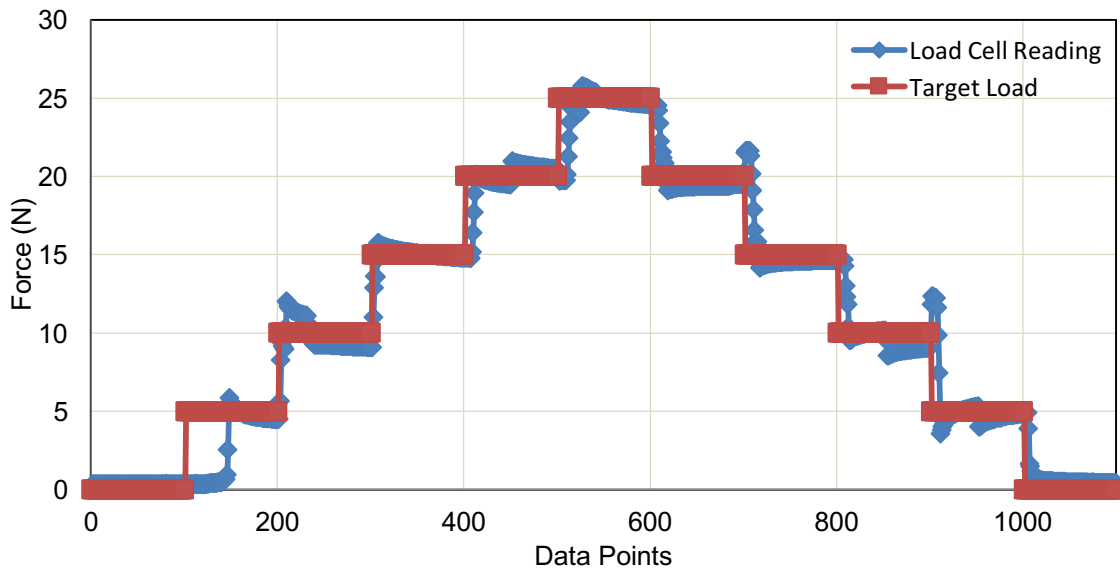


**Figure A.2.3.1: Response Graph for Derivative Gain D = 0.005**
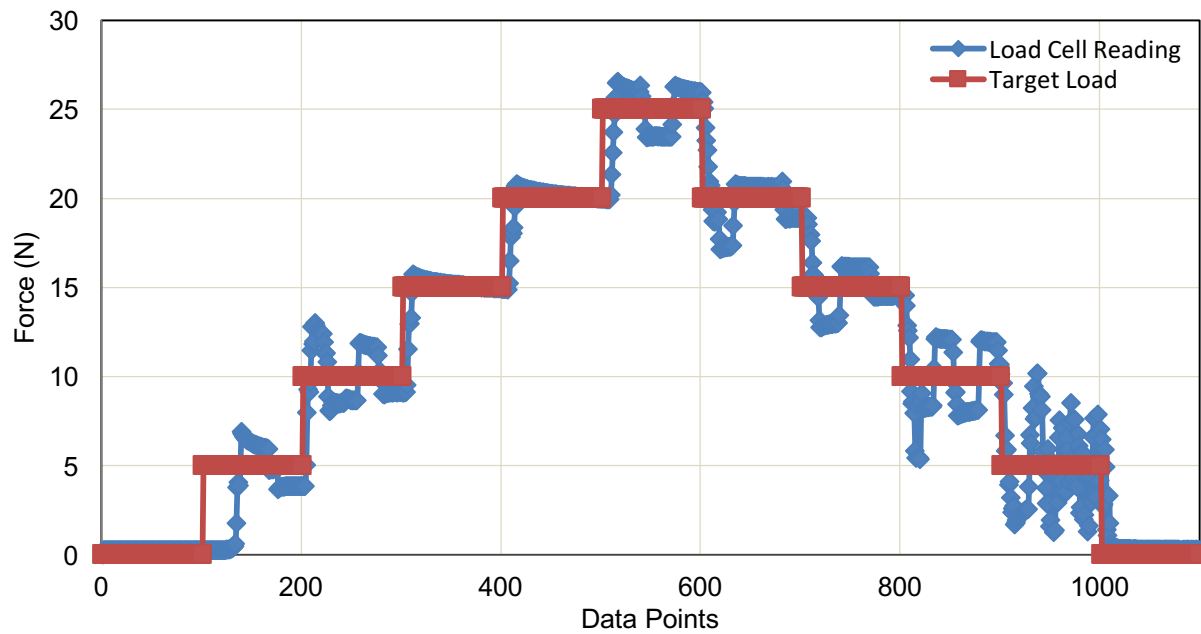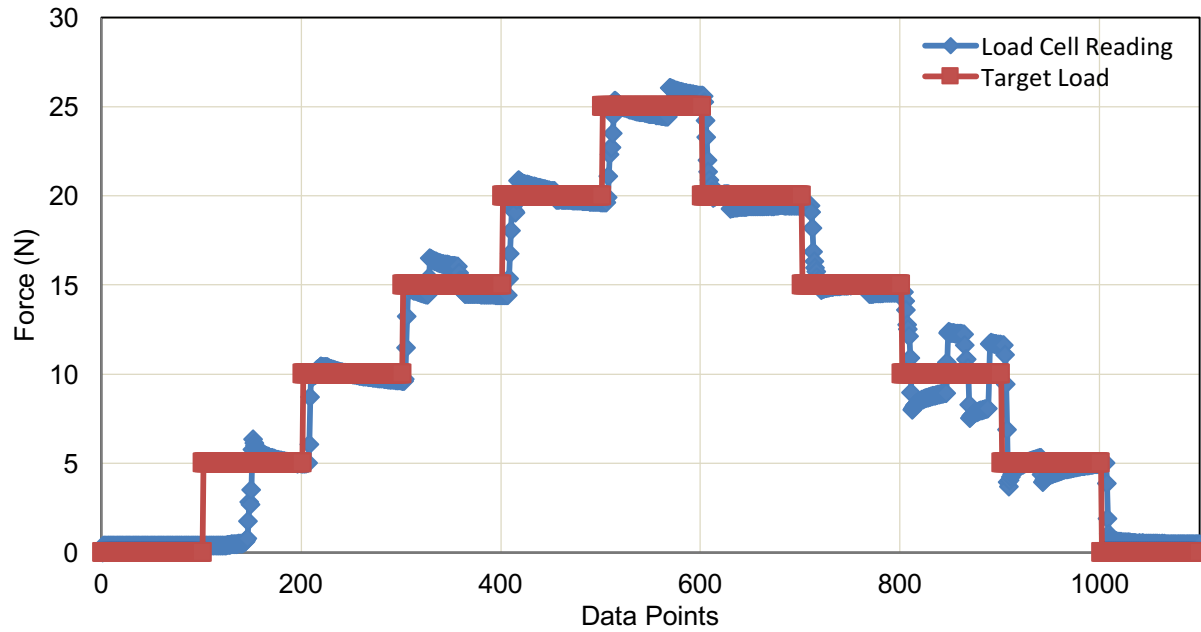
**Figure A.2.3.2: Response Graph for Derivative Gain D = 0.007 and D= 0.05**

*D= 0.007 (top) and D= 0.05 (bottom)*

# Appendix B: Technical Drawings/Pictures of Simulator Components

-All measurements illustrated in inches.

2

1

14.00

0.50

B

18.00

B

0.50

14.00

A

A

| | | DIMENSIONS ARE IN INCHES | | NAME | DATE | | | |
| | | TOLERANCES: | | | | | | |
| | | FRACTIONAL ± | DRAWN | | | | | |
| | | ANGULAR: MACH ± BEND ± | CHECKD | | | | | |
| | | TWO PLACE DECIMAL ± | ENG APPR. | | | | | |
| | | THREE PLACE DECIMAL ± | MFG APPR. | | | | | |
| | | | Q.A. | | | | | |
| | | MATERIAL | COMMENTS | | | | | |
| NEXT ASSY | USED ON | FINISH | | | | SIZE DWG. NO. | Back Base | REV. |
| APPLICATION | | DO NOT SCALE DRAWING | | | | A | | |
| | | | | | | SCALE: 1:8 WEIGHT: | SHEET 1 OF 1 | |

5.00

0.43

0.53

3.10

4.15

2.50

2.00

2.00

2.00

2.50

11.00

0.25

Ø0.2660

0.2660

100°

| | | | DIMENSIONS ARE IN INCHES TOLERANCES: FRACTIONAL± ANGULAR: MACH± BEND ± TWO PLACE DECIMAL ± THREE PLACE DECIMAL ± | | NAME | DATE | | | |
|---|---|---|---|---|---|---|---|---|---|
| | | | | DRAWN | | | | | |
| | | | | CHECKED | | | | | |
| | | | | ENG APPR | | | | | |
| | | | | MFG APPR | | | | | |
| | | | MATERIAL | Q.A | | | | | |
| | | | | COMMENTS: | | | | | |
| NEXT ASSY | USED ON | FINISH | | | | SIZE A | DWG NO | Base Plate | REV |
| APPLICATION | | DO NOT SCALE DRAWING | | | | SCALE:1:5 | WEIGHT | SHEET 1 OF 1 | |

6.00
5.5
5.00
5.75
0.25

0.25
0.25
0.3125

0.25
5.50
0.31250
6.00

B

B

A

A

2

1

| | | DIMENSIONS ARE IN INCHES | | NAME | DATE | | | |
| TOLERANCES: | | | | | | | | |
| FRACTIONAL± | | | | DRAWN | | | | |
| ANGULAR: MACH± BEND ± | | | | CHECKED | | | | |
| TWO PLACE DECIMAL ± | | | | ENG APPR | | | | |
| THREE PLACE DECIMAL ± | | | | MFG APPR | | | | |

MATERIAL
Q.A.
COMMENTS:

NEXT ASSY    USED ON
APPLICATION

FINISH
DO NOT SCALE DRAWING

SIZE A    DWG NO    **Front Base**    REV

SCALE:1:100    WEIGHT    SHEET 1 OF 1

2

1

Vertical Upright

2 1

4.00

R3.00

4.00

6.00

0.25

7.00

18.00

4.00

0.25

0.25

1.00

B B

A A

| | | DIMENSIONS ARE IN INCHES TOLERANCES: FRACTIONAL± ANGULAR: MACH± BEND ± TWO PLACE DECIMAL ± THREE PLACE DECIMAL ± | | NAME | DATE | | |
|---|---|---|---|---|---|---|---|
| | | | DRAWN | | | | |
| | | | CHECKED | | | | |
| | | | ENG APPR | | | | |
| | | | MFG APPR | | | | |
| | | MATERIAL | Q.A. | | | | |
| | | | COMMENTS: | | | | |
| NEXT ASSY | USED ON | FINISH | | | | SIZE DWG. NO | Dome | REV |
| APPLICATION | | DO NOT SCALE DRAWING | | | | A | | |
| | | | | | | SCALE: | SHEET | |

2 1

2

1

Ø0.10

2.20

3.00

0.55

4.37

0.40

3.00

4.00

B                                                                B

0.98

0.46

0.55

R0.33

2.75

2.20

0.40

A                                                                A

| | | DIMENSIONS ARE IN INCHES | | NAME | DATE | | |
| | | TOLERANCES: | DRAWN | | | | |
| | | FRACTIONAL± | CHECKED | | | | |
| | | ANGULAR: MACH± BEND ± | ENG APPR | | | | |
| | | TWO PLACE DECIMAL ± | | | | | |
| | | THREE PLACE DECIMAL ± | MFG APPR | | | | |
| | | | Q.A | | | | |
| | | MATERIAL | COMMENTS: | | | | |
| NEXT ASSY | USED ON | FINISH | | | SIZE A | Motor Lower Mount | REV |
| APPLICATION | | DO NOT SCALE DRAWING | | | SCALE:1:2 WEIGHT: | | SHEET 1 OF 1 |

2

1

2      1

3.58

Ø0.20

1.27

B

3.00

B

R1.40

0.31

A

A

| | | |
|---|---|---|
| DIMENSIONS ARE IN INCHES | | |
| TOLERANCES: | | |
| FRACTIONAL± | | |
| ANGULAR: MACH±  BEND ± | | |
| TWO PLACE DECIMAL    ± | | |
| THREE PLACE DECIMAL  ± | | |

| | NAME | DATE |
|---|---|---|
| DRAWN | | |
| CHECKED | | |
| ENG APPR. | | |
| MFG APPR. | | |
| Q.A. | | |
| COMMENTS: | | |

MATERIAL

FINISH

NEXT ASSY | USED ON

APPLICATION | DO NOT SCALE DRAWING

**Motor Upper Mount**

SIZE A | SCALE:1:2 | WEIGHT: | SHEET 1 OF 1

2      1

R0.39

2.00

1.00

4.00

1.00

0.50

3.50

2.00

0.50

DIMENSIONS ARE IN INCHES
TOLERANCES:
FRACTIONAL±
ANGULAR: MACH± BEND ±
TWO PLACE DECIMAL ±
THREE PLACE DECIMAL ±

NAME | DATE
DRAWN
CHECKED
ENG APPR
MFG APPR
Q.A
COMMENTS:

MATERIAL

FINISH

NEXT ASSY | USED ON

APPLICATION | DO NOT SCALE DRAWING

SIZE **A**

**Rod Guide**

REV

SCALE:1:2 | WEIGHT: | SHEET 1 OF 1

**Figure B.1: Top View Assembly of Simulator**

*with a phantom hand representing a cadaver*
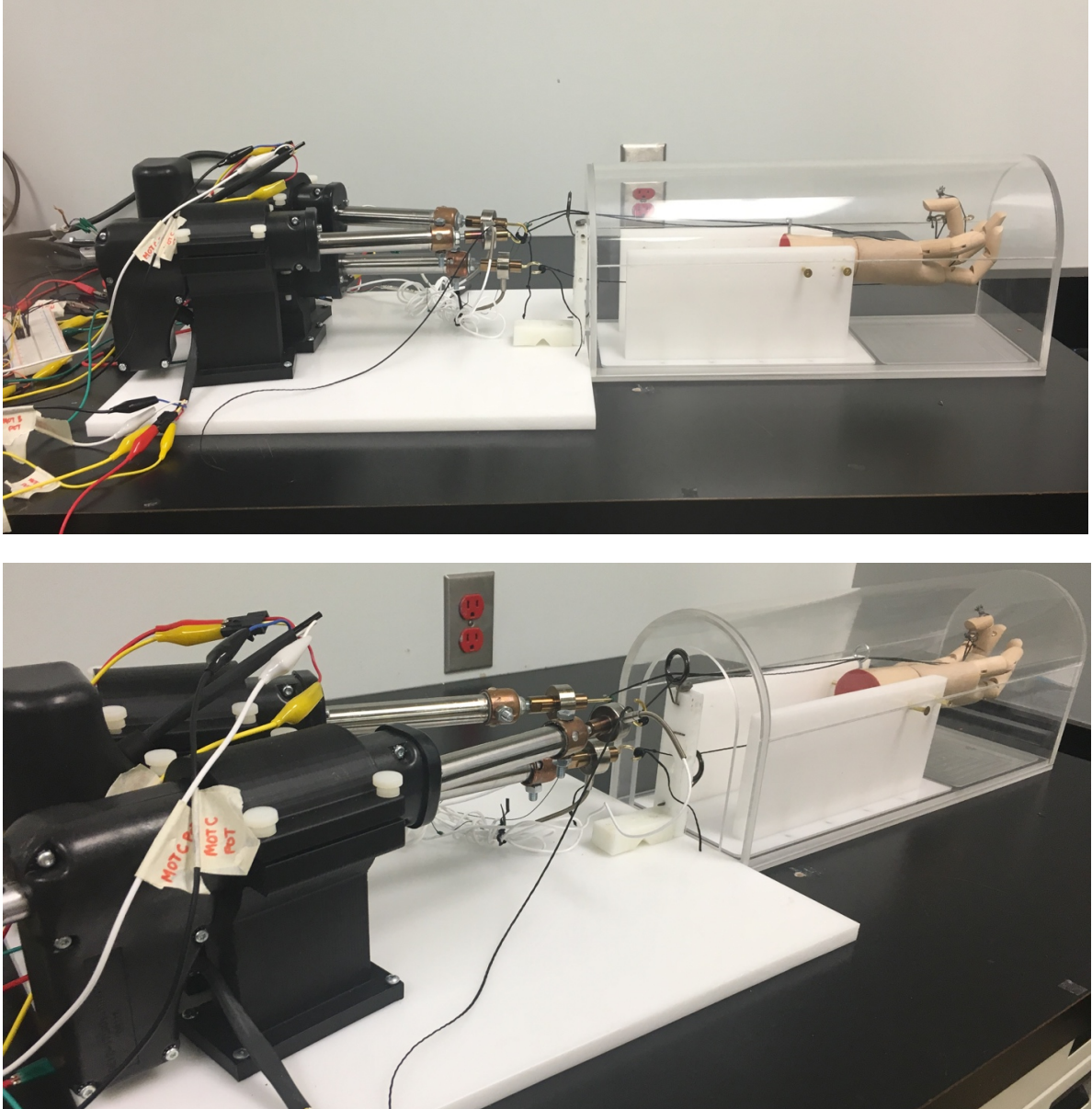
**Figure B.2: Different Views of Simulator**

*Side view (top), Isometric view (bottom)*

**Figure B.3: Cap, Rod Guide, and Motor Mount**

*Cap design for mounting the load cell onto the motor (top), Rod guide assembly (bottom left),*

*and 3D printed motor mount (bottom right)*

# Appendix C: Arduino Code

## C.1 Main code file

```
#include "L298MotorDriver.h"
const int tolerance = 3;
//speedPin, in13, in24, potPin, tolerance, (bool) printStatements

L298MotorDriver motor1('1', 2, 4, 5, 1, 0, 234, tolerance);
L298MotorDriver motor2('2', 6, 8, 7, 4, 0, 234, tolerance);
L298MotorDriver motor3('3', 9, 10, 11, 3, 0, 234, tolerance);

void setup() {
        Serial.begin(115200);
        Serial.println("Mutli-Motor driver testing V1.0");
        delay (1000);
}
bool m1updated = false, m2updated = false, m3updated = false;
void loop ()
{
        if (m1updated)
        {motor1.update();} else
        {m1updated = motor1.update();}
        if (m2updated)
        {motor2.update();}
        else
        {m2updated = motor2.update();}
        if (m3updated)
        {motor3.update();}
        else
        {m3updated = motor3.update();}
if (m1updated && m2updated && m3updated)
        {Serial.println();
                m1updated = false;
                m2updated = false;
                m3updated = false;}
}
void serialEvent () {
        char motor = char (Serial.read());
        delay (10);
        char command = char (Serial.read());
        Serial.println(motor);
        Serial.println(command);
        String val = "";

delay(5);
        char currentChar = ' ';
        while (Serial.available()) {
                currentChar =
char(Serial.read());
                if (currentChar == '$')
                        break;
                val += currentChar;
                delay(5);
        }
        switch (motor)
        {case '1':

        motor1.parseCommand(command, val);
                break;
        case '2':

        motor2.parseCommand(command, val);
                break;
        case '3':

        motor3.parseCommand(command, val);
                break;
        default:
                Serial.print("Motor '");
                Serial.print(motor);
                Serial.print("' is not a valid
option.");
                break;
        }
}
```

## C.2 Motor Driver File

```cpp
#include "L298MotorDriver.h"
L298MotorDriver::L298MotorDriver(
        char id, int speedPin,
        int in13, int in24,
        int potPin, int tolerance,
        int potMin, int potMax,
        bool printStatements)
        : _id(id)
{
        this->_enAB = speedPin;
        this->_in13 = in13;
        this->_in24 = in24;

        this->_pot = potPin;

        this->_tolerance = tolerance;

        this->_printStatements = printStatements;

        this->_rawSpeed = 0;
        this->_rawPosCmd = 0;

        this->_speed = 100;

        this->_stmt = -1;

        this->_potMin = potMin;
        this->_potMax = potMax;

        pinMode(this->_enAB, OUTPUT);
        pinMode(this->_in13, OUTPUT);
        pinMode(this->_in24, OUTPUT);

        analogWrite(this->_enAB, 0);
        digitalWrite(this->_in13, LOW);
        digitalWrite(this->_in24, LOW);
}

bool L298MotorDriver::update()
{
        static bool printed = false;

        _tNow = millis();
        if (_printStatements && (_tNow - _tPrev >
_updatePeriod)) {
                _tPrev = _tNow;

                Serial.print("Id: ");

                Serial.print(", stmt: ");
                        Serial.print(_stmt);

                        Serial.print(", actualPosCmd:
");
                        Serial.print(_actualPosCmd);

                        Serial.print(", Raw Motor
Pos:");

                Serial.println(analogRead(_pot));

                        printed = true;
        } else
        {
                printed = false;
        }

        int actualPos = analogRead(_pot);
        if (actualPos < (_actualPosCmd -
_tolerance)) {
                digitalWrite(_in13, HIGH);
                digitalWrite(_in24, LOW);
                analogWrite(_enAB, _speed);
                _stmt = 0;
        }
        else if (actualPos >(_actualPosCmd +
_tolerance)) {
                digitalWrite(_in13, LOW);
                digitalWrite(_in24, HIGH);
                analogWrite(_enAB, _speed);
                _stmt = 1;
        }
        else {
                digitalWrite(_in13, LOW);
                digitalWrite(_in24, LOW);
                analogWrite(_enAB, 0);
                _stmt = 2;
        }

        return printed;
}
```

```cpp
Serial.print(_id);
void L298MotorDriver::parseCommand(char cmd, String& args)
{switch (cmd) {
        case 'd': // distance
                _rawPosCmd = args.toFloat();
                if (_rawPosCmd < 0 || _rawPosCmd > 100) {
                        Serial.println("Position out of range.  Please select between 0 and 100.");}
                else {_actualPosCmd = map(_rawPosCmd, 0, 100, _motMinPot, _motMaxPot);
                        Serial.print("Id: ");
                        Serial.print(_id);
                        Serial.print(", Received pos command: ");
                        Serial.print(_rawPosCmd);
                        Serial.print(", actualPosCommand: ");
                        Serial.print(_actualPosCmd);
                        Serial.print(", pot pos: ");
                        Serial.println(analogRead(_pot));}
break;
        case 's': // speed
                _rawSpeed = args.toInt();
                if (_rawSpeed < 0 || _rawSpeed > 100) {
                        Serial.print("Id: ");
                        Serial.print(_id);
                        Serial.println(", Speed out of range.
                        Choose between 0 and 100.");
                        _speed = 0;}
                else {_speed = map(_rawSpeed, 0, 100, 0,
255);
                        Serial.print("Id: ");
                        Serial.print(_id);
                        Serial.print(", Raw speed: ");
                        Serial.print(_rawSpeed);
                        Serial.print(", Speed mapped to: ");
                        Serial.println(_speed);}
                break;
        case 't': // tolerance
                _tolerance = args.toInt();
                if (_tolerance < 0 || _tolerance >
                _maxTolerance) {
                        Serial.print("Id: ");
                        Serial.print(_id);
                        Serial.println(", tolerance out of range.
                        Choose between 0 and 10.");}
                else {  Serial.print("Id: ");
                        Serial.print(_id);
                        Serial.print(", Tolerance set to: ");
                        Serial.println(_tolerance);}
                break;
case 'p': // print values
                Serial.print("Id: ");
                Serial.print(_id);

                Serial.print(", position command: ");
                        Serial.print(_actualPosCmd);
                        Serial.print(", current position:
");
                        Serial.print(analogRead(_pot));
                        Serial.print(", Speed: ");
                        Serial.print(_speed);
                        Serial.print(", Tolerance: ");
                        Serial.println(_tolerance);
                        break;
                default:
                        Serial.print("Id: ");
                        Serial.print(_id);
                        Serial.print(", command: '");
                        Serial.print(cmd);
                        Serial.println("' not supported.");
                        break;}
}

void L298MotorDriver::printStatements(bool flag)
{_printStatements = flag;}
char L298MotorDriver::getId() const
{return _id;}
```

## C.3 Header/Library File

```
// L298MotorDriver.h

#ifndef _L298MOTORDRIVER_h
#define _L298MOTORDRIVER_h

#if defined(ARDUINO) && ARDUINO >= 100
        #include "arduino.h"
#else
        #include "WProgram.h"
#endif
class L298MotorDriver
{public:
        L298MotorDriver(
                char id, int speedPin,
                int in13, int in24,
                int potPin, int tolerance,
                int potMin, int potMax,
                bool printStatement = true);
        bool update();

        void printStatements(bool flag);
        void parseCommand(char cmd, String& args)
        char getId() const;

private:
        int _enAB, _in13, _in24, _pot;
        uint32_t _tNow, _tPrev;
        int _stmt;
        int _actualPosCmd, _tolerance;
        float _rawPosCmd;
        int _rawSpeed;
        int _speed;
        int _potMin, _potMax;
        bool _printStatements;
        const char _id;
        static const uint32_t _updatePeriod = 1000;
        static const int _maxTolerance = 10;
        static const int _motMinPot = 0;
        static const int _motMaxPot = 254;
};
#endif
```
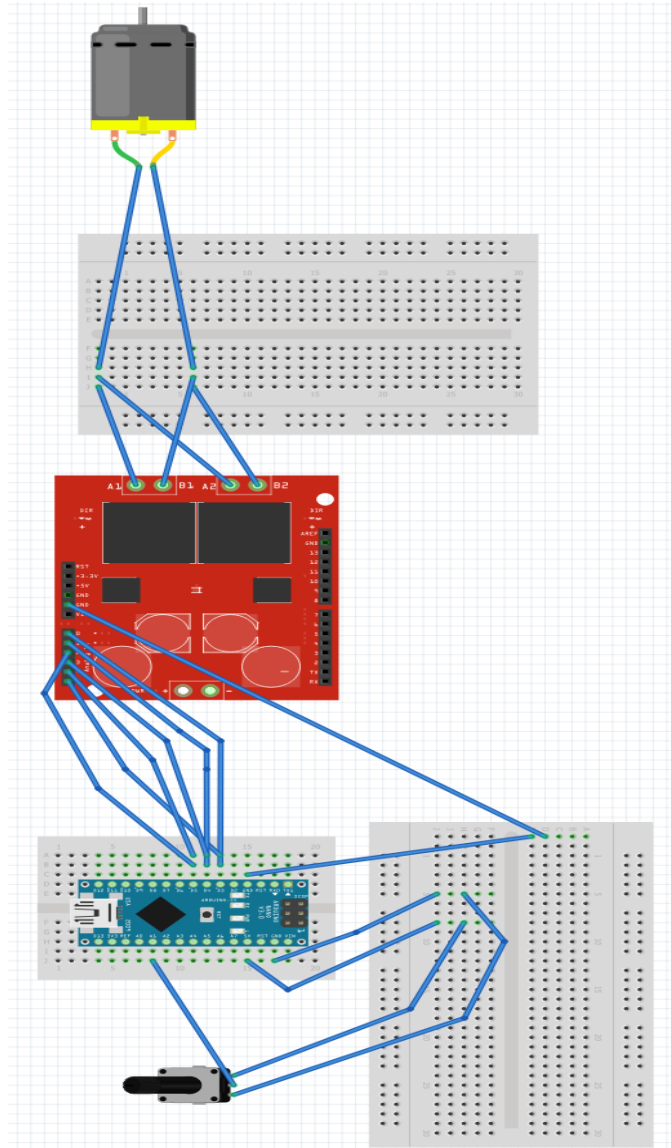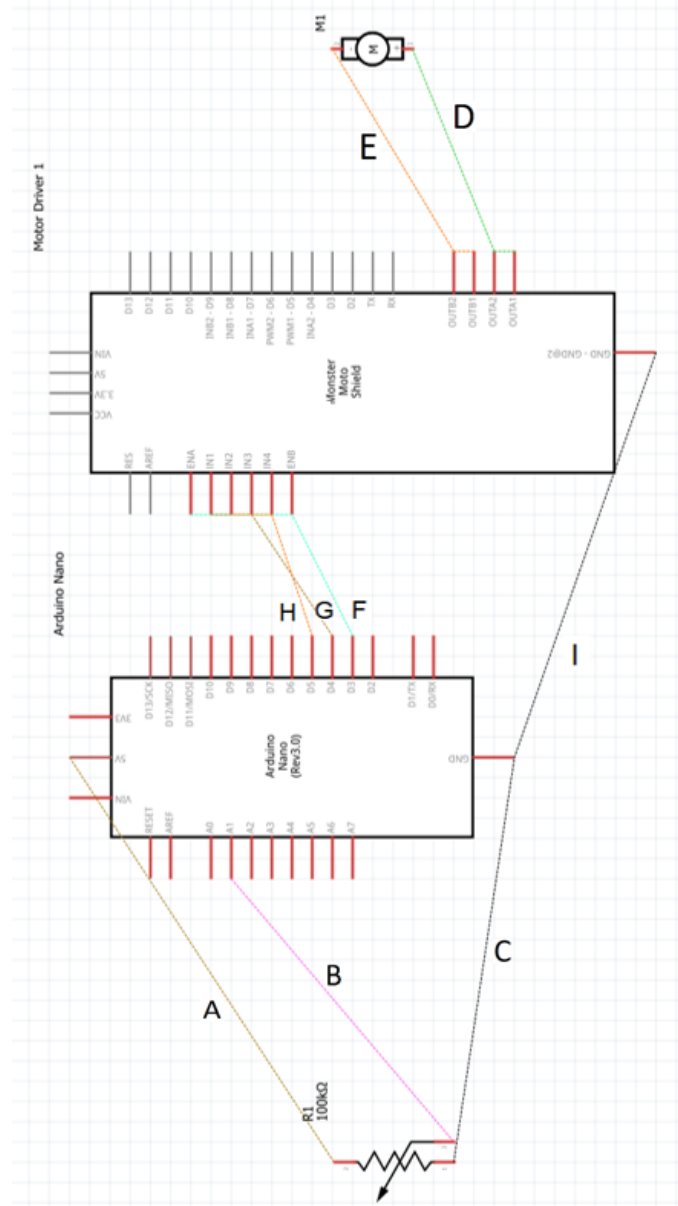
# Appendix D: Electrical Diagram & Circuit Schematic



**Figure D.1: Electrical Circuit Diagram**

*connection for one of three motors*

**Figure D.2: Electrical Schematic Connection**

*For one of three motors*

**Table D.1: Circuit Connections and Components**

| | |
|---|---|
| A | 5V Arduino Nano to positive (+) terminal on Potentiometer |
| B | Analog pin (A1) on Arduino to potentiometer input terminal |
| C | Ground (GND) to negative (-) terminal on Potentiometer |
| D | OUTA1 & OUTA2 pins on Motor Shield Driver to positive (+) terminal on Motor |
| E | OUTB1 & OUTB2 pins on Motor Shield Driver to negative (-) terminal on Motor |
| F | ENA and ENB pins on Motor Shield Driver to Digital pin (D3) on Arduino Nano |
| G | IN1 and IN3 pins on Motor Shield Driver to Digital pin (D4) on Arduino Nano |
| H | IN2 and IN4 pins on Motor Shield Driver to Digital pin (D5) on Arduino Nano |
| I | Ground (GND) to Motor Shied Driver |
| **Components** | **Name/ Part number** |
| Arduino (x1) | ATmega328 Arduino Nano |
| Motor Shield Drivers (x3) | Keyes L298 Motor Driver |
| Linear Motors (x3) | E050 Thomson Linear Motors w/10kΩ Potentiometers |
| Breadboard (x3) | Solderless Breadboard Terminal Strip |
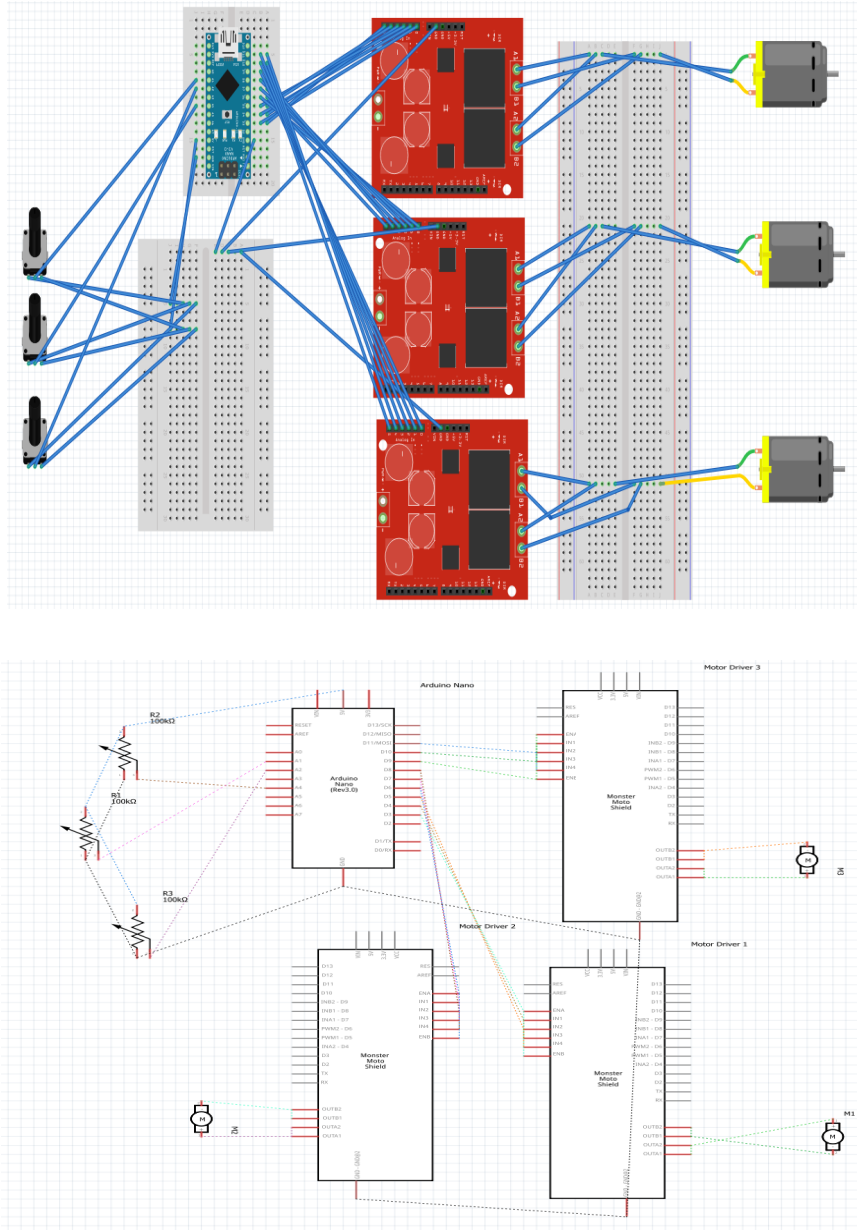
**Figure D.3: Final Circuit Diagram**

*Including all 3 motors*

# Appendix E: Sample Size Calculation

G*Power is a software tool with many statistical benefits including determining the correct number of samples required to achieve significance within data. Illustrated below is a step by step outline on how to attain such value in a G*Power software using metrics retrieved from statistical analysis files.

*Step 1 – Identifying type of statistical test & output metric of interest*

The desired outcome is sample size; given effect size and power within a repeated measures

| Test family | Statistical test |
|---|---|
| F tests | ANOVA: Repeated measures, within factors |

Type of power analysis
A priori: Compute required sample size – given α, power, and effect size

Input Parameters

| | | |
|---|---|---|
| Determine => | Effect size f | 0.261 |
| | α err prob | 0.05 |
| | Power (1−β err prob) | 0.8 |
| | Number of groups | 1 |
| | Number of measurements | 10 |
| | Corr among rep measures | 0.7 |
| | Nonsphericity correction ε | 0.527 |

Output Parameters

| | |
|---|---|
| Noncentrality parameter λ | |
| Critical F | |
| Numerator df | |
| Denominator df | |
| Total sample size | |
| Actual power | |

***Step 2*** *– Determining the Effect size & Alpha*



***Step 3*** *– Selecting a statistical power & number of groups/measurements*

***Step 4*** *– Correlation measures & nonsphericity correction*
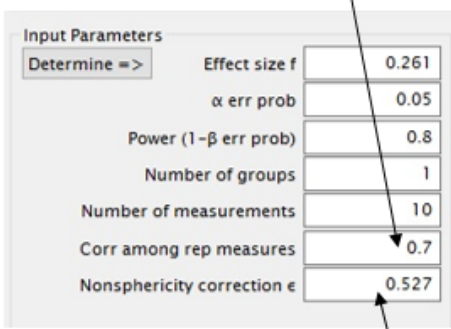


Mauchly's Test of Sphericity[a]

Measure: MEASURE_1

| Within Subjects Effect | Mauchly's W | Approx. Chi-Square | df | Sig. | Epsilon[b] Greenhouse-Geisser |
|---|---|---|---|---|---|
| Pulley_Level | .003 | 39.231 | 44 | .830 | .527 |
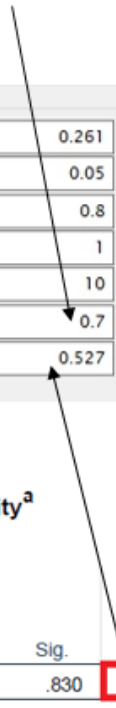
**Step 5** – *Compute the required sample size*
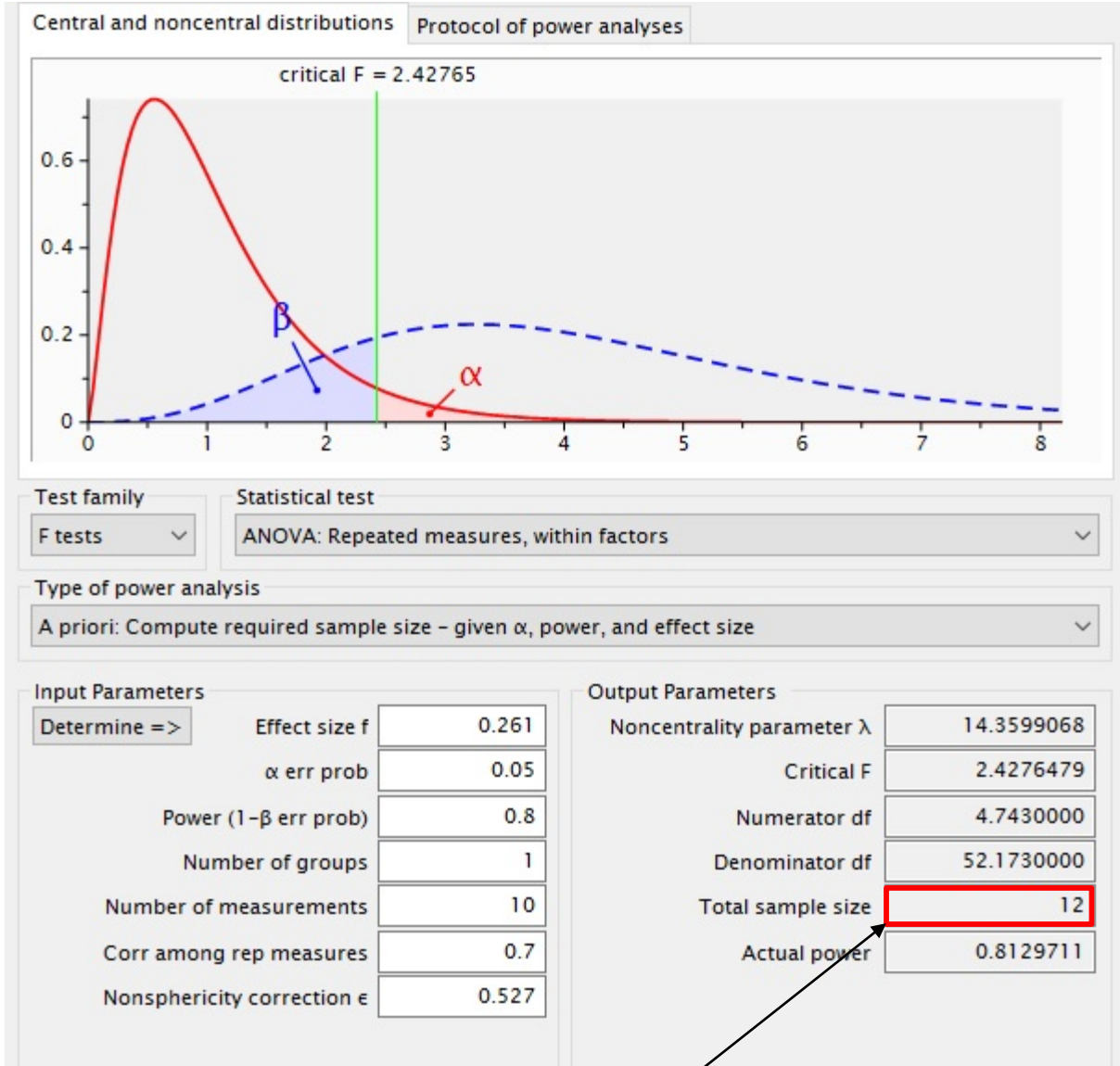


The equated sample size reveals that a minimum of 12 samples is required to achieve significance within 80% statistical power

# Appendix F: Specimen demographics

**Table G.0.2: Chapter 2 Demographics**

| Specimen | Number | Age | Sex |
|----------|----------|-----|--------|
| 1 | 13-07017 | 87 | Female |
| 2 | 13-08049 | 64 | Female |
| 3 | 13-11068 | 72 | Male |
| 4 | 13-12003 | 60 | Male |
| 5 | 13-12023 | 68 | Male |

**Table G.0.3: Chapter 3 Demographics**

| Specimen | Number | Age | Sex |
|----------|----------|-----|------|
| 1 | 15-10049 | 78 | Male |
| 2 | 16-05020 | 64 | Male |

**Table G.0.4: Chapter 4 Demographics**

| Specimen | Number | Age | Sex |
|---|---|---|---|
| 1 | 16-05014 | 60 | Female |
| 2 | 15-05021 | 80 | Male |
| 3 | 15-07052 | 69 | Female |
| 4 | 16-01032 | 66 | Female |
| 5 | 15-02069 | 84 | Male |

# Curriculum Vitae

## MOHAMMAD HADDARA

*Roth|McFarlane Hand and Upper Limb Centre St. Joseph's Health Care, London, ON*
*CMHR University Hospital, London, ON.*
*CIHR Strategic Training Program in Musculoskeletal Health Research and Leadership, London, ON.*

### OBJECTIVE

To obtain a position where my skills are utilized to their maximum potential and where I can maximize my leadership skills, quality assurance, program development, and training experience

### EDUCATION

**Masters of Engineering Science (MESc), Biomedical Engineering, Biomechanics**

Western University                                    *London, Ontario 2015- Expected graduation 2017*

Supervisor: Dr. Louis M. Ferreira

Research Project: Development of an Active Finger Motion Simulator: With In-Vitro Assessments of Tendon Loads and Joint Kinematics

**Bachelor of Engineering Science (BESc), Mechatronics Engineering**

Western University                                    *London, Ontario 2011- 2015*

### RELEVANT RESEARCH EXPERIENCE

**Graduate Research Assistant, Biomechanics**

*Roth|McFarlane Hand and Upper Limb Centre St. Joseph's Health Care, London, ON*

**Joint Motion Program (JuMP)**

University Hospital                                    *London, Ontario   Summer of 2013*

Supervisor: Dr. Louis M. Ferreira, Dr. Timothy Burkhart

Research Project: Tendon Excursion and Adhesion Simulation in Cadaver Hands Specimens: Comparative Force and Kinematic Analysis.

**Work Study**

Mechatronics Laboratory, St. Joseph's Hospital                    *London, Ontario    November 2012- 2013*
Western University
Supervisor: Dr. Louis M. Ferreira
Modifying a MotionSation project on LabVIEW; debugging
Testing different scripts using a Certus tracking camera
Creating codes and functions on LabVIEW
Working with Refman and Reworks databases.

## RELEVANT ACADEMIC EXPERIENCE

**SunStang Solar Car Project**
Western University                            *London, Ontario   September 2012- Present*
Supervisors: Lesley Mounteer
Non-Technical Co-Manager

**Mechatronics Capstone Project**
Western University                            *London, Ontario   September 2014- April 2015*
Supervisor: Dr. Michael Naish
Designing and Building a 5mm diameter SmartCable for the Davinci surgical instrument that can feedback
tensile forces exerted onto them; protecting the patient.

## FUNDING AND SCHOLARSHIPS

**Joint Motion Program (JuMP)**
University Hospital                              *London, Ontario*
CIHR Fellowship in Musculoskeletal Health Research and Leadership - $6000  *Summer of 2013*

CMHR Fellowship in Musculoskeletal Health Research and Leadership - $1500 *2015 – 2017* Western
University

## TEACHING

**Graduate Teaching Assistant**

**ES1050: Engineering Design**
Western University                            *London, Ontario   September 2015- Summer 2017*
Professor: Dr. Jonathan Southen
Assisting students with their critical thinking and design development.
Evaluating 50 students through presentations, reports, and exams.

**BUS 2299E: Engineering Business**
Western University                            *London, Ontario   September 2015- Summer 2017* Professor: Dr.
David House
Evaluating 100 students through exams and reports

**ENGSCI 4498F: Engineering Ethics**

Western University                                                *London, Ontario   Summer 2015*
Professor: Dr. Ayman El Ansary
Evaluated 54 students through exams and assignment

## SUPERVISION

**Secondary School Students (co-supervised)**              *London, Ontario   Summer 2015*

James Han, High-School Co-Operative Education Program, *Lucas Secondary School*
**Research Project:** Tendon Excursion and Adhesion Simulation in Cadaver Hands
Specimens: Comparative Force and Kinematic Analysis.

## ACADEMIC AWARDS

**3MT Engineering Competition - $150**                     *London, Ontario    April 2017*

## PRESENTATIONS & CONFRENCES

*\*Presenting Author is underlined*

**Haddara M**, Byers B, Ferreira LM, <u>Suh N.</u> (January 2018) The Effect of Wrist Position on Tendon Loads Following Pulley Sectioning and Operative Reconstruction. American Association for Hand Surgery: AAHS. Phoenix, Arizona. (U.S.) (Podium) (Grad)

**Haddara M**, Byers B, Ferreira LM, <u>Suh N.</u> (January 2018) The Effect of Sequential Flexor Tendon Pulley Sectioning and Reconstruction on Joint Range of Motion and Tendon Load. American Association for Hand Surgery: AAHS. Phoenix, Arizona. (U.S.) (E-Poster) (Grad)

<u>**Haddara M**,</u> Ferreira LM. (September 2017) Development of an Active Finger Motion Simulator. Western University Thesis Seminar Presentation. London, ON. (Local) (Podium) (Grad)

<u>**Haddara M**</u>, Ferreira LM. (May 2017) Tendon Excursion and Adhesion Simulation: A Cadaveric Force and Kinematic Study. Western University Biomedical Research Day. London, ON. (Local) (Poster) (Grad)

<u>**Haddara M**</u>, Ferreira LM.  (February 2016) Tendon Excursion and Adhesion Simulation: A Cadaveric Force and Kinematic Study. Western University Thesis Seminar Presentation. London, ON. (Local) (Podium) (Grad)

<u>**Haddara M**</u>, Ferreira LM.  (April 2015) Kinematics of Tendon Excursion and Adhesion Simulation in Cadaveric Hands. Western University Thesis Presentation. London, ON. (Local) (Podium) (Undergrad)

<u>**Haddara M**</u>, Ferreira LM. (April 2015) Use of FBG cables for Force Feedback Analysis on The DaVinci Surgical Tool. Fourth Year Capstone Project. London, ON. (Local) (Poster) (Undergrad)